UNIVERSITETET I AGDER

# ULTRA RELIABLE COMMUNICATION IN 5G NETWORKS: A DEPENDABILITY-BASED AVAILABILITY ANALYSIS IN THE SPACE DOMAIN

HANDUNNETHTHI VIMARSHA KALPANIE MENDIS

SUPERVISOR
Professor Frank Yong Li

**University of Agder, 2017**
Faculty of Engineering and Science
Department of Information and Communication Technology

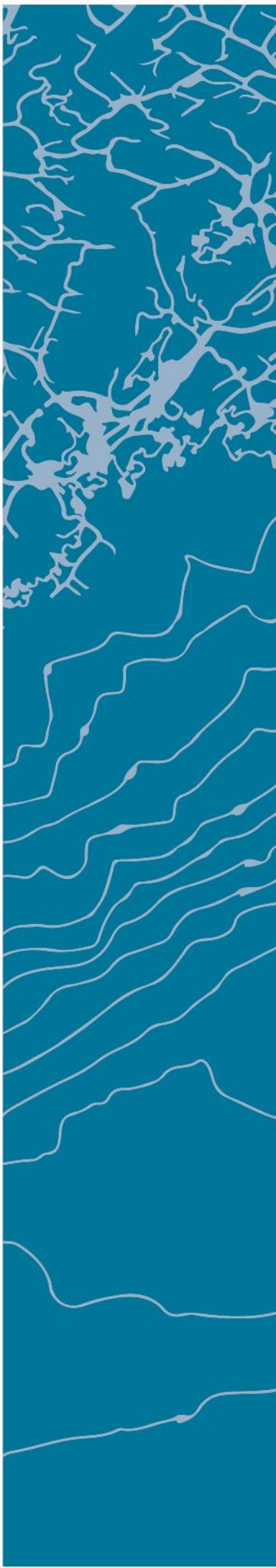

# Ultra Reliable Communication in 5G Networks: A Dependability-based Availability Analysis in the Space Domain

by

**Handunneththi Vimarsha Kalpanie Mendis**

**Supervisor:**

Professor Frank Yong Li

**IKT-591: Master's Thesis**

*This masters thesis is carried out as a part of the education at the University of Agder and is therefore approved as a part of this education. However, this does not imply that the University answers for the methods that are used or the conclusions that are drawn.*

University of Agder
Faculty of Engineering and Science
Department of Information and Communication Technology
Grimstad

May 22, 2017

**Abstract**

As our daily life is becoming more dependent on wireless and mobile services, seamless network connectivity is of utmost importance. Wireless networks are expected to handle the growing demand for applications which require higher capacity, without failure. Therein, wireless connectivity is regarded as an essential requirement for a wide range of applications in order to support flexible and cost-effective services. As part of the fifth generation (5G) communication paradigm, ultra reliable communication (URC) is envisaged as an important technology pillar for providing anywhere and anytime services to end users. While most existing studies on reliable communication are not pursued from a dependability perspective, those dependability based studies tend to define reliability merely in the time domain.

The main objective of this thesis work is to advocate the concept of URC from a dependability perspective *in the space domain*. Accordingly, we define cell availability, system availability, and guaranteed availability for cellular networks. Poisson point process (PPP) and Voronoi tessellation are adopted to model the spatial characteristics of cell deployment in cellular networks. The spatially modeled cellular networks are used to analyze availability and initiate definitions on cell availability and system availability. Correspondingly, the availability as well as the probability of providing a guaranteed level of availability in a network are analyzed both/either cell-wise and/or system-wise. From this perspective, we investigate in depth the relationship between the signal to interference noise ratio (SINR), capacity or user requirement and achievable availability levels.

Extensive simulations are performed for various network scenarios and cell deployments to obtain numerical results based on the cell and system availability definitions. For SINR-based and capacity-based studies, threshold contours are identified in each case in order to further study cell availability under different conditions. The importance of deploying different types of cells for a cellular network is also highlighted by studying the tradeoff between the required transmission power and the obtained system availability. Moreover, definitions are developed for availability from users' perspective concerning PPP distributed users as well.

In a nutshell, this thesis proposes a novel concept referred to as *space domain availability* as a contribution to the ongoing research activities on URC for future 5G networks.

**Key words:** *5G and URC, dependability and availability, space domain analysis, PPP and Voronoi tessellation, simulations.*

# Preface

This report serves as a Masters Thesis to partially fulfill the requirements of the Masters Program in Information and Communication Technology (ICT) at the Faculty of Engineering and Science, University of Agder (UiA) in Grimstad, Norway. It is based on the work performed in the context of IKT591 Master thesis, which counts 60 ECTS credits towards the degree of MSc in ICT. The thesis work started on 29th August 2016 and ended on 21st May 2017. Followed by studying the preliminaries underlying the availability analysis and URC, we propose definitions for connectivity-based availability in the space domain. The thesis work is furthermore extended to define availability in the context of SINR and capacity of 5G cellular networks. Lastly, availability is defined in the user-perspective to facilitate 5G service providers to obtain a better overview of achieving URC. The results based on chapter 3 of the thesis was disseminated in the form of a journal paper in IEEE Communication Letters.

With great pleasure I take an opportunity to acknowledge the efforts of the people whose guidance, cooperation were vital to reach the goal of the thesis. I am very grateful to my supervisor Prof. Frank Yong Li. His careful supervision, encouragement, visionary ideas, and constant support helped me a lot in moulding my efforts into favorable outcomes. The credit should be given to him for initiating this study with a novel and innovative topic. My sincere gratitude goes to Dr. Indika A. M. Balapuwaduge who is a Post-doctoral Fellow at the Department of ICT in UiA, for his valuable comments and illuminating discussions for the improving the quality of the thesis work. He has been an inspiration with his dedication, innovative ideas and excellent research quality. Last, but certainly not the least, I would like to acknowledge the commitment, sacrifice and support of my parents, my brother and friends for their affection which always kept me going through thick and thin. Finally, I would like to express my deepest gratitude to my husband, Madhawa who was a continuous source of encouragement and determination for me. The completion of this thesis would not be possible without his immense love and support.

Handunneththi Vimarsha Kalpanie Mendis
Grimstad, Norway
May 22, 2017

# Contents

**Contents** ii

**List of Figures** v

**List of Tables** viii

**List of Abbreviations** ix

**List of Nomenclature** xi

**1 Introduction** 1

1.1 5G and URC . . . 1
1.2 Fundamentals of Dependability Theory . . . 2
1.2.1 Dependability . . . 3
1.2.2 Reliability . . . 3
1.2.3 Availability . . . 3
1.3 Motivation and Problem Statement . . . 4
1.4 Research Methodology . . . 6
1.5 Thesis Organization . . . 6

**2 Related Work and Theoretical Preliminaries** 8

2.1 Related Work on URC . . . 8
2.2 Related Work on Dependability . . . 9
2.3 Related Work on SG as a Tool for Dependability Analysis . . . 11
2.4 Dependability Metrics . . . 12
2.4.1 Reliability metrics . . . 13
2.4.2 Availability metrics . . . 14
2.5 Geometry of Cellular Networks . . . 15
2.5.1 Traditional cellular network model in the space domain . . . 15
2.5.2 SG framework . . . 16
2.5.3 Point processes . . . 16
2.5.4 PPP . . . 17
2.5.5 Voronoi tessellation . . . 17

2.5.6 Size of a PV cell . . . 18
2.6 Preliminaries on SINR and Capacity . . . 20
2.6.1 SINR . . . 20
2.6.2 Capacity and Shannon capacity . . . 21
2.7 Chapter Summary . . . 22

**3 Connectivity-based URC Concepts and Analysis 23**
3.1 System Model . . . 23
3.1.1 HomNets and HetNets . . . 24
3.1.2 Network topologies . . . 25
3.2 Availability Definition from the Space Domain . . . 26
3.3 Cell Availability . . . 27
3.3.1 Single cell single topology (SCST) . . . 27
3.3.2 Single cell multiple topology (SCMT) . . . 27
3.3.3 Multiple cell single topology (MCST) . . . 28
3.3.4 Multiple cell multiple topology (MCMT) . . . 28
3.4 System Availability . . . 29
3.4.1 Single topology (ST) . . . 29
3.4.2 Multiple topology (MT) . . . 29
3.5 Guaranteed Availability . . . 30
3.5.1 The normalized size of a PV polygon: A stochastic view . . . 31
3.5.2 Guaranteed cell availability . . . 31
3.6 Space Domain Availability in a PV Network . . . 33
3.6.1 Generating Voronoi diagram . . . 33
3.6.2 Size of a Voronoi polygon: A deterministic expression . . . 34
3.6.3 Cell and system availability for HomNets . . . 34
3.6.4 Cell and system availability for HetNets . . . 41
3.6.5 Availability and transmission power tradeoff . . . 43
3.6.6 Guaranteed cell availability . . . 45
3.7 Chapter Summary . . . 46

**4 SINR-based URC Concepts and Analysis 47**
4.1 System Model . . . 47
4.2 SINR and Coverage . . . 47
4.3 SINR-based Cell Availability . . . 49
4.4 SINR-based System Availability . . . 49
4.5 SINR Threshold Contours . . . 49
4.6 SINR-based Cell Availability of a PV Network . . . 52
4.7 SINR-based System Availability of a PV Network . . . 57
4.8 Chapter Summary . . . 59

**5 Capacity-based URC Concepts and Analysis** **60**
5.1 System Model . . . 60
5.2 Capacity and Coverage . . . 60
5.3 Capacity-based Cell Availability . . . 61
5.4 Capacity-based System Availability . . . 62
5.5 Capacity Threshold Contours . . . 62
5.6 Capacity-based Cell Availability of a PV Network . . . 65
5.7 Capacity-based System Availability of a PV Network . . . 71
5.8 Chapter Summary . . . 73

**6 User-oriented URC Concepts and Analysis** **75**
6.1 System Model . . . 75
6.2 Individual User Availability . . . 76
6.3 User-oriented System Availability . . . 77
6.4 Individual User Availability of a PV Network with PPP Distributed Users . . 77
6.5 User-oriented System Availability of a PV Network with PPP Distributed Users 79
6.6 PPP Distributed Users with Specific Resource Requirements . . . 82
6.6.1 Homogeneous resource requirements . . . 82
6.6.2 Heterogeneous resource requirements . . . 83
6.7 Chapter Summary . . . 87

**7 Conclusions** **88**
7.1 Conclusions . . . 88
7.2 Major Contributions . . . 89
7.3 Future Work . . . 89

**Bibliography** **91**

**Appendices** **96**

**A A Published Paper based on Chap. 3** **96**

**Appendix A: References** **106**

**B Example of MATLAB Codes** **107**
B.1 MATLAB Code for Connectivity-based System Availability of HetNet Scenario 107
B.2 MATLAB Code for Creating SINR Threshold Contour and Finding The Cell Availability of The RC . . . 120

# List of Figures


1.1 Key capabilities for different usage scenarios of 5G system. . . . . 2
1.2 Real life traffic pattern. . . . . 2

2.1 System times in a repairable system assuming that the system is initially in the operational state. . . . . 13
2.2 Hexagonal grid model of cellular networks. . . . . 15
2.3 Voronoi tessellation generated by a random sample of points. . . . . 18
2.4 The BSs and mobile users modeled as PPPs. The cell boundaries of each BS form a PVT. . . . . 18

3.1 A PV distributed homogeneous cellular network with N = 10 cells/BSs. The cell boundaries are shown and the cells together form a Voronoi tessellation. The Voronoi cell boundaries which create the actual geographical area of each cell are indicated in blue (solid) lines. The BS coverage which the BS can communicate with the UEs within each cell is indicated in red (dashed) lines. . 24
3.2 HomNets and HetNets. . . . . 25
3.3 Topology 1 of a PPP distributed cellular network with $N = 10$ cells/BSs. . . 25
3.4 Different topologies for a PPP distributed cellular network with $N = 10$ cells/BSs. 26
3.5 Illustration of the overlapping areas among neighboring BSs and the exurban areas of outer-tier cells in topology 1 of the PPP distributed cellular network. Shown in green color and yellow color are the exurban areas and overlapping areas respectively. . . . . 30
3.6 The Voronoi cells normalized area-distribution function in 2D. . . . . 32
3.7 Illustration of the RC ($i = 6$) in topology 1 of the PPP distributed cellular network. . . . . 35
3.8 Illustration of the outbound coverage area of the RC ($i = 6$) in topology 1 of the PPP distributed cellular network. . . . . 35
3.9 SCST cell unavailability of the RC ($i = 6$) for topology $j = 1$ as BS the coverage increases. . . . . 36
3.10 SCST and SCMT cell unavailability of the RC $i = 6$ for $M = 5$ topologies as the BS coverage increases. . . . . 37

3.11 SCST, MCST cell and ST system unavailability in a HomNet with N = 10 cells for topology $j = 1$. . . . 39
3.12 SCMT, MCMT cell and MT system unavailability in a HomNet with $N = 10$ cells for $M = 5$ topologies. . . . 41
3.13 SCST, MCST cell and ST system unavailability in a HetNet with 3(7) T2(T1) cells for topology $j = 1$ . . . . 43
3.14 Comparison of MCST cell/ST system unavailability in a HomNet with $N = 10$ cells and HetNet with 3(7) T2(T1) cells for topology $j = 1$ . . . . 44
3.15 The probability for providing a guaranteed cell availability level. . . . 46

4.1 The coverage contour for a low SINR threshold. . . . 51
4.2 The coverage contour for a high SINR threshold. . . . 51
4.3 SCST cell unavailability of the RC ($i = 6$) for topology $j = 6$ as SINR threshold increases. . . . 53
4.4 SCST and SCMT cell unavailability for $i = 6$ and $M = 5$ topologies as SINR threshold increases. . . . 54
4.5 SCST and MCST cell unavailability for $N = 10$ cells of topology $j$ as SINR threshold increases. . . . 55
4.6 MCMT cell unavailability for $N = 10$ cells and $M = 5$ topologies as SINR threshold increases. . . . 57
4.7 Illustration of the overlaps between SINR threshold contours. . . . 58

5.1 The coverage contours for various capacity thresholds. . . . 64
5.2 The achieved capacity variation over distance. . . . 64
5.3 SCST cell unavailability of the RC ($i = 6$) for topology $j = 6$ as capacity threshold increases. . . . 66
5.4 SCST cell unavailability of the RC ($i = 6$) for topology $j = 6$ as capacity threshold increases assuming QAM. . . . 66
5.5 SCST and SCMT cell unavailability for $i = 6$ and $M = 5$ topologies as capacity threshold increases. . . . 68
5.6 SCST and MCST cell unavailability for $N = 10$ cells of topology 1 as capacity threshold increases. . . . 69
5.7 MCST and MCMT cell unavailability for $N = 10$ cells and $M = 5$ topologies as capacity threshold increases. . . . 71
5.8 ST and MT system unavailability as capacity threshold increases. . . . 73

6.1 A cellular network of N = 10 BSs modeled with a homogeneous PPP of intensity $\lambda_B = 10$ and a collection of UEs following an independent homogeneous PPP of intensity $\lambda_U = 1500$ in the Euclidean plane. . . . 76
6.2 The individual user unavailability for a randomly chosen UE which lies in the middle of a cell. . . . 78

6.3 The individual user unavailability for a randomly chosen UE which lies closer to an edge of a cell. . . . . 79
6.4 The individual user unavailability for a randomly chosen UE which lies in between the SINR threshold contours. . . . . 79
6.5 The variation of user-oriented system unavailability as the SINR threshold increases. . . . . 81
6.6 The variation of user-oriented system unavailability with the SINR threshold variation for different user distributions. . . . . 81
6.7 User-oriented system unavailability for users with homogeneous user requirements. . . . . 84
6.8 A PV network consisting of 10 BSs and LRR (illustrated by empty circles) and HRR (illustrated by cross symbols) users which follow 2 independent homogeneous PPP distributions of both having intensity of $\lambda_U = 500$. . . . . 84
6.9 user-oriented system unavailability variation for LRR and HRR users when the capacity threshold increases. . . . . 85

A.1 A PV distributed cellular network with $N = 10$ cells/BSs. The cell boundaries are shown and the cells together form a Voronoi tessellation. The Voronoi cell boundaries which create the actual geographical area of each cell are indicated in blue (solid) lines. The BS coverage which the BS can communicate with the UEs within each cell is indicated in red (dashed) lines. . . . . 99
A.2 Cell unavailability of the reference cell as BS coverage increases. . . . . 102
A.3 Cell and system unavailability in a HomNet with $N = 10$ cells. . . . . 103
A.4 Cell/system unavailability in a HetNet with 3(7) T2(T1) cells. . . . . 103
A.5 The probability for providing a guaranteed cell availability level. . . . . 105

# List of Tables


3.1 Comparison of SCST and SCMT cell availability . . . . . 37
3.2 Comparison of MCST and MCMT cell availability for $N = 10$ cells and $M = 5$ topologies . . . . . 40
3.3 Comparison of ST and MT system availability . . . . . 41
3.4 The tradeoff between availability and transmission power . . . . . 45

4.1 Comparison of SCST and SCMT SINR-based cell availability . . . . . 54
4.2 SINR-based SCST and MCST cell availability for $N = 10$ cells in topology 1 . 56
4.3 Average SINR-based MCST and MCMT cell availability for $N = 10$ cells and $M = 5$ topologies . . . . . 57

5.1 Comparison of SCST and SCMT capacity-based cell availability . . . . . 68
5.2 Capacity-based SCST and MCST cell availability of $N = 10$ cells in topology 1 70
5.3 Average capacity-based MCST and MCMT cell availability for $N = 10$ cells and $M = 5$ topologies . . . . . 71
5.4 Comparison of ST and MT system availability . . . . . 72

6.1 Numerical results of user-oriented system availability for PPP and uniform distributions . . . . . 82

A.1 The Tradeoff between Availability and Transmission Power . . . . . 104

B.1 Summary of the MATLAB codes . . . . . 107

# List of Abbreviations

| | |
|---|---|
| 3GPP | 3rd Generation Partnership Project |
| 4G | Fourth generation |
| 5G | Fifth generation |
| ACK | Acknowledgment |
| ARQ | Automatic repeat request |
| ASE | Area spectral efficiency |
| BS | Base station |
| BER | Bit error rate |
| BPP | Binomial PP |
| CCDF | Complementary cumulative distribution function |
| CDF | Cumulative distribution function |
| D2D | Device-to-device |
| EIRP | Effective isotropic radiated power |
| FEC | Forward error correction |
| Gbps | Giga bits per second |
| HCPP | Matérn hard core point process |
| HRR | High resource requiring |
| IEEE | Institute of electrical and electronics engineers |
| KPI | Key performance indicator |
| LRR | Low resource requiring |
| LTE | Long term evolution |
| MDT | Mean down time |
| METIS | Mobile and wireless enablers for the twenty-twenty information society |
| MTBF | Mean time between failures |
| MTFF | Mean time to first failure |
| MTTF | Mean time to failure |
| MTTR | Mean time to repair |
| MUT | Mean up time |
| OFDM | Orthogonal Frequency Division Multiplexing |
| PCP | Poisson cluster process |
| PDR | Packet delivery ratio |
| PDF | Probability density function |

| | |
|---|---|
| PPP | Poisson point process |
| PRR | Packet reception ratio |
| PV | Poisson Voronoi |
| PVT | Poisson Voronoi tessellation |
| QAM | Quadrature amplitude modulation |
| RC | Reference cell |
| SG | Stochastic geometry |
| SINR | Signal to interference and noise ratio |
| SIR | Signal to interference ratio |
| SNR | Signal to noise ratio |
| TCP/IP | Transport control protocol/Internet protocol |
| T1 | Type 1 |
| T2 | Type 2 |
| UE | User equipment |
| URC | Ultra reliable communication |
| WLAN | Wireless local area network |

# List of Nomenclature

| | |
|---|---|
| $M$ | Number of network topologies |
| $N$ | Number of cells |
| $A_s^c(i,j)$ | Cell availability of cell $i$ of topology $j$ |
| $A_s^c(i,:)$ | Average cell availability of cell $i$ considering $M$ network topologies |
| $A_s^c(:,j)$ | Average cell availability of topology $j$ considering $N$ cells |
| $\bar{A}_s^c$ | Average cell availability considering $N$ cells and $M$ network topologies |
| $A_s^s(j)$ | System availability of topology $j$ |
| $\bar{A}_s^s$ | Average system availability |
| $A_s^u(m)$ | Individual availability of user $m$ |
| $A_s^u$ | User-oriented system availability |
| $U_s^c(i,j)$ | Cell unavailability of cell $i$ of topology $j$ |
| $U_s^c(i,:)$ | Average cell unavailability of cell $i$ considering $M$ network topologies |
| $U_s^c(:,j)$ | Average cell unavailability of topology $j$ considering $N$ cells |
| $\bar{U_s^c}$ | Average cell unavailability considering $N$ cells and $M$ network topologies |
| $U_s^s(j)$ | System unavailability of topology $j$ |
| $\bar{U}_s^s$ | Average system unavailability |
| $U_s^u(m)$ | Individual unavailability of user $m$ |
| $U_s^u$ | User-oriented system unavailability |
| $C(i,j)$ | Covered area of the cell $i$ of topology $j$ |
| $S(i,j)$ | Area of the cell $i$ of topology $j$ |
| $C_{SINR}$ | Area covered by the SINR threshold |
| $C_{cap}$ | Area covered by the capacity threshold |
| $R$ | Radius of the BS coverage |
| $R_1$ | Radius of the BS coverage of a T1 cell |
| $R_2$ | Radius of the BS coverage of a T2 cell |
| $v$ | Number of vertices of a cell |
| $\eta$ | Cell area threshold which determines the type of a cell |
| $\Delta$ | overlap between the BS coverages |
| $y$ | Normalized PV cell area |
| $f_Y(y)$ | Probability distribution function of the normalized Voronoi cell sizes |
| $F_Y(y)$ | CDF of $f_Y(y)$ |
| $P\left(A_s^c \geq \beta\right)$ | Probability for providing a guaranteed availability level greater than or equal to $\beta$ |

| | |
|---|---|
| $W$ | Total bandwidth |
| $d$ | distance between the UE and the BS |
| $\alpha$ | Path loss coefficient |
| $T_{sys}$ | Temperature of the system |
| $E_b$ | Energy per bit |
| $f_s$ | Baud rate |
| $MCA$ | Mean covered area |
| $MUA$ | Mean uncovered area |
| $R(t)$ | Reliability function |
| $C_{Ch}$ | Channel capacity |
| $Th$ | SINR/ capacity threshold |
| $R_b$ | Instantaneous bit rate |
| $N_{FFT}$ | Total number of subcarriers |
| $N_{used}$ | Number of used subcarriers |
| $M_{mod}$ | Number of data symbols in the constellation |
| $G$ | Ratio of guard time for an OFDM symbol to useful OFDM symbol time |
| $n$ | Oversampling factor |
| $R_{err}$ | Error-correcting code rate |
| $p$ | Ratio of the number of data subcarriers to the number of pilot subcarriers and data subcarriers |
| $S_r$ | Received signal power |
| $N_0$ | Additive white Gaussian noise |
| $\Delta f$ | Frequency spacing between subcarriers |
| $k$ | The Boltzmanns constant |
| $I$ | Cochannel interference |
| $P_T$ | Effective isotropic radiated power from the BS |
| $P_R$ | Reception power at the UE |
| $L_p$ | Propagation loss between the transmitter and the receiver |
| $u_g$ | Gains provided by the system |
| $u_l$ | Propagation-related losses between the transmitter and the receiver |
| $G_T$ | Transmitter antenna gain |
| $G_R$ | Received antenna gain |
| $L$ | System loss factor |
| $\lambda$ | Wavelength of the transmitted signal |
| $N_{UE}$ | Number of users in the system |
| $(UE)_{covered}$ | Number of users covered |
| $\lambda_U$ | Intensity of the user PPP distribution |
| $\lambda_B$ | Intensity of the BS PPP distribution |
| $\mathbb{R}^d$ | Real coordinate space of $d$ dimensions |

# Chapter 1

# Introduction

*This chapter provides background information regarding the concept of ultra reliable communication (URC) in the fifth generation (5G) networks with a focus on the reliability aspects in the space domain. The problem statement is stated along with the motivation of the thesis, followed by the research methodology. Lastly, an outline of the thesis chapters is provided.*

## 1.1 5G and URC

As an advancement from the fourth generation (4G), 5G will continue to provide services at higher data rates with higher carrier frequencies and wider bandwidths to satisfy the growing user demand. Apart from 4G advancements, it is foreseen to become highly integrative by combining 5G air interface and spectrum together with long term evolution (LTE) and WiFi to expand the coverage at higher rates and to facilitate seamless user experience [1]. In consequence, the European Union's mobile and wireless enablers for the twenty-twenty information society (METIS) 5G program has introduced URC as one of the key requirements for future 5G networks. Fig. 1.1 shows how the importance of key capabilities in different usage scenarios has been identified by ITU-R M.2083 recommendations.

The terminology, URC refers to achieving almost 100% reliability at a certain (satisfactory) level of services [2]. Achieving reliable communication may be particularly challenging in wireless mobile networks. URC is expected to support applications such as traffic, safety, emergency response, industry and other areas where reliability concerns are considered to be paramount. URC may support mission-critical applications, such as industrial automation, public safety and vehicular communications [3]. These applications will require ultra reliable connectivity with guaranteed availability and reliability of service [4].

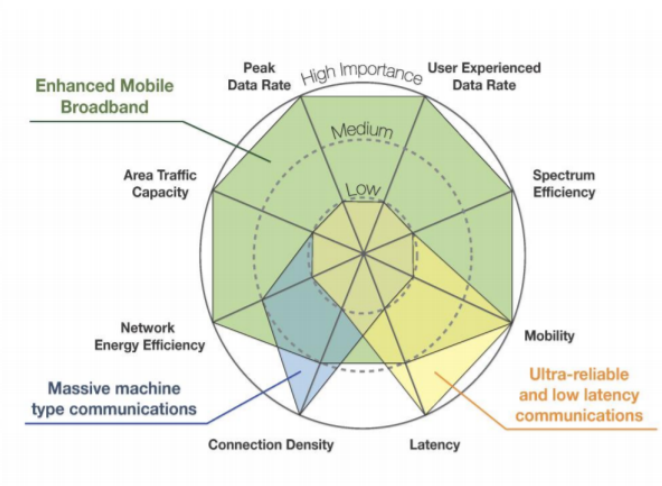


Figure 1.1: Key capabilities for different usage scenarios of 5G system [5].

## 1.2 Fundamentals of Dependability Theory

Reliability and availability in its simplest form can be explained as having the connectivity to a system anywhere and anytime. A system can be either a mechanical system, software system, electrical system or a cellular network etc. However, in the context of this thesis, we will be referring to a cellular network in wireless communication as the system in interest.

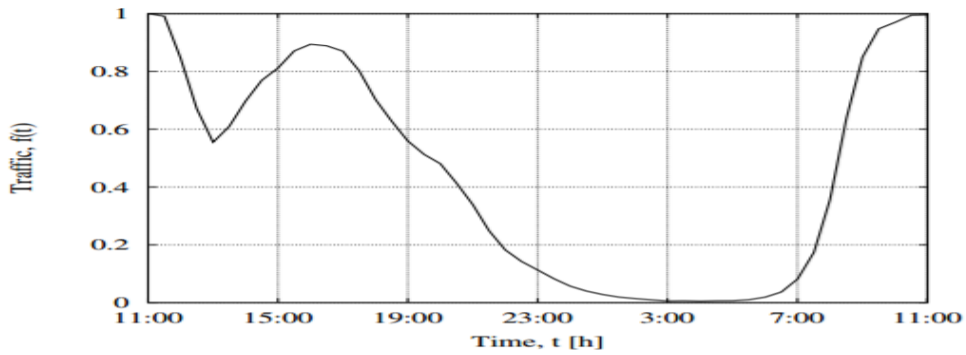


Figure 1.2: Real life traffic pattern [6].

Fig. 1.2 shows the daily cellular traffic pattern in a suburban area. As indicated, several peak times are reported in the 24-hour time span, in which there could be a higher probability of unsuccessful call attempts. For example, at the peak load point, all channels can be occupied by the demanding users therefore, the communication system can be saturated and unavailable for further call attempts. Apart from that, a communication system can be still unavailable to a user, when he/she is not covered by the base station (BS) even though there are unoccupied communication channels. A user at an edge of a cell may experience difficulty to connect to the cellular network because the received signal power is not satisfactory.

### 1.2.1 Dependability

Dependability is *the ability of a system to behave as it is specified when facing with failures of components to deliver its intended level of services to its users* [7]. It is important to analyze dependability attributes of a system since they describe essential properties which are expected from a system for a successful operation. Dependability attributes may be utilized to appropriately evaluate a system behavior, depending on its application. There are three primary attributes of dependability which represent the properties that are expected from a communication system, i.e., reliability, availability and safety [8]. When the system is in a state in which it can operate all the user requests successfully, the system is said to be in the operational state whereas, the system is said to be in the failure state, when the system fails to perform the required function.

### 1.2.2 Reliability

Reliability, as one of the primary attributes of the dependability theory, has been widely deemed as an important aspect of wireless mobile networks [9]. A particular system may be required to perform various functions with different reliability levels of each. The reliability of a system is defined as *the probability that a system will perform its intended functions without failure for a given interval of time under specified operating conditions* [10].

Alternatively, we can define the probability that the system fails to perform is intended functions for a given interval of time under specified operating conditions as unreliability. Therefore, unreliability expresses the probability of failure. The reliability and the unreliability can be related as, $Unreliability = 1 - Reliability$.

### 1.2.3 Availability

In reality, only handful of systems can operate continuously without interruption and failure. Most of the time we are not only interested in the probability of failure but also the fraction of time or space in which the system is in the operational mode, expressed via availability. Reliability can be attained when the communication system is available to users. Therefore, availability of communication systems is an important and a fundamental aspect of dependability theory which has to be studied extensively. Availability is closely related to reliability, however, reliability is often confused as availability.

According to ITU-T Recommendation E.800 availability is defined as *the ability of an item to be in a state to perform a required function at a given instant of time or at any instant of time within a given time interval, assuming that the external resources, if required, are provided* [11]. More straightforwardly, availability is the probability that the system is functioning correctly at the instant of time or point of space.

Alternatively, we can define the probability that the system is failing to perform is intended functions for a given instant of time or space as unavailability. The availability and the unavailability can be related as, $Unavailability = 1 - Availability$.

## 1.3 Motivation and Problem Statement

Reliable communication from an end-user perspective can be explained as having connectivity to the network at anywhere and anytime. However, most researches on reliability analysis have merely emphasized on the anytime connectivity or the time domain analysis. So far very little work has been done regarding the anywhere aspect of reliable communication or the space domain analysis.

URC is a novel and a promising feature which is intended to enhance the future 5G systems. It is vital to facilitate mission critical, safety and emergency response applications. The terminology of URC is introduced by the METIS project which had then objective of laying the foundation for 5G technologies. A 3rd generation partnership project (3GPP) technical report [12] included also the concept of URC in their ongoing work, but URC was dropped in the newer (December 2016) version, probably due to its immaturity. However, there exist no studies which elaborate the method to achieve URC, specifically in the space domain. Triggered by this observation, we aim to centre our attention to find possible ways to achieve URC.

Most of the reliability metrics cope with the conventional understanding of reliable communication, but they do not address the reliability issue from a dependability theory point of view. Moreover, most dependability terminologies are however applicable to the time domain, not the space domain. It is vital to conduct the analysis in the space domain in addition to the time domain, since the dependability of a system may differ with the space domain. Availability analysis in the space domain will facilitate to comprehend how it can be used to enhance the reliability levels in mobile networks.

Above interpretations can be incorporated in achieving URC. However, a proper definition of availability in the space domain is lacking from the dependability theory's perspective. To the best of our knowledge, so far no definition exists on the availability of User Equipments (UEs) in the space domain dedicated to URC. Triggered by this fact, we aim to introduce the following definitions and terminologies considering the space domain in this thesis.

Therefore, it is necessary to advocate extending the concept of URC from the dependability perspective considering the space domain. Moreover, it is important to initiate availability definitions considering cell-wise, system-wise and user-wise. The scenarios and the specific requirements have to be identified such that URC can be achieved considering circular BS

coverage, signal to interference ratio (SINR)-based BS coverage and capacity-based BS coverages. These observations lead the way to propose a novel analysis focusing on space domain modeling in which stochastic geometry (SG) is utilized to evaluate the availability of cellular networks.

### Research objectives

The main objective of this work is to advocate dependability-based availability definitions in the space domain as a contribution for the research work undergoing in the context of URC. More specifically, we have the following objectives.

- **Objective 1** Develop a system model for both homogenous and heterogeneous cellular networks which employs the characteristics of SG and propose definitions for availability of a cellular network.
- **Objective 2** Create the coverage areas of the BS in a cellular network defined by the minimum SINR threshold and propose definitions for availability of a cellular network based on the BS coverage defined by the minimum SINR threshold.
- **Objective 3** Create the coverage areas of the BS in a cellular network defined by the minimum capacity threshold and propose definitions for availability of a cellular network based on the BS coverage defined by the minimum capacity threshold.
- **Objective 4** Advocate definitions by accommodating randomly positioned users in a cellular network considering user requirements.

### Research questions

This thesis makes efforts to answer the following research questions.

- **Question 1** From the perspective of dependability theory, how to define availability in the space domain by considering characteristics of real-life cellular networks?
- **Question 2** How to find the locations of a Poisson Voronoi (PV) network which receive the minimum SINR threshold and how to define availability of a PV network based on the BS coverage defined by the minimum SINR threshold?
- **Question 3** How to find the locations of a PV network which attain the minimum capacity requirement and how to define availability of a PV network based on the minimum capacity threshold?
- **Question 4** How to define user-oriented availability considering spatially distributed users with different resource requirements?

## 1.4 Research Methodology

Followed by a thorough literature review on the areas relevant to the thesis topic, the general concepts and related research work were studied. Equipped by that knowledge, the target was to develop a system model which will enable to formulate definitions for availability. Various schemes were proposed such that availability is analyzed considering factors such as BS coverage, SINR and capacity. The proposed schemes were implemented by developing algorithms and performing extensive simulations using MATLAB® software.

- While spatially modeling the locations of the nodes in a cellular network, it was inevitable that SG has to be in-cooperated in order to obtain tractable results. Thus, the network may adapt Poisson point process (PPP) and Voronoi tessellation, and may be referred to as a PV network. Assuming BS antenna is omni-directional, circular BS coverages were presumed and cell availability, system availability, guaranteed availability etc. were defined.
- Based on a predefined SINR threshold and the random BS locations, the contours which define the boundary of the SINR threshold were created. Consequently, cell availability, system availability were defined.
- Adapting a similar concept as in above, availability along with the respective contours were also defined based on the minimum capacity requirement. Therein, cell availability, system availability were defined.
- To initiate the user-oriented availability, users were also considered as PPP distributed inside the network. Then the availability or rather the user connectivity was measured considering circular-based, SINR-based and capacity-based BS coverage scenarios.

## 1.5 Thesis Organization

The rest of the thesis is organized into seven chapters and the main points of each chapter are summarized below.

- In Chap. 2, the background work and the theoretical knowledge required to develop the proposed scheme are discussed in detail. The basic system model is also introduced.
- Chap. 3 is dedicated to present the availability analysis conducted for a circular BS coverage within a cell assuming that each BS uses an omni-directional antenna. The definitions for cell availability, average cell availability, system availability, average system availability and guaranteed availability are presented in a detailed manner. All the algorithms used for Matlab simulations are also listed.

- In Chap. 4, the detailed model of cellular network with SINR-based BS coverage is explained. It described how the SINR threshold contours can be found for different SINR thresholds. Then the definitions for cell availability, average cell availability, system availability, average system availability are presented in a detailed manner. All the algorithms used for Matlab simulations are also listed.

- Chap. 5 carries out the availability analysis for capacity-based BS coverage. Capacity threshold contours are created for various capacity thresholds and cell and system availability and their averages are also investigated.

- Chap. 6 consists of the analysis related to user availability in cellular networks. PPP distributed users are considered and the availability is defined in terms of minimum SINR threshold and capacity threshold. All the algorithms used for Matlab simulations are also listed.

- Finally, the main contributions and conclusions of the thesis are summarized in Chap. 7 and some directions for future research are also pointed out.

- A paper which has been published in IEEE Communications Letters is reproduced in Appendix A.

- Two examples of implemented MATLAB codes in the study are disclosed in Appendix B.

# Chapter 2

# Related Work and Theoretical Preliminaries

*In order to propose novel definitions and terminologies, it is important to study the existing literature and concepts relevant to the area of interest. First part of this chapter describes the studies that has been conducted in the areas of URC and dependability aspects. Second part provides a brief introduction of some fundamentals of SG theory, such as properties of the PPP, which will be extensively used in the following chapters.*

## 2.1 Related Work on URC

Very little work has been done on URC in 5G communication networks although it has become an active research topic recently. The authors in [2] gave an insight to the terminology URC and also for solving the new engineering problems posed by URC in 5G along with several motivating scenarios for supporting URC in future wireless applications. Considering applying URC in the time domain, the authors of [13] investigated the tradeoff between mobile energy and latency for mobile cloud computing applications over fading channels by applying wireless URC service composition at the application layer. Furthermore, [14] provided a review of recent advances for short packet communications through three examples in order to achieve massive, ultra reliable and low latency wireless communications.

To estimate the latency and reliability of a communication system and therein to achieve URC, [15] proposed an analysis framework from the combination of traditional reliability models with technology specific latency probability distributions. With the system level improvements proposed in [16], the authors expected to support the high reliable requirements which are to be realized by 5G communications by focusing on the need of reduced control signaling and improved end-to-end latency in network assisted device to device communications.

In [17], the authors showed the viability of using a simple air interface to achieve very low

error rates and latencies for high reliability communication. They suggested that the spatial diversity is important to ensure high reliability and low latency using short transmission intervals without retransmissions, which could limit the coverage area of the BS. [18] evaluated the viability of different diversity and interference management techniques to achieve the required downlink SINR outage probability for URC using a realistic network.

The authors of [19] invented a method to achieve cooperative URC using a master node and slave nodes in an orthogonal frequency division multiplexing (OFDM) wireless network in which all the resources are used for the down link transmission to increase the the probability for reliable reception by the slaves. Several methods and apparatus were disclosed by [20] for URC. An example method is, setting up a reliability estimate (or a threshold reliability) before the communication link is established between the UEs and establishing the communication link upon when the received reliability estimate exceeds a threshold reliability. The authors in [21] introduced *availability* as a novel metric for URC, that estimate the presence or absence of link reliability at the time of transmission. They developed a system model which compute the availability and indicated it to the applications by means of a possible implementation for automotive scenarios.

URC is a novel topic which emerged along with 5G networks, therefore not many researches have been conducted yet in its field. Therefore, there exists a void in the space domain analysis of dependability in order to find the means of achieving URC, specifically for availability in the space domain.

## 2.2 Related Work on Dependability

Research work done in relation to dependability can be identified under any of the dependability metrics, more particularly as reliability or availability for wireless cellular networks. In [22], the authors presented few architectures to improve the dependability of wireless networks. They also obtained fault-tolerant architectures with variable sizes, which are able to improve in both network availability and survivability attributes. Two configurations using redundant access points for IEEE 802.11e wireless local area networks (WLANs) were proposed in [23] have higher dependability than the scheme without any redundancy techniques.

The authors of [24], defined several reliability and availability metrics for channel access in multichannel cognitive radio networks with analogous to the dependability theory. They developed Markov-chain-based models to analyze these metrics such as steady-state channel availability, the mean time to channel unavailability, and the mean channel available time.

One of the many ways to ensure reliability at the transport layer is for the receiver to acknowledge the data it receives from the sender. Transport control protocol (TCP) in trans-

port layer guarantees reliable transmission where congestion is the primary cause of packet loss. This is performed by setting a timeout at the initiation of data transmission and retransmitting data in the case of non-receipt of acknowledgment (ACK) of data within the timeout. In [25], a new TCP-aware link layer retransmission scheme was developed which is able to offer almost full reliable transmission over a wireless link. Their focus was on efficiently recovering the loss from out-of-order packets and avoiding false actions of TCP source. [26] introduced modifications to the transport control protocol/internet protocol (IP) stack, to improve end-to-end reliable transport performance in wireless mobile networks where significant data losses are incurred due to bit errors and hand-offs.

The authors in [27] defined the reliability as the probability that the packet is successfully decoded in at most retransmissions. For an ad hoc network, delay-reliability, and throughput-delay-reliability tradeoffs were derived for single hop and multi hop transmission with automatic repeat request (ARQ) on each hop. In [28], the authors optimized modulation constellation size to minimize the bit energy consumption under average BER constraints. Furthermore, the link reliabilities and retransmission probabilities were determined using outage probabilities under log-normal shadowing effects.

Apart from the traditional approaches of achieving reliable information transmission over an error-prone network which employs either forward error correction (FEC) or retransmission techniques, it has been proven that network coding schemes could improve the reliability of error-prone networks by reducing the number of packet retransmissions. The reliability gain is also an important measure to quantify the reliability of wireless networks which was analyzed by the work of the authors in papers [29–32].

The authors in [33] have investigated the relationship between packet loss rate at the physical layer and the signal to noise ratio (SNR) in IEEE 802.15.4 networks. They demonstrated that the packet loss rate reaches zero as long as the SNR exceeds the threshold. Their results discuss the implications of using SNR as a reliability metric considering that SNR and physical level packet loss rate do not share a linear relationship. In [34], a measure on reliable throughput was proposed to investigate the efficient transmission rate and outage probability for Rician fading channels which has indicated better tradeoff between the efficient transmission rate and the outage probability.

The authors in [35] provided a framework for modeling, analyzing and prediction of the wireless link reliability. They started with the first techniques presented in reliability engineering [36] and analyzed the theoretical reliability of the wireless link based on factors such as fading, mobility, interference etc. The work in [37] introduced an approach to availability prediction and reliability analysis of a wireless transmission assuming a repairable system with variable failure and repair rates. It also introduced point availability and reliability

function $R(t)$ as two key performance indicators (KPIs) for analyzing reliable transmission.

The authors in [38] proposed a new availability measure and its application to a three tier architecture considering availability in network design. The availability and reliability of wireless multi-hop networks were evaluated in [39] by considering stochastic link failures. The availability of wireless links was improved by placing redundant nodes at appropriate locations in the existing network. In [40], based on a random-walk mobility model in ad-hoc networks, expressions for the probability of link and path availability was derived for different initial conditions. The analytical results were validated using discrete event simulation. The proposed link availability measure places a bound on the probability of path failure and the probabilistically determined path availability measure is expected to increase node mobility.

Mathematical expressions were derived for the coverage probability and rate coverage by analyzing the SINR distribution based on a cell association scheme for non-uniform heterogeneous cellular networks in [41]. The obtained numerical results demonstrate that the achieved rate by UEs through small cell deployment increases and also a higher coverage probability can be obtained after employing appropriate level of cell biasing.

However, none of the above studies has carried out an extensive study to define availability in the space domain for individual cells of the system and to evaluate system availability. Also none of them has introduced the metric guaranteed availability which relates to the BS coverage, those which we study in this thesis.

## 2.3 Related Work on SG as a Tool for Dependability Analysis

SG is powerful mathematical tool which allows studying random spatially distributed patterns in the real world. Many applications of SG into wireless cellular network can be found in the literature. The following only brings out the literature which is related to the work presented in this thesis.

In the work done in [42–44] BSs in cellular networks were modeled using homogeneous PPPs. However no expressions were derived to analyze coverage, SINR or capacity. In the letter [45], SG was adopted to model BSs and the mobile outage probability was analyzed in order to optimize the BS density and achieve an optimal network performance.

The authors in paper [46], used PPP to model one tier networks and obtained a tractable result for SINR, coverage probability and average rate of users. They have assumed that the down-link SINR complementary cumulative distribution function (CCDF) is equivalent

to the coverage probability and have derived some closed form expressions. A model to analyze the coverage probability for PPP based heterogeneous networks was presented in [47]. Therein, a method was proposed to compute the location-specific coverage probability inside the inscribing ball of a weighted Voronoi cell in three tier heterogeneous networks.

The probability of the user being connected to a macro cell or open access femto cell was computed in [48] by using realistic SG models. The locations of the BSs in a three tier network were used to find the SINR in a closed form. The authors of [49] developed a sequence of equivalence relations for heterogeneous networks to derive semi analytical expressions for the coverage probability at the mobile station when the transmissions from each BS may be affected by random fading with arbitrary distributions as well as attenuation following arbitrary path loss models.

The authors in [50] investigated the outage probability, the coverage probability, and the average achievable rate for $K$ tier heterogeneous networks. They modeled the locations of BSs according to a PPP and a Poisson cluster process (PCP) which clusters the transmitting nodes and attempted to find better ways to characterize the aggregate interference of clustered BSs. A tractable framework for SINR in downlink heterogeneous cellular networks with flexible cell association was presented in [51]. The authors derived the outage probability over SINR threshold which is equivalently the cumulative distribution function (CDF) of SINR for a randomly selected mobile in the network. Their study also extended to analyze spectral efficiency for the proposed model, the average ergodic rate of a random user, and the minimum average user throughput.

Although some of the above approaches have employed SG for BS modeling and some of the studies have investigated coverage probability, SINR profile or outage probability, proper definitions for cell availability in the space domain have not been determined yet. Through the presented work in this thesis we aim to fulfill that gap in research and initiate an in depth analysis for availability cell-wise and system-wise. We adopt SG tools to model the randomness incorporated in cellular networks. As a result, we may obtain more tractable analysis, for availability in a dependability perspective.

## 2.4 Dependability Metrics

In the context of the dependability theory, metrics such as mean up time (MUT), mean down time (MDT), mean time to failure (MTTF), mean time to first failure (MTFF), mean time between failures (MTBF), and mean time to repair (MTTR) have been defined to investigate reliability aspects of a system.

Generally, a system may undergo a series of failures and be repaired over time. The

available time or uptime (UT) is the time during which the system is operational. The unavailable time or downtime (DT) is the time during which the system is not operational. MUT is the average time that a system is in the operational state and MDT is the average time that a system is in the non-operational (failed) state. TFF is the time from the system initiation instant until it fails for the first time. MTTF describes the expected average time to failure for a non-repairable system. MTFF is the mean time until the first failure occurs. MTBF is used to estimate the expected lifetime of a system and it is the mean time between two consecutive failures in a repairable system. MTTR is the mean time needed to repair a failed system. Therefore, $MTFF = E\{TFF\}$; $MUT = E\{UT\}$ and $MDT = E\{DT\}$, where $E\{X\}$ denotes the expected value of a random variable $X$ and $MTBF = MUT + MDT$. Fig. 2.1 illustrates the system times i.e. operational times and failed times regarding the failures and repairs of a repairable system.

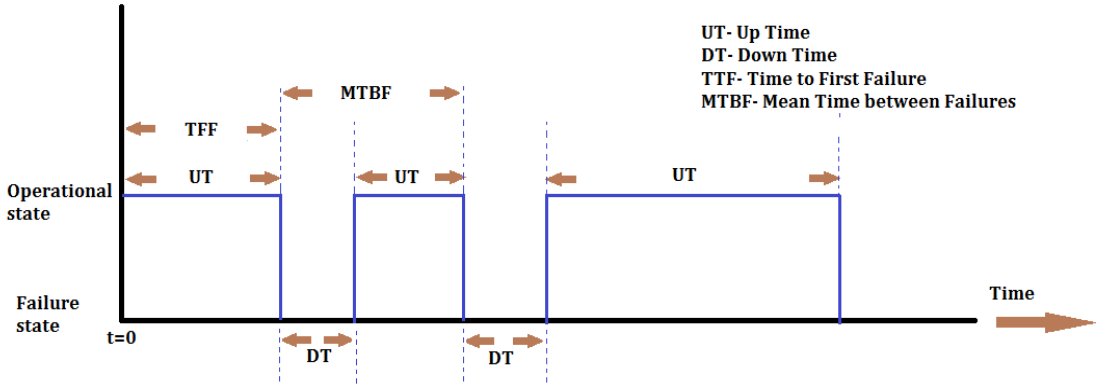


Figure 2.1: System times in a repairable system assuming that the system is initially in the operational state [52].

### 2.4.1 Reliability metrics

With respect to the metrics used to characterize reliable communication, parameters such as packet delivery ratio (PDR), packet reception ratio (PRR), bit error rate (BER), SINR, outage probability are popular ones.

PDR is defined as the ratio of the number of packets successfully received by all receivers to the number of packets transmitted. This is a transmitter-centric reliability index evaluating how a packet from a sender (or tagged node) is received by all intended receivers. PRR is the percentage of nodes that successfully receive a packet from the tagged node among the intended receivers at the moment that the packet is sent out. Therefore, PRR is a receiver centric reliability index evaluating how a packet from a sender (or tagged node) is received by all intended receivers.

BER is the number of bit errors per unit time or the number of bit errors divided by the total number of transferred bits during a time interval. It is an indication of how often a packet has to be retransmitted in the occasion of an error. It serves as a reliable indicator in both noise and interference-limited conditions. Any communication system is concerned with an important parameter called the SINR, at the receiver. This parameter defines how much signal power is received compared to the combination of the noise power and the interference at the receiver. Here, the interference is the powers from other sources, such as adjacent (sub)carriers in frequency or nearby cells in space. Indeed, the outage probability is defined as the probability of failing to reach a minimum (or threshold) SINR required to satisfy a given service i.e., $Outage\ Probability = P(Achieved\ SINR < Threshold\ SINR)$.

### 2.4.2 Availability metrics

Availability can be measured using the metrics such as instantaneous (or point) availability, interval availability (or mean availability), steady state availability, inherent availability, achieved availability and operational availability.

Instantaneous (or point) availability is the probability that a system is operational at a specific time of interest, t [53]. The mean availability is the proportion of time period that the system is available for use [53]. It represents the mean value of the instantaneous availability function over the period $(0, T]$. The steady state availability of the system is the limit of the availability function as time tends to infinity. Steady state availability is also called the long-run or asymptotic availability [53].

Inherent availability is the probability that an item will operate satisfactorily at a given point in time when used under stated conditions in an ideal support environment [53]. It excludes logistics time, waiting or administrative downtime, and preventive maintenance downtime. It includes corrective maintenance downtime. It is calculated as,

$$Inherent\ Availability = \frac{MTTF}{MTTF + MTTR}. \tag{2.1}$$

Achieved availability is the probability that an item will operate satisfactorily at a given time when used under a set of stated conditions in an ideal support environment [53]. It excludes logistics time and waiting or administrative downtime. It includes active preventive and corrective maintenance downtime.

Operational availability is the probability that an item will operate satisfactorily at a given point in time when used in an actual or realistic operating and support environment [53].

It includes logistics time, ready time, and waiting or administrative downtime, and both preventive and corrective maintenance downtime. Moreover,

$$Operational\ Availability = \frac{MTBF}{MTBF + MDT}. \tag{2.2}$$

## 2.5 Geometry of Cellular Networks

The geometry of a cellular network or the location of the nodes (BSs, UEs) plays a vital role with regard to the metrics such as coverage, achieved SINR and data rate. A mobile user's connectivity to a network is largely affected by the node locations in terms of the BS and the user itself.

### 2.5.1 Traditional cellular network model in the space domain

Cellular networks are usually modeled by placing the BSs on a grid, where the UEs are either randomly scattered or placed deterministically within the grid. The conventional hexagonal grid model is the conceptual and is the simplistic model of the radio coverage for each BS in a cellular network [54], [55]. However, the actual radio coverage is not reflected by this model, because it has to be determined using propagation models or from field measurements [56]. But the hexagonal grid model is widely adopted since it provides a manageable analysis of a cellular network. A hexagonal shape has been chosen among other sensible choices of geometric shapes such as circle, an equilateral triangle or square, as it could cover an entire region without any overlap, and has the largest area given the farthest perimeter points from the center of the polygon. However, the actual cellular footprint has to be determined by the contour in which a given BS serves the UEs successfully.

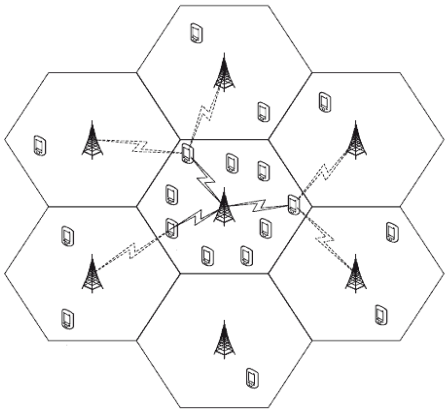

Figure 2.2: Hexagonal grid model of cellular networks.

Although this model has been utilized extensively, it is important to realize that it is both highly idealized and not very tractable [46]. For example, it is inaccurate to model the heterogeneous cell deployment in urban or suburban areas where the radio coverage can considerably vary due to the deviations in transmission power and BS and UE densities. Therefore, traditional hexagonal grid planning can no longer be used to capture the deployment of BSs nowadays.Hence, it is desirable to study more tractable models to model the spatial distribution of nodes in a cellular network.

### 2.5.2 SG framework

SG is a valuable analytical tool to model cellular networks which captures the spatial randomness inherent in cellular networks. Moreover, it takes into account for other sources of uncertainties such as fading, shadowing, path loss and power control [57]. In a nutshell, SG allows to study the average behavior over many spatial realizations of a network whose nodes are placed according to some probability distribution. It is intrinsically related to the theory of point processes [58].

### 2.5.3 Point processes

Point Processes (PPs) are the most fundamental objects studied in the context of SG. A PP can be visually illustrated as a random collection of points in space. More formally, *a PP is a measurable mapping $\phi$ from some probability space to the space of point measures (a point measure is a measure which is locally finite and which takes only integer values) on some space $E$* [59].

A few dichotomies concerning PPs on Euclidean space $\mathbb{R}^d$ are as follows where $\mathbb{R}^d$ denotes the real coordinate space of $d$ dimensions:

- A PP can be simple or not. It is simple if the multiplicity of a point is at most one (no two points are at the same location). By simple, we mean there are no two points at the same location.
- A PP can be stationary or not. Stationarity holds if the law of the point process is invariant by translation.
- A PP can be Poisson or not.
- A PP can be isotropic or not. Isotropy holds if the law of the PP is invariant to rotation. Homogeneous PPPs are isotropic. If a PP is isotropic and stationary, it is called motion-invariant.
- A PP can be marked or not; marks assign labels to the points of the process, and they are typically independent of the PP and i.i.d. The study of marked point processes may require the handling of Palm calculus.

There are four categories of PPs that have been widely studied to model wireless networks, namely, PPP, binomial PP (BPP), PCP and Matérn hard core PP (HCPP). PPP provides the baseline model for the other PPs, i.e., PPP can be converted into the other PPs [59]. Moreover, among other PPs, PPP has provided a convenient mathematical framework to model random wireless networks.

### 2.5.4 PPP

Recently, many studies tend to model the location of the nodes in a cellular network as random, following a PPP. In the following, we define the PPP and the homogeneous PPP.
**PPP** A PP $\Phi \triangleq \{x_i\} \in \mathbb{R}^d$ is a PPP if and only if

- for an arbitrary set $A \in \mathbb{R}^d, \Phi(A)$ is a Poisson RV.
- for any two disjoint subsets $A_i, A_j \in \mathbb{R}^d, \Phi(A_i)$ and $\Phi(A_j)$ are independent [59].

**Homogeneous PPP** If the intensity measure $\Lambda$ of a PPP $\Phi$ satisfies $\Lambda(A) = \lambda |A|$, i.e., the product of a constant value $\lambda$ and Lebesgue measure $|A|$, then $\Phi$ is a homogeneous PPP with intensity $\lambda$. $\lambda$ can be simply introduced as the mean number of points per unit of area. Homogeneous PPP is a simple, isotropy, and stationary PP. Mathematical analysis can be greatly simplified by using homogeneous PPP. Therefore, unless otherwise specified, the PPP in the following refers solely to the homogeneous PPP on a two dimensional plane $\mathbb{R}^2$ .

**A key property on PPP** Among the key properties of PPPs, the following is the mostly used key property. *For a PPP $\Phi \subset \mathbb{R}^2$ and an arbitrary finite region $A, \Phi(A)$ is a Poisson random variable with mean $\lambda |A|$.* Therefore,

$$\mathbb{P}\{\Phi(A) = n\} = e^{-\lambda |A|} \frac{(\lambda |A|)^n}{n!} \tag{2.3}$$

where $|A|$ denotes the area of $A$. Eq. (2.3) gives the probability that $n$ points are located inside the area indicated by finite region $A$.

### 2.5.5 Voronoi tessellation

By definition, *a tessellation is a collection of open, pairwise disjoint polyhedra (or polygons in the case of $\mathbb{R}^2$ ) whose closures cover the space, and which is locally finite (i.e., the number of polyhedra intersecting any given compact set is finite)* [60]. Given a set of centers or seeds, a Voronoi tessellation can divide the space in to specific regions, known as Voronoi regions. Each of the regions contains those points of space that are closest to the same center. A Voronoi tessellation in $\mathbb{R}^2$ would look like the polygons sketched in Fig. 2.3.

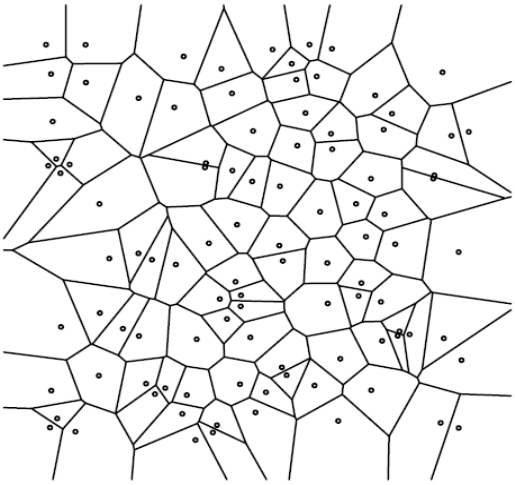

Figure 2.3: Voronoi tessellation generated by a random sample of points [60].

When the centers are randomly distributed and uncorrelated in a Voronoi tessellation, it is called as a Poisson Voronoi Tessellation (PVT). A PVT is constructed from the perpendicular lines bisecting the distances between each two neighboring nodes of a PPP. In a cellular network, the coverage regions of the BSs defined by these boundaries or the bisectors, form a PVT, as shown in Fig. 2.4.

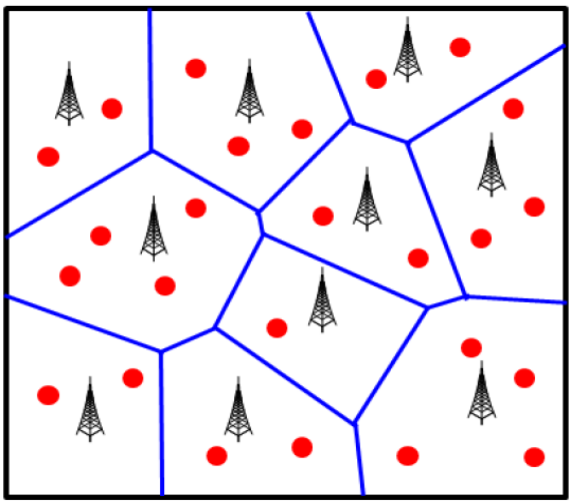

Figure 2.4: The BSs and mobile users modeled as PPPs. The cell boundaries of each BS form a PVT.

### 2.5.6 Size of a PV cell

In our study, we are particularly interested in the average size or the area of a PV cell. Unfortunately, calculating the average size of a PV cell has been an open mathematical problem to date and there does no exist a closed form expression until today. It is yet one of the most

debated and less clarified aspect in SG.

A linear relationship between the mean cell area $A(n)$ and the number of edges $n$ in a PV cell was presented by *Lewis law* [61] as below,

$$A(n) = \frac{n - n_0}{6 - n_0}\bar{a}_0 \tag{2.4}$$

for a constant $n_0$ where $\bar{a}_0 = \frac{1}{\lambda_0}$ and $\lambda_0$ denotes the mean number of cells per unit area. The value 6 in the denominator indicates the mean number of edges a random PV cell could possess. Substituting $n_0 = 3/2$, [62] proposes,

$$A(n) = \frac{2n - 3}{9}\bar{a}_0. \tag{2.5}$$

However it is not reasonable to say, that the average PV cell size can solely depend on the number of edges, since edge length has to be considered in this case. Therefore, it was decided not to rely on this findings for the continuation of our study.

Numerous researchers have studied the characteristics of the PV cells using computer simulations [63], [64], [65]. Their results have been able to provide an approximate numerical solution for PV cell size distribution by fitting it into a generalized three parameter ($a, b$ and $c$) Gamma distribution. The Gamma function is an extension of the factorial function, with its argument shifted down by 1, to real and complex numbers.

$$f(y) = \frac{c\ b^{\frac{a}{c}}}{\Gamma(\frac{a}{c})} y^{a-1} exp(-by^c). \tag{2.6}$$

However, some researches [66], [67] have also suggested that a simpler two parameter ($a$ and $b$) Gamma function can also fit.

$$f(y) = \frac{b^a}{\Gamma(a)} y^{a-1} exp(-by). \tag{2.7}$$

Using Monte Carlo-type computer simulations, the authors in [68] found that the probability density function (PDF) of a *normalized* PV cell area $y$ in a $d$ dimensional space, i.e., $\mathbb{R}^d$ can be approximated as Eq. (2.8); by finding appropriate values for $a, b$ and $c$ in Eq. (2.6),

$$f_d(y) = \frac{\left(\frac{3d+1}{2}\right)^{\left(\frac{3d+1}{2}\right)}}{\Gamma\left(\frac{3d+1}{2}\right)}\ y^{\left(\frac{3d-1}{2}\right)}\ exp\left(-\left(\frac{3d+1}{2}y\right)\right). \tag{2.8}$$

For 2 dimensional space, i.e. $d = 2$ we can rewrite Eq. (2.8) as,

$$f_Y(y) = \frac{343}{15}\sqrt{\frac{7}{2\pi}} y^{2.5} exp\left(-3.5y\right). \tag{2.9}$$

We will be using Eq. (2.9), for our work in order to satisfy the requirement of a good fit to the size distribution of a PV cell.

## 2.6 Preliminaries on SINR and Capacity

In this section we recall the theoretical preliminaries behind SINR and capacity which will be extensively used in the rest of this thesis.

### 2.6.1 SINR

Ensuring reliability in a cellular network can be also defined in terms of minimum SINR requirement, which in turn satisfies the coverage requirement to serve an estimated number of users. Satisfying the coverage requirement is an essential part at the initial configuration of any cellular network design. Therefore, evaluating the intensity of received signals and interference at a particular location is fundamental and critical. Not only the received signal power is random due to the random spatial distribution of the users, the interference is also a function of the network geometry which is also dependent upon the path loss and the fading characteristics of the propagation environment.

#### SINR of an OFDM system

Due to the increased signal bandwidths, OFDM has been adopted as the modulation technique in 4G LTE cellular networks which is built on IEEE 802.16 [69]. 5G cellular systems have agreed to deliver a capacity of the order of giga bits per second (Gbps) which is an increase up to three orders of magnitude with respect to current 4G LTE systems. Therefore, it is natural to appraise OFDM as the dominant signaling format for high-speed wireless communication facilitated by 5G networks.

For an OFDM based system, received signal power $S_r^{i,j}$ for the $j^{th}$ subcarrier of the $i^{th}$ user is given by,

$$S_r^{i,j} = P_T^{i,j} L_p^i u_g^i u_l^i G_R^i, \tag{2.10}$$

where, $P_T^{i,j}$ is the effective isotropic radiated power (EIRP) for the $j^{th}$ subcarrier of the $i^{th}$ user (in the direction of the receiver for user $i$), $L_p^i$ is the propagation loss between the transmitter and the receiver for user $i$, $u_g^i$ consists of other gains provided by the system (e.g., transmit diversity gain, macro diversity gain) for user $i$, $u_l^i$ consists of other propagation-related losses between the transmitter and the receiver (e.g., log-normal shadowing loss, fast fading loss) for user $i$, and $G_R^i$ is the received antenna gain in the direction of the transmitter for user $i$ [70].

In the context of an OFDM based system, interference can occur when two users in neighboring cells occupy subcarriers at the same frequency at the same time. Such interference

degrades the achieved SINR of individual subcarriers. The received cochannel interference $I^{0,j}$ observed by the $j^{th}$ subcarrier of the $0^{th}$ user is (assuming that user 0 is the user for whom the SINR is calculated),

$$I^{0,j} = \sum_{i=1}^{M} P_T^{i,j} L_p^i u_g^i u_l^i G_R^i, \tag{2.11}$$

where, $M$ is the number of cochannel interfering users [70]. It is obvious that, $P_T^{i,j}$ where $i \neq 0$ contributes to the interference received by user 0.

The noise power $N_0$ received by a single subcarrier is given by,

$$N_0 = kT_{sys}\Delta f, \tag{2.12}$$

where, $k$ is the Boltzmanns constant ($1.38 \times 10^{-23}$ watt/HzK), $T_{sys}$ is the system temperature, and $\Delta f$ is the frequency spacing between subcarriers [70].

Provided the above expressions, $SINR^{0,j}$ for the $j^{th}$ subcarrier of user 0 can be derived simply as,

$$SINR^{0,j} = \frac{S_r^{0,j}}{N_0 + I^{0,j}}. \tag{2.13}$$

Note that above expression calculates SINR per subcarrier and is valid for both the uplink and the downlink.

### 2.6.2 Capacity and Shannon capacity

For an effective system design of cellular networks, we should not only consider the coverage, but also should take into account the capacity of the system. As the demand is expected to rise as more UEs is become accustomed to being connected anywhere, anytime, it is important to ascertain how many bps of capacity can be supplied by a BS utilizing a given amount of spectrum. An effective design enables a the cellular service provider to serve the offered traffic in a given area with fewer BSs.

The capacity of a communication system is the maximum data-rate in bits per second that can be reliably transferred from transmitter to receiver. Claude Shannon invented the information theory in 1948 in order to characterize the limitations of reliable communication [71]. Shannons formula can be used as a tool to determine the maximum rate, which is also known as the channel capacity by which the information can be transferred over a communication channel. Let $W$ be the bandwidth available, $S$ be the received signal power and the $N$ be the additive white Gaussian noise, channel capacity $C_{Ch}$ can be simply expressed as,

$$C_{Ch} = W\ log_2\left(1 + \frac{S_r}{N_0}\right). \tag{2.14}$$

From 2.14, it is evident that the two factors limiting the maximum achievable rate is the $W$ and $S_r/N_0$ which is the average SNR.

**Capacity of an orthogonal frequency division multiplexing system**

For an OFDM system, the instantaneous bit rate corresponds to the amount of bits in an OFDM symbol that can be transmitted through the channel within the duration of an OFDM symbol. The instantaneous bit rate $R_b$ over an OFDM symbol in bps is yielded by,

$$R_b = \frac{nW(N_{used} - 1)log_2 M_{mod}}{N_{FFT}(1 + G)} R_{err} p, \tag{2.15}$$

where, $W$ is the total bandwidth, $N_{FFT}$ is the total number of subcarriers, $N_{used}$ is the number of used subcarriers, $M_{mod}$ is the number of data symbols in the constellation, $G$ is the ratio of guard time for an OFDM symbol to useful OFDM symbol time, $n$ is the oversampling factor, $R_{err}$ is the error-correcting code rate, and $p$ is the ratio of the number of data subcarriers to the number of pilot subcarriers and data subcarriers [70].

## 2.7 Chapter Summary

This chapter begins with summarizing the work done by several researches on our area of interest. After a thorough literature we have highlighted the void to be filled in relation to dependability theory analysis and URC in 5G systems. Second part of this chapter has been dedicated to brief out the relevant theoretical preliminaries which enabled us to carry out the research work. The most important and relevant principles in SG are presented. Moreover, techniques of evaluating size of PV cells and measuring SINR and capacity of an OFDM based system is described before winding up the chapter.

# Chapter 3

# Connectivity-based URC Concepts and Analysis

*The importance of adapting SG tools to model typical cellular networks was elaborated in Chap. 2. In Chap. 3, we propose the system model using SG, which will enable to derive more realistic expressions for cell availability, system availability and guaranteed availability. The highlight in this analysis is that the BS coverage at each cell is circular assuming omni-directional antennas at the BS.*

## 3.1 System Model

Consider a cellular network which is modeled using PV principles. For the ease of our analysis, we only focus on a $1 \times 1$ unit region of a cellular network, covered by a Voronoi tessellation with $N$ number of cells as shown in Fig. 3.1. We establish the system model based on the following underlying assumptions.

- All BSs are formed based on a homogeneous PPP of intensity $\lambda_B$ in the Euclidean plane. This is in contrast with the typical modeling of cellular networks which locates the BSs on a hexagonal grid assuming a deterministic approach.
- In each cell, one BS is deployed and one omni-directional antenna is mounted on each of them. Hence, the coverage of each BS is considered to be a circular one.
- Same channel type and propagation condition are considered always.

The following terminologies are important to be clarified before explaining the proposed model. Fig. 3.1 would provide more clarification to the above two terms.

**Covered area of the BS** means the geographical area in which the BS can communicate with the UEs distributed randomly within the cell, assuming the BS antenna is omni-directional.

**Area of the cell** means the actual geographical area defined by the Voronoi cell boundaries.

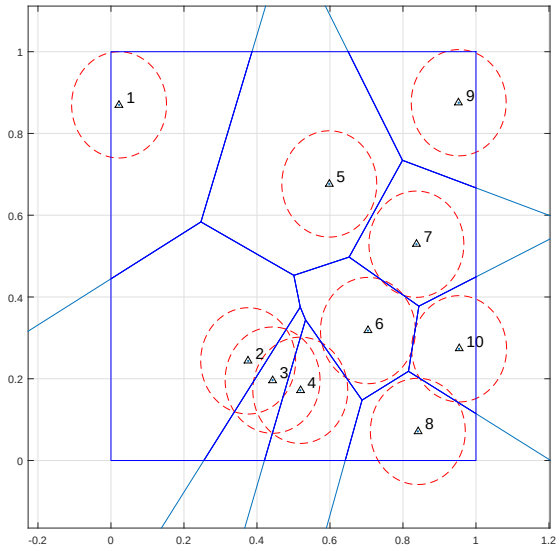


Figure 3.1: A PV distributed homogeneous cellular network with N = 10 cells/BSs. The cell boundaries are shown and the cells together form a Voronoi tessellation. The Voronoi cell boundaries which create the actual geographical area of each cell are indicated in blue (solid) lines. The BS coverage which the BS can communicate with the UEs within each cell is indicated in red (dashed) lines.

### 3.1.1 HomNets and HetNets

We consider two cellular network deployment scenarios referred to as HomNets and HetNets. The main difference between them is that, while in the cell size transmission power for all BSs is considered to be identical in the former case, two transmission power levels are considered in HetNets to represent two types of cells, i.e., type 1 (T1) cells and type 2 (T2) cells.

- HomNet: All BSs transmit with an identical transmission power level and have the same coverage radius, $R_2$. Therefore, the network only consists of one type of cells, i.e., T2 cells.
- HetNet: This network deployment consists of both types, i.e., T1 and T2 cells. A T2 cell is deployed when its Voronoi cell size is greater than a predefined threshold value, $\eta$. Otherwise a T1 cell with radius $R_1$, where $R_1 < R_2$, is deployed for these small-size cells.

In Fig. 3.2 the two network deployments are illustrated. T2 cells are indicated in red (dot-dashed) lines and T1 cells are indicated in red (solid) lines.

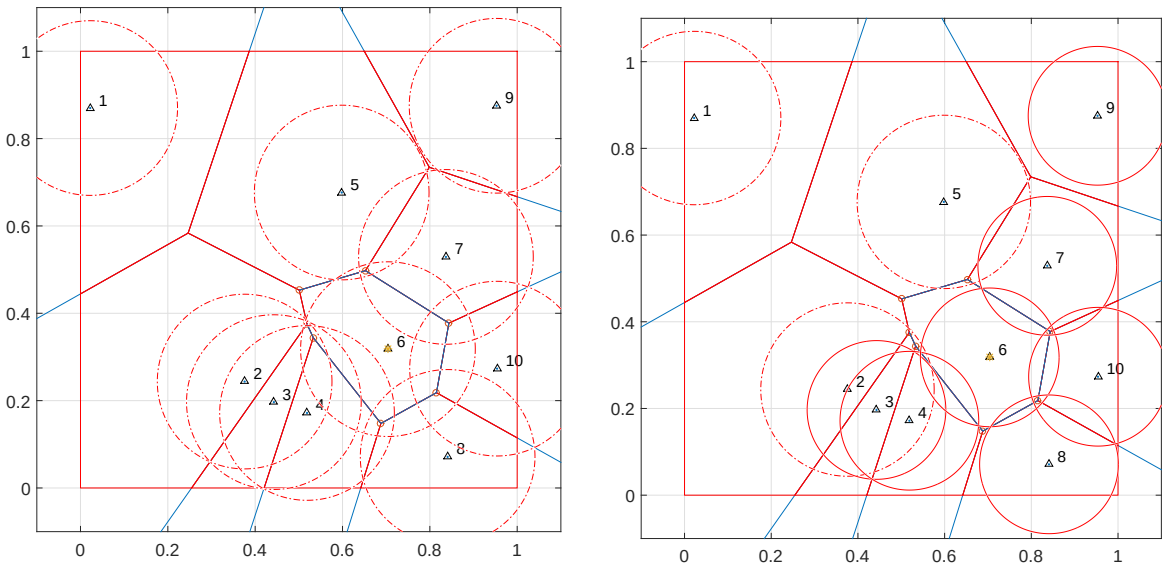


(a) HomNet scenario (b) HetNet scenario

Figure 3.2: HomNets and HetNets.

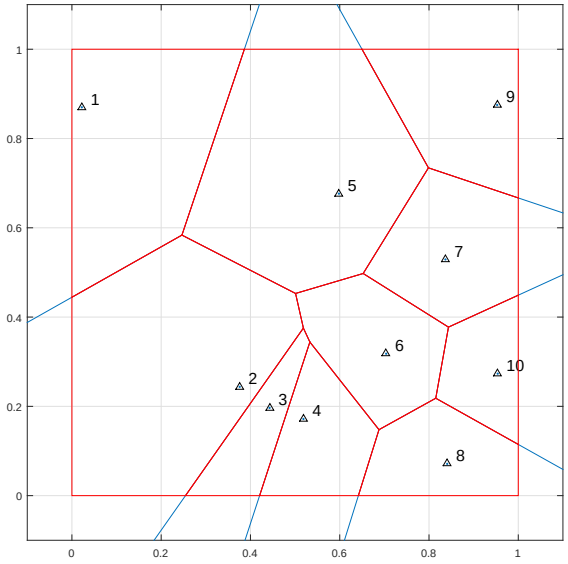


Figure 3.3: Topology 1 of a PPP distributed cellular network with $N = 10$ cells/BSs.

### 3.1.2 Network topologies

The $N$ cells considered in this model can be spatially distributed in multiplicity of topologies, within a unit region. Any system we consider is a particular topology of many random topologies the Voronoi cell system can take. In Fig. 3.3 and Fig. 3.4, we illustrate 5 random topologies that a PPP distributed cellular network with N = 10 cells/BSs could take. Fig. 3.3 illustrates the topology we adhere to, for single topology scenario and Fig. 3.4 illustrates the four other topologies we refer to, in multiple topology scenario.

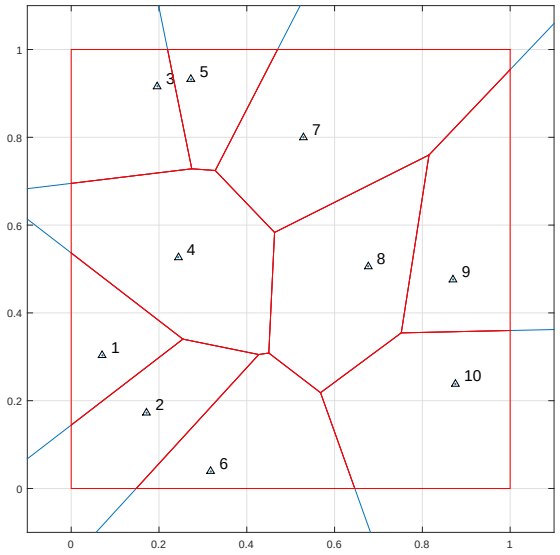

(a) Topology 2

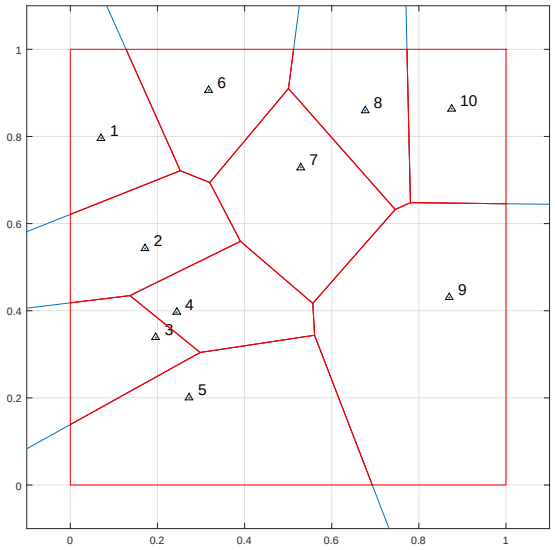

(b) Topology 3

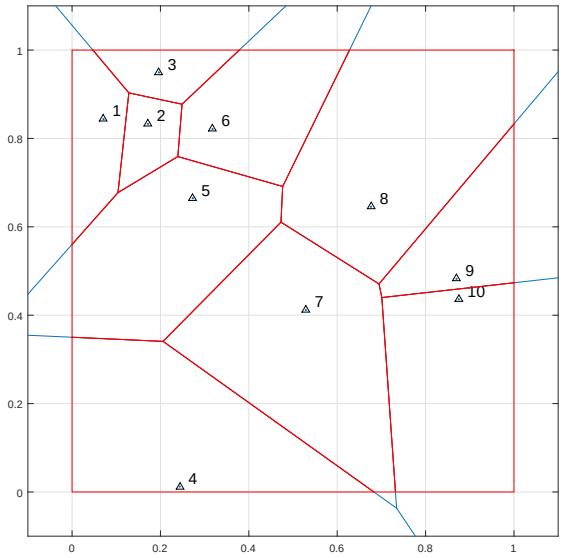

(c) Topology 4

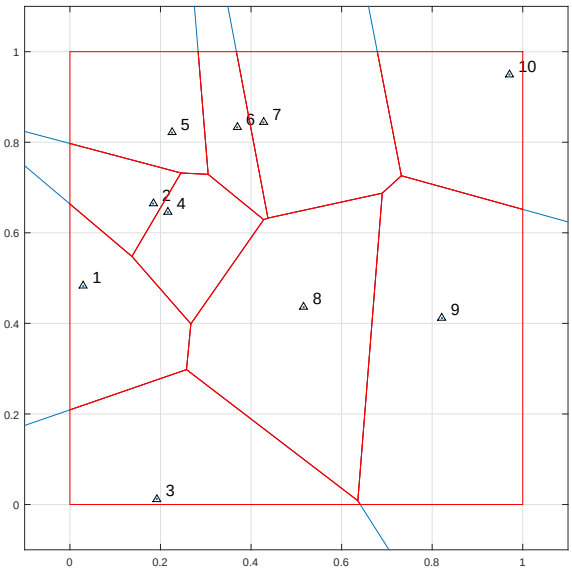

(d) Topology 5

Figure 3.4: A PPP distributed cellular network with $N = 10$ cells/BSs.

## 3.2 Availability Definition from the Space Domain

Firstly, it is important to revisit the time domain definition of availability, before developing our concept which defines network availability in the space domain. The space domain network availability deals with the anywhere aspect of URC. The steady state availability in the time domain, $A_t$, can be expressed as,

$$A_t = \frac{MUT}{MUT + MDT}. \tag{3.1}$$

Analogous to the time domain, we adopt a similar ratio to define the space domain avail-

ability of a cellular network. Conceptually, the network availability in the space domain is defined as the ratio between the covered area by the BS(s) and the total area of a cell or network of interest. Consider the randomness of cell sizes in SG cellular networks and denote the mean covered area and the mean uncovered area as MCA and MUA respectively. We can express the availability in the space domain, $A_s$, as,

$$A_s = \frac{MCA}{MCA + MUA}. \tag{3.2}$$

Bringing forward the above concept, we further define more explicit availability terminologies as follows.

## 3.3 Cell Availability

Cell availability, is the availability defined in the context of one cell in interest.

### 3.3.1 Single cell single topology (SCST)

In this scenario, cell availability is expressed for a BS located in a Voronoi cell $i$ considering a particular topology $j$ of many random topologies the Voronoi cell system can take. Thus, cell availability, i.e., $A_s^c$ is defined as the covered area by the BS of an individual cell of interest divided by the area (or size) of the Voronoi cell. More simply, it is the ratio of covered area and the area of the cell. Denote these two areas by $C(i,j)$ and $S(i,j)$ respectively for a randomly selected cell $i$, in a given network topology $j$. We have,

$$A_s^c(i,j) = \begin{cases} \frac{C(i,j)}{S(i,j)}, & \text{if } C(i,j) < S(i,j); \\ 1, & \text{otherwise.} \end{cases} \tag{3.3}$$

Note that, we are interested in defining cell availability for a particular cell, under a particular network topology using Eq. (3.3). For example, considering cell 6 of topology 1 shown in Fig. 3.3, we calculate the cell availability of cell 6, i.e., $A_s^c(6,1)$.

Furthermore, the cell unavailability of cell $i$ under network topology $j$, denoted by $U_s^c(i,j)$ is defined as,

$$U_s^c(i,j) = 1 - A_s^c(i,j). \tag{3.4}$$

### 3.3.2 Single cell multiple topology (SCMT)

Consider, M randomly deployed topologies of the system with $N$ cells. We can obtain a more generalized definition for availability of a particular cell $i$ by defining the cell availability $A_s^c(i,:)$ as follows.

$$A_s^c(i,:) = \frac{1}{M}\sum_{j=1}^{M}\left(\frac{C(i,j)}{S(i,j)}\right) \tag{3.5}$$

where $C(i,j)$ and $S(i,j)$ denote the covered area and the cell size of cell $i$ corresponding to $j^{th}$ topology. Here, denoted by $A_s^c(i,:)$ is the SCMT cell availability defined for the cell $i$ considering *all $M$ network topologies*. It is worth to mention that, one can argue the above definition as *average cell availability of cell $i$*. The only difference is that a single topology is considered in Eq. (3.3) while the average of multiple topologies is considered in Eq. (3.5). For example, for the same cell of interest, cell 6 we further calculate the cell availability $A_s^c(6,:)$ as defined by Eq. (3.5) by considering all 5 random topologies, i.e., topology 1,2,3,4 and 5 of Fig. 3.3 and Fig. 3.4.

Furthermore, the cell unavailability of cell $i$ under $M$ network topologies, denoted by $U_s^c(i,:)$ is defined as,

$$U_s^c(i,:) = 1 - A_s^c(i,:). \tag{3.6}$$

### 3.3.3 Multiple cell single topology (MCST)

Considering a given topology, we can also calculate the average cell availability for the whole system, by calculating cell availability for *all the cells* in the network, and then by taking the average. Cell availability specified for this scenario can be also argued as *average cell availability of any cell in a system*, since it is the average over cell availabilities of the $N$ cells in a particular topology. Therefore, for a randomly selected cell in a a given network topology $j$ consisting of $N$ cells, the average cell availability $A_s^c(:,j)$ is expressed as,

$$A_s^c(:,j) = \frac{1}{N}\sum_{i=1}^{N} A_s^c(i,j). \tag{3.7}$$

Furthermore, the cell unavailability for the network topology $j$, denoted by $U_s^c(:,j)$ is defined as,

$$U_s^c(:,j) = 1 - A_s^c(:,j). \tag{3.8}$$

### 3.3.4 Multiple cell multiple topology (MCMT)

For a randomly selected cell, among $M$ randomly deployed topologies of a system with $N$ cells, the average cell availability $\bar{A}_s^c$ can be expressed as,

$$\bar{A}_s^c = \frac{1}{M}\sum_{j=1}^{M} A_s^c(:,j) = \frac{1}{N}\sum_{i=1}^{N} A_s^c(i,:), \tag{3.9}$$

and also,

$$\bar{A}_s^c = \frac{1}{N}\sum_{i=1}^{N}\left(\frac{1}{M}\sum_{j=1}^{M} A_s^c(i,j)\right). \tag{3.10}$$

Therefore,

$$\bar{A}_s^c = \frac{1}{N\ M}\sum_{i=1}^{N}\sum_{j=1}^{M} A_s^c(i,j). \tag{3.11}$$

It should be highlighted that, this is the most generalized definition of cell availability, by the virtue of taking into account random cell and topology occurrences. Furthermore, the average cell unavailability can be defined as,

$$\bar{U_s^c} = 1 - \bar{A}_s^c. \tag{3.12}$$

## 3.4 System Availability

System availability is the availability defined for the whole system considering the total coverage area composed of all the cells within it.

### 3.4.1 Single topology (ST)

For a specific network topology $j$, the system availability, $A_s^s(j)$ is defined as the ratio between the sum of the total covered area of all individual cells and the total area of the network including all $N$ cells. That is,

$$A_s^s(j) = \begin{cases} \frac{\sum_{i=1}^{N} C(i,j) - \Delta}{\sum_{i=1}^{N} S(i,j)}, & \text{if } \sum_{i=1}^{N} C(i,j) - \Delta < \sum_{i=1}^{N} S(i,j); \\ 1, & \text{otherwise} \end{cases} \tag{3.13}$$

where $\Delta$ represents those overlapped coverage areas among neighboring BSs and the 'exurban' areas of outer-tier cells. While an overlapping area is an area mutually covered by two or more neighboring BSs, an exurban area is the area which belongs to an outer-tier cell but falls outside the region of interest, i.e., beyond the $1 \times 1$ border as illustrated in Fig. 3.5.

Furthermore, system unavailability of topology $j$, denoted by $U_s^s(j)$ is defined as,

$$U_s^s(j) = 1 - A_s^s(j). \tag{3.14}$$

### 3.4.2 Multiple topology (MT)

The system availability, can also be defined considering multiple topologies to obtain a more generalized expression. For $M$ randomly deployed topologies of a system with $N$ cells, $\bar{A}_s^s$ is given by,

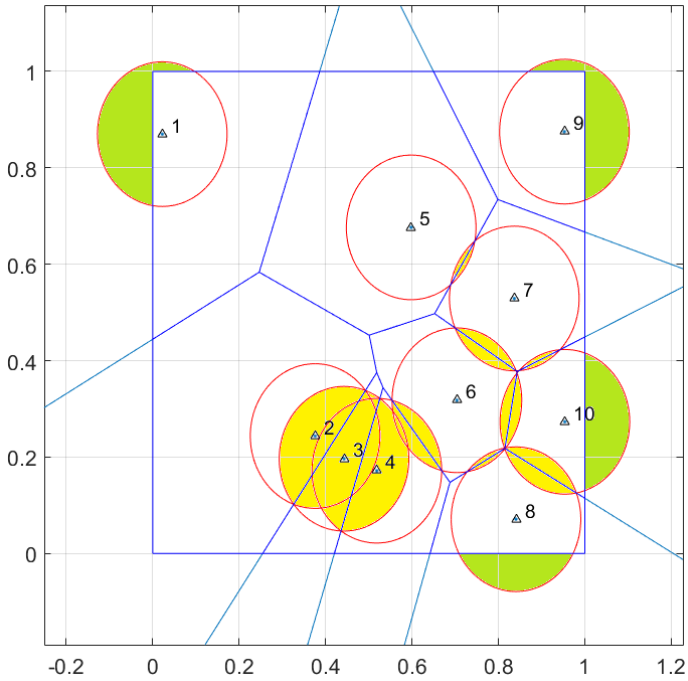


Figure 3.5: Illustration of the overlapping areas among neighboring BSs and the exurban areas of outer-tier cells in topology 1 of the PPP distributed cellular network. Shown in green color and yellow color are the exurban areas and overlapping areas respectively.

$$\bar{A}_s^s = \frac{1}{M} \sum_{j=1}^{M} A_s^s(j). \tag{3.15}$$

Moreover, the average system unavailability $\bar{U}_s^s$ is given by,

$$\bar{U}_s^s = 1 - \bar{A}_s^s. \tag{3.16}$$

The goal of achieving URC in the space domain is to diminish cell and system unavailability to a sufficiently low level.

## 3.5 Guaranteed Availability

Even though a high level of availability is expected for applications such as mission critical applications, safety applications so on, there is no guarantee that it can be obtained in a network everywhere. The average availability itself does not provide a complete view regarding the obtained availability from the system's point of view. Network operators may additionally be interested in obtaining the probability of achieving a given level of availability. In this section, we introduce another dependability measure of guaranteed availability of a network using a stochastic approach. The importance of this measure is that, it could expresses the probability of providing a predetermined or guaranteed level of availability [72].

### 3.5.1 The normalized size of a PV polygon: A stochastic view

There is no standard closed form expression provided for the average area of a Voronoi cell in the literature. Instead of obtaining an explicit expression for $g(S)$, it is more convenient to use a general $f_Y(y)$ distribution function to express the normalized cell sizes $y = S/\bar{S}$, where $S$ is the area of Voronoi cell and $\bar{S} = \frac{1}{N}\sum_{i=1}^{N} S(i)$. In other words, $\bar{S}$ denotes the average size of a PV cell. Rewriting, the PDF of a *normalized* PV cell area $y$ in a two-dimensional space as [68],

$$f_Y(y) = \frac{343}{15}\sqrt{\frac{7}{2\pi}}y^{2.5}exp\left(-3.5y\right). \tag{3.17}$$

Furthermore, from the CDF of Eq. (3.17), which is given by Eq. (3.18), we can obtain the probability that the normalized Voronoi cell area $y$ is smaller than or equal to a value $c$ and it is given by Eq. (3.19).

$$F_Y(y) = P(Y \leq y) = \int_0^y f_Y(u)\ du. \tag{3.18}$$

$$P\left(y \leq c\right) = \int_0^c f_Y\left(y\right) dy. \tag{3.19}$$

According to the simulations done in [68], the PV cells normalized area distribution function in two dimension can be illustrated as in Fig. 3.6. Empty circles are simulation results which fits into a Gamma distribution and the point-dashed line is the corresponding CDF.

### 3.5.2 Guaranteed cell availability

As defined in Eq. (3.3), the cell availability equals to one when the cell size is smaller than or equal to the covered area of the BS. Accordingly, Eq. (3.19) is equivalent to the probability that $A_s^c = 1$ given that the value $c$, i.e., the upper limit of the integral, is equal to the normalized covered area of the BS covering that cell. Mathematically, it is expressed as

$$P\left(A_s^c = 1\right) \equiv P\left(c \geq y\right) = \int_0^c f_Y\left(y\right) dy. \tag{3.20}$$

Note that availability equals to one implies that full connectivity is obtained everywhere in the cell, indicating that URC can be achieved in this cell in the space domain.

Let us now target at a general guaranteed cell availability level of $\beta$ where $(0 < \beta < 1)$. Then the probability for providing a guaranteed availability level greater than or equal to $\beta$ by the cell is given by,

$$P\left(A_s^c \geq \beta\right) \equiv P(y \leq y_i) = \int_0^{y_i} f_Y\left(y\right) dy \tag{3.21}$$

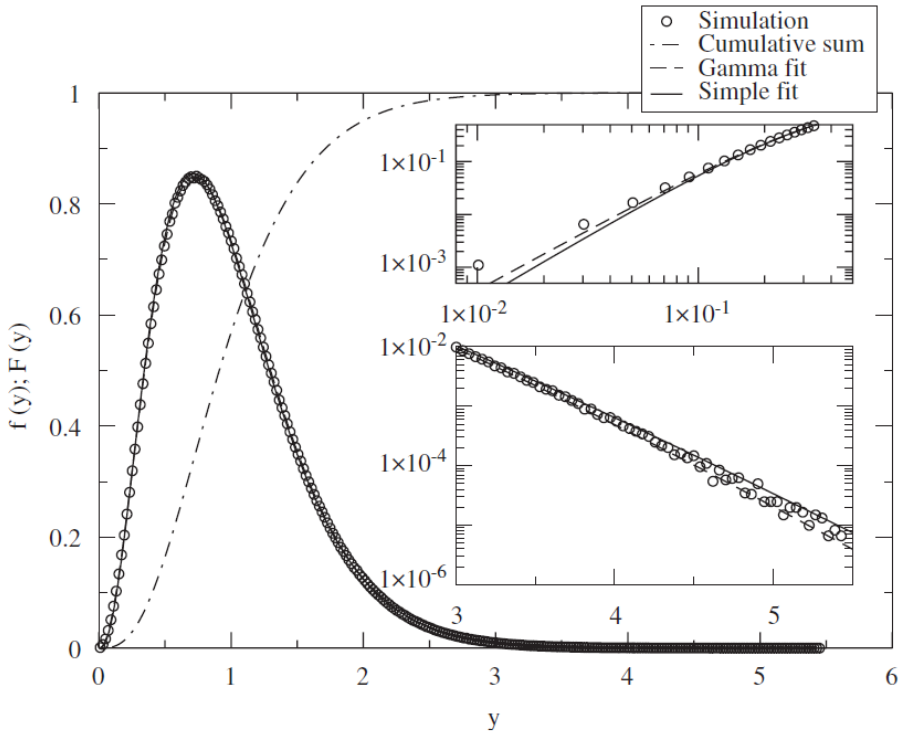


Figure 3.6: The Voronoi cells normalized area-distribution function in 2D [68].

where $y_i = MCA/(\bar{S}\beta)$ is the corresponding *normalized cell area*.

This can be explained elaborately, using the following example with reference to the topology 1 of the system as shown in Fig. 3.3. The cell areas calculated using the Shoelace formula is as , $S(1) = 0.1489\ km^2$, $S(2) = 0.2163\ km^2$, $S(3) = 0.0354\ km^2$, $S(4) = 0.054\ km^2$, $S(5) = 0.2094\ km^2$, $S(6) = 0.0733\ km^2$, $S(7) = 0.0828\ km^2$, $S(8) = 0.0575\ km^2$, $S(9) = 0.08\ km^2$ and $S(10) = 0.0423\ km^2$.

Then, we can find $\bar{S}$ as,

$$\bar{S} = \frac{\sum_{i=1}^{10} S(i)}{10} = 0.1\ km^2 \tag{3.22}$$

Normalized cell area $y$ for each cell is calculated using Eq. (3.23), and $y(1) = 1.4891$, $y(2) = 2.1631$, $y(3) = 0.3542$, $y(4) = 0.5404$, $y(5) = 2.0938$, $y(6) = 0.7328$, $y(7) = 0.8282$, $y(8) = 0.5746$, $y(9) = 0.8003$ and $y(10) = 0.4234$.

$$y(i) = \frac{S(i)}{\bar{S}} \tag{3.23}$$

Therein, the general distribution function to express the normalized cell sizes $y = S/\bar{S}$, is given by Eq. (3.17).

Let us now assume that a particular cell in the system, which is chosen randomly, is required to provide a guaranteed availability, $\beta = 0.9$. If we limit the BS's transmission power to a pre-determined value, i.e. assume the BS coverage is governed by $R = 0.15\ km$, we can find the normalized cell area that the cell in interest should occupy, when $\beta = 0.9$,

$$y(i) = \frac{MCA}{\bar{S}\ \beta},$$

$$MCA = \pi * R^2 = \pi * 0.15^2\ km^2,$$

$$y(i) = \frac{\pi * 0.15^2\ km^2}{0.1\ km^2 \times 0.9} = 0.785.$$

From Eq. (3.21) and the CDF plotted in Fig. 3.6, we know that,

$$P\left(A_s^c \geq 0.9\right) \equiv P(y \leq 0.785) = \int_0^{0.785} f_y\left(y\right) dy \approx 0.44.$$

## 3.6 Space Domain Availability in a PV Network

In the previous sections, we introduced the definitions and the terminologies which we propose in order to analyze the space domain availability of any cellular network. In this section, we explain how those preliminaries can applied to evaluate the space domain availability in a PV network.

### 3.6.1 Generating Voronoi diagram

Given a set of random seeds or centers, a Voronoi diagram for the two-dimensional case, was sketched using the the perpendicular bisectors method [73], [74]. Starting from a given center ($C_0$), the nearest neighboring seed ($C_1$) to it, was detected. Then the perpendicular bisector on the $C_0C_1$ line was created which formed the first edge of the Voronoi polygon corresponding to $C_0$. Then the second nearest neighboring seed ($C_2$) was detected and the perpendicular bisector on $C_0C_2$ became the second edge of the Voronoi polygon. This algorithm was continued with the third ($C_3$), fourth ($C_4$),. . . nearest seeds, until the perpendicular bisectors on $C_0C_3, C_0C_4$,.. . . created a closed polygon which does not change after considering any more distant points. Repeating the above algorithm for all centers in the considered system generated the Voronoi tessellation of the whole system.

### 3.6.2 Size of a Voronoi polygon: A deterministic expression

To deterministically compute the areas of each Voronoi polygon in a PVT, the well-known shoelace formula can be adopted. It is a mathematical algorithm to calculate the area of a simple two-dimensional polygon whose vertices are represented by ordered pairs in the plane [75]. Let $(x_l, y_l)$ be the coordinates of vertex $l$, $v$ be the number of edges of the Voronoi polygon, and $S$ be the area of the polygon. Then the formula to calculate the area of the Voronoi polygon is expressed as,

$$S = \frac{1}{2}\left|\sum_{l=1}^{v-1} x_l y_{l+1} + x_v y_1 - \sum_{l=1}^{v-1} x_{l+1} y_l - x_1 y_v\right|. \tag{3.24}$$

The individual cell areas are calculated from Eq. (3.24) and they are used to compute the cell and system availability metrics defined in Sec. 3.3 and Sec. 3.4 by replacing $S$ with $S(i,j)$ for cell $i$ under topology $j$.

### 3.6.3 Cell and system availability for HomNets

The cell availability for SCST scenario was simulated using Alg. 1 as shown below. Simulations were carried out for the cell number 6 in Fig. 3.7 which is considered as the reference cell (RC) in this study. The outbound coverage area is the BS coverage which extends beyond the boundaries of the cell in interest as highlighted (in yellow color) in Fig. 3.8.

**Algorithm 1: Algorithm to estimate the cell availability for SCST.**

**Input:** $x_B, y_B$ : Cartesian coordinates of the BS
**Input:** $R$ : Radius of the BS coverage
**Output:** $A_s^c(i,j)$ : Cell availability of the corresponding BS $i$ under the $j_{th}$ topology
[1] Calculate $C(i,j) = \pi R^2$
[2] Generate the Voronoi diagram using $(x_B, y_B)$ pairs
[3] Find the vertices of the cell, $(x_l, y_l)$ of the Voronoi diagram
[4] Input $(x_l, y_l)$ pairs to calculate the cell area $S(i,j)$ using the Shoelace formula Eq. (3.24)
[5] Calculate $C_{out}(i,j)$, i.e., exurban coverage area
[6] **if** $C(i,j) - C_{out}(i,j) \leq S(i,j)$ **then**
[7] $\quad A_s^c(i,j) = \frac{C(i,j) - C_{out}(i,j)}{S(i,j)}$
[8] **else**
[9] $\quad A_s^c(i,j) = 1$
[10] **end**

Fig. 3.9 illustrates the obtained $U_s^c(i,j)$ variation for the RC as the BS coverage, i.e., $\pi R^2$ increases. It is observed that smaller the BS coverage is, higher the unavailability turns. BS coverage is dependent on the transmission power level. Thus, we can also state that the unavailability decreases monotonically to a substantially low level, as the transmission power of the BS increases. By providing favorable conditions and sufficiently large transmission power to the BS, cell unavailability can be reduced to zero, implying that all the users residing in the RC are connected to the network through the coverage of the serving BS. Also, attaining

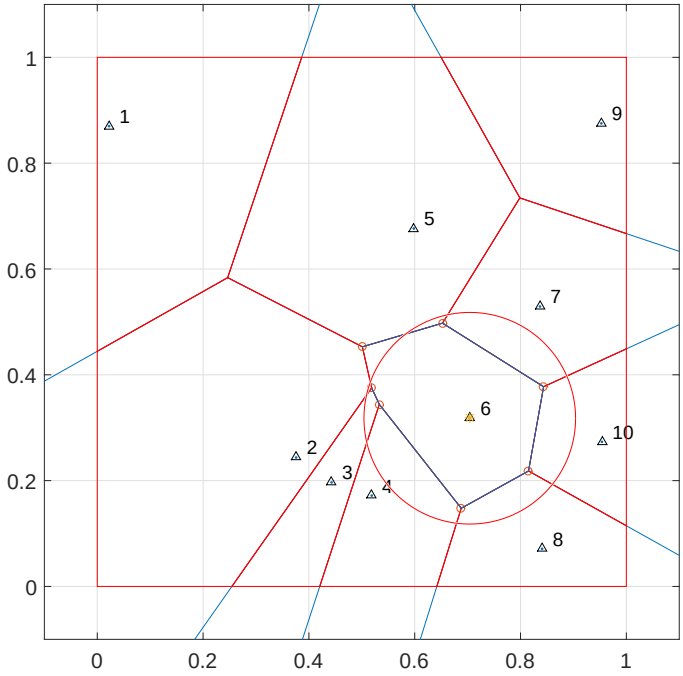


Figure 3.7: Illustration of the RC ($i = 6$) in topology 1 of the PPP distributed cellular network.

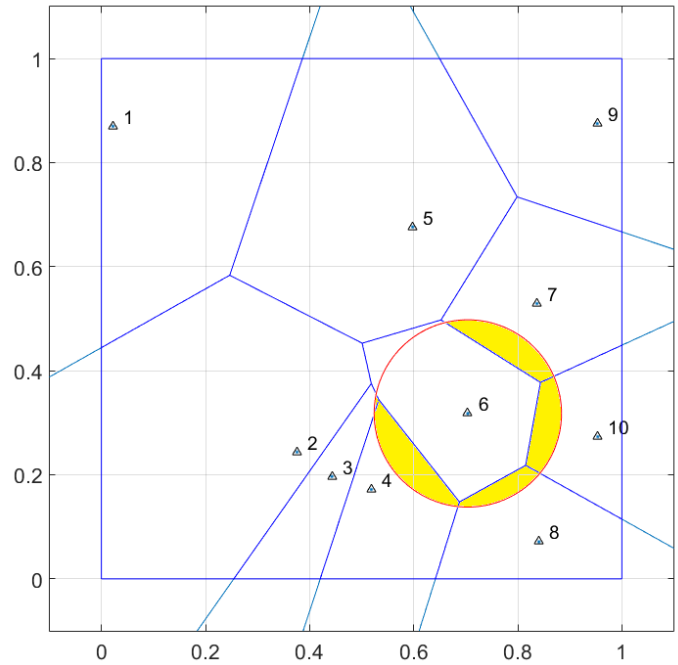


Figure 3.8: Illustration of the outbound coverage area of the RC ($i = 6$) in topology 1 of the PPP distributed cellular network.

cell unavailability closer to zero means achieving URC within the cell.

To further investigate cell unavailability, we deploy $M = 5$ different topologies for the same PV network with $N = 10$ cells but still select the cell in the center of the network topology as the RC as shown in Fig. 3.7. The algorithm presented in Alg. 2 is used to run the simulations for SCMT scenario.

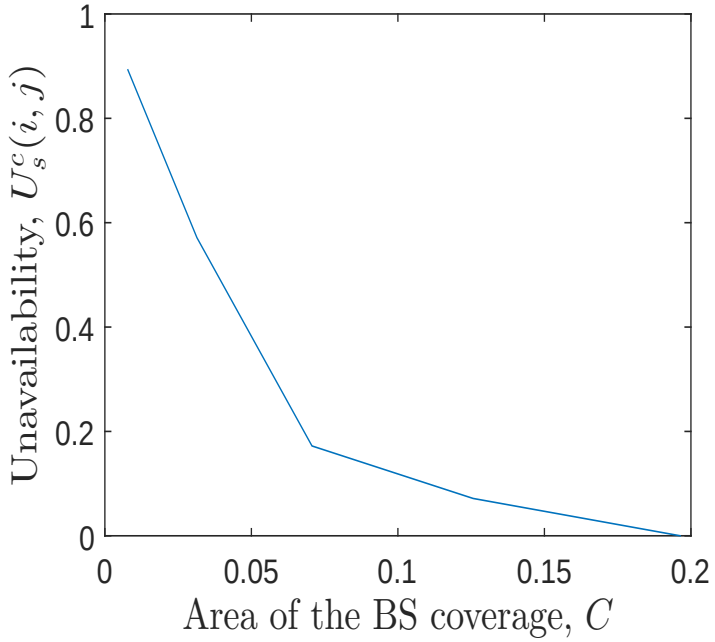


Figure 3.9: SCST cell unavailability of the RC ($i = 6$) for topology $j = 1$ as BS the coverage increases.

**Algorithm 2: Algorithm to estimate the cell availability for SCMT.**

**Input:** $M$ : Number of topologies
**Input:** $x_B(i,j), y_B(i,j)$ : Cartesian coordinates of the BS of the $j^{th}$ topology
**Input:** $R$ : Radius of the BS coverage
**Output:** $A_s^c(i,:)$ : The average availability of the cell in interest considering $M$ topologies
**[1]** **for** *j=1:M* **do**
**[2]** | Run Alg. 1 to find $A_s^c(i,j)$
**[3]** **end**
**[4]** $A_s^c(i,:) = \frac{1}{M}\sum_{j=1}^{M} A_s^c(i,j)$

Fig. 3.10 illustrates the individual cell unavailability behavior for the RC under each topology in colored (dashed) plots (obtained based on Eq. (3.3) under SCST scenario) and averaged over 5 topologies in blue (solid with triangle marks) line (obtained based on the defined $A_s^c(i,:)$ in Eq. (3.5) under SCMT scenario). It is evident that the relationship between the cell unavailability and the BS coverage agrees with what is observed in Fig. 3.9. When the BS coverage area increases, a large portion of the PV cell can be covered. Therefore, the availability of the cell increases. The gap between the cell availability curves related to each topology are governed by the randomness of each deployment. As a consequence, higher unavailability is entailed where RC occupies a larger cell area in the respective topology where as lower unavailability is observed where RC occupies a smaller cell area. This result implies also that it may not be beneficial to deploy the same type of cells in a PV network where a mix of small-sized and large-sized cells are placed if URC is required.

Shown among the plots is the average unavailability of the different topologies. This

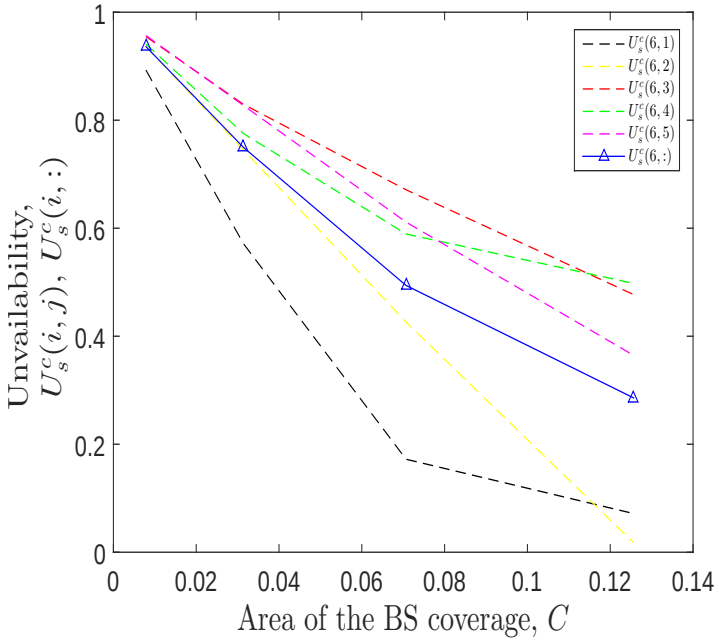


Figure 3.10: SCST and SCMT cell unavailability of the RC $i = 6$ for $M = 5$ topologies as the BS coverage increases.

Table 3.1: Comparison of SCST and SCMT cell availability

| R(km) | 0.05 | 0.1 | 0.15 | 0.2 |
|---|---|---|---|---|
| $A_s^c(6,1)$ | 0.1072 | 0.4287 | 0.8278 | 0.9284 |
| $A_s^c(6,2)$ | 0.0638 | 0.2546 | 0.5071 | 0.7610 |
| $A_s^c(6,3)$ | 0.0452 | 0.1706 | 0.3288 | 0.5230 |
| $A_s^c(6,4)$ | 0.0590 | 0.2248 | 0.4107 | 0.5022 |
| $A_s^c(6,5)$ | 0.0432 | 0.1728 | 0.3887 | 0.6355 |
| $A_s^c(6,:)$ | 0.0637 | 0.2503 | 0.4926 | 0.6700 |

provides overall and general insight about the cell unavailability variation without any attachment to a specific topology deployment. Although this also depicts a similar trend with gradually decreasing unavailability with the increasing BS coverage, it is worth to get the general behavior of any randomly selected cell in any deployment scenario.

Tab. 3.1 shows the numerical results obtained for above illustrated network topologies. Note that $A_s^c(6,j)$ and $A_s^c(6,:)$ are obtained via Eq. (3.3) and Eq. (3.5) respectively. The cell of interest is cell number $i = 6$ and there are $M = 5$ topologies, i.e., $j = 1, 2, 3, 4, 5$.

In MCST and MCMT scenarios we need to include all cells in the studied network. Since we consider the whole network for defining average cell availability or the system availability, we may deploy either the same type of cells (i.e., HomNets) or two types of cells (i.e., HetNets). For the HetNet scenario, the threshold to distinguish a cell as a T1 or T2 cell is configured as $\eta = 0.085$ unit$^2$ as described in Sec. 3.1.1. The radius of the BS coverage for

a T1 or T2 cell varies as $R_1 = 0.1 \sim 0.16$ or $R_2 = 0.1 \sim 0.2$ unit respectively. These units would represent kilometers in real-life scenarios, since the average cell size can vary between one to few *kilometers*.

Alg. 3 proposes the algorithm which was used to carry out the MATLAB simulations for MCST scenario and Alg. 4 proposes the algorithm for average cell availability in MCMT scenario. Algorithms for calculating system availability are depicted in Alg. 5 and Alg. 6 for ST scenario and MT scenario respectively.

**Algorithm 3: Algorithm to estimate the cell availability for MCST in HomNets.**

**Input:** $x_B, y_B$ : Cartesian coordinates of the BS
**Input:** $N$ : Number of cells in the topology
**Input:** $R$ : Radius of the BS coverage
**Output:** $A_s^c(:, j)$ : The average availability of any cell in the topology j

**for** *i=1:N* **do**
  Run Alg. 1 to find $A_s^c(i, j)$
**end**
Calculate $A_s^c(:, j) = \frac{1}{N} \sum_{i=1}^{N} A_s^c(i, j)$

**Algorithm 4: Algorithm to estimate the cell availability for MCMT in HomNets.**

**Input:** $x_B, y_B$ : Cartesian coordinates of the BS
**Input:** $N$ : Number of cells in the topology
**Input:** $M$ : Number of topologies
**Input:** $R$ : Radius of the BS coverage
**Output:** $\bar{A}_s^c$ : The average availability of any cell in any given topology

**for** *i=1:N* **do**
  Run Alg. 1 to find $A_s^c(i, j)$
**end**
$\bar{A}_s^c = \frac{1}{M} \sum_{j=1}^{M} \left( \frac{1}{N} \sum_{i=1}^{N} A_s^c(i, j) \right)$

**Algorithm 5: Algorithm to estimate the system availability for ST in HomNets.**

**Input:** $x_B, y_B$ : Cartesian coordinates of the BS
**Input:** $N$ : Number of cells in the topology
**Input:** $R$ : Radius of the BS coverage
**Output:** $A_s^s(j)$ : System availability of topology $j$

Generate the Voronoi diagram using $(x_B, y_B)$ pairs
Find the vertices of the cell, $x_l, y_l$ of the Voronoi diagram
Input $(x_l, y_l)$ pairs to calculate the area of each cell $S(i, j)$ for each topology using Eq. (3.24)
Calculate the total exurban BS coverage outside the unit square region $C_{exurban}(j)$ for each topology
Calculate the total overlaps between BS coverages $C_{overlap}(j)$ for each topology
Calculate $C_{tot}(j) = N \times \pi R^2 - C_{exurban}(j) - C_{overlap}(j)$
**if** $C_{tot}(j) \leq \sum_{i=1}^{N} S(i, j)$ **then**
  $A_s^s(j) = \frac{C_{tot}(j)}{\sum_{i=1}^{N} S(i,j)}$
**else**
  $A_s^s(j) = 1$
**end**

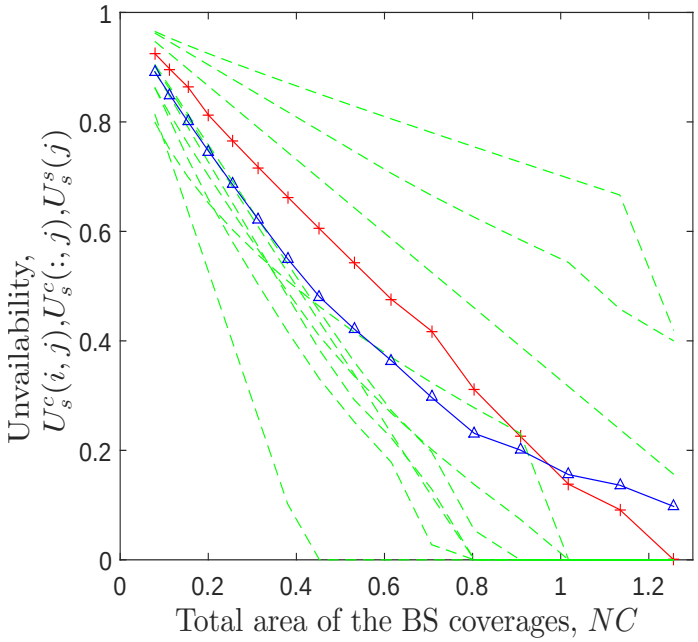


Figure 3.11: SCST, MCST cell and ST system unavailability in a HomNet with N = 10 cells for topology $j = 1$.

Fig. 3.11 depicts the change of unavailability with the change of coverage of BS for the HomNet scenario considering topology 1 cell deployment. The plots shown in green (dashed) are the unavailability of individual cells and the average cell unavailability is shown in blue (solid with triangle marks) plot. The average of the individual cell availabilities of the 10 cells has been calculated as the average unavailability for MCST scenario. The system unavailability is plotted in red (solid with plus marks) as the BS coverage increases. The illustrated system unavailability is falling under the ST scenario since it is calculated solely for topology 1.

When the coverages of the BSs are at its minimum the unavailability of the system is the highest, because most probably a user could fall inside the uncovered area. Increasing the radius of the BS coverage will obviously reduce the system unavailability of the whole circular system but as shown from the plot many cells reach the zero unavailability before the average unavailability reaches there. While cells which occupies a larger geographical area, need a higher transmit power to reduce the high levels of unavailability, smaller cells require comparably low transmit power to reach the same level of unavailability. This implies that URC can be achieved by increasing the transmit power of the BSs and thereby increasing the BS coverages. Because of the diversity of cell sizes in a PV network, it is not necessary and meaningful to uplift the radius of the coverage or the transmit power for the whole system simultaneously. Therein, we perceive the need of deploying HetNets. Thus, it is appreciable to analyze the unavailability for HetNets.

Tab. 3.2 shows the numerical results obtained for above illustrated network topologies,

Table 3.2: Comparison of MCST and MCMT cell availability for $N = 10$ cells and $M = 5$ topologies

| R(km) | 0.05 | 0.1 | 0.15 | 0.2 |
|---|---|---|---|---|
| $A_s^c(:,1)$ | 0.1085 | 0.3789 | 0.7031 | 0.9025 |
| $A_s^c(:,2)$ | 0.0980 | 0.3605 | 0.6651 | 0.9170 |
| $A_s^c(:,3)$ | 0.1008 | 0.3625 | 0.7376 | 0.8736 |
| $A_s^c(:,4)$ | 0.1301 | 0.4341 | 0.6992 | 0.8959 |
| $A_s^c(:,5)$ | 0.0961 | 0.3892 | 0.7141 | 0.9139 |
| $\bar{A}_s^c$ | 0.1067 | 0.3850 | 0.7038 | 0.5386 |

i.e. $N = 10$ cells in a system and $M = 5$ topologies. Note that $A_s^c(:,j)$ and $\bar{A}_s^c$ are obtained via Eq. (3.7) and Eq. (3.11) respectively.

To obtain more general definitions, it is worth to analyze multiple topology scenarios and take the averages. Thus, availability of HomNet was also evaluated for cell availability in MCMT scenario and system availability considering MT scenario. The algorithm used to evaluate the system availability under $M$ topologies is given in Alg. 6.

**Algorithm 6: Algorithm to estimate the system availability for MT in HomNets.**

**Input:** $x_B, y_B$ : Cartesian coordinates of the BS
**Input:** $N$ : Number of cells in the topology
**Input:** $M$ : Number of topologies
**Input:** $R$ : Radius of the BS coverage
**Output:** $\bar{A}_s^s$ : Average system availability
**[1]** **for** *j=1:M* **do**
**[2]** | Run Alg. 5 to find $A_s^s(j)$
**[3]** **end**
**[4]** Calculate $\bar{A}_s^s = \frac{1}{M}\sum_{j=1}^{M} A_s^c(j)$

As illustrated in Fig. 3.12, green (dashed) curves are the SCMT cell unavailability variations for individual cells with the total BS coverage of the system. Blue (solid with triangle marks) plot indicates the MCMT average cell unavailability of 10 cells over 5 topologies. It also follows the same trend as in SCST ans SCMT scenarios but provides a more realistic analysis of the average cell availability. The average system unavailability behavior for $M = 5$ topologies can be observed by the red (solid with plus marks) curve which shows a approximate linear relationship with the coverage radius. But it should be noted that this curve does not reflect the 100% accurate variation of the system unavailability, since we had to ignore the coverage area overlapping of more than 3 coverage areas due to calculation complexity. Same applies to the system unavailability calculations in ST scenario as well.

Tab. 3.3 shows the numerical results obtained for the above illustrated network topologies. Note that $A_s^s(j)$ and $\bar{A}_s^s$ are obtained via Eq. (3.13) and Eq. (3.15) respectively. The system of interest consists of $N = 10$ cells and there are M = 5 topologies.

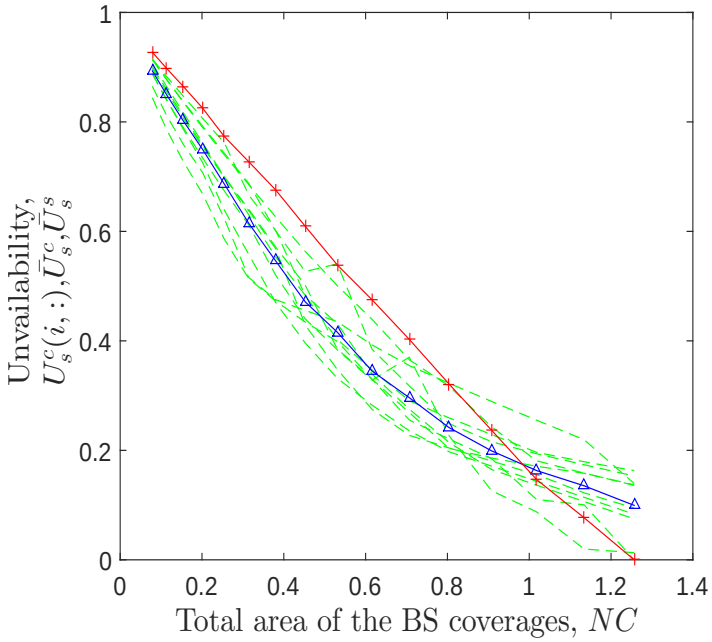


Figure 3.12: SCMT, MCMT cell and MT system unavailability in a HomNet with $N = 10$ cells for $M = 5$ topologies.

Table 3.3: Comparison of ST and MT system availability

| R(km) | 0.05 | 0.1 | 0.15 | 0.2 |
|---|---|---|---|---|
| $A_s^s(1)$ | 0.0751 | 0.2833 | 0.5820 | 1.0000 |
| $A_s^s(2)$ | 0.0758 | 0.2770 | 0.5748 | 1.0000 |
| $A_s^s(3)$ | 0.0729 | 0.2591 | 0.6324 | 1.0000 |
| $A_s^s(4)$ | 0.0725 | 0.2721 | 0.6156 | 1.0000 |
| $A_s^s(5)$ | 0.0670 | 0.2714 | 0.5973 | 1.0000 |
| $\bar{A}_s^s$ | 0.0727 | 0.2726 | 0.5908 | 1.0000 |

### 3.6.4 Cell and system availability for HetNets

Now we convert the same PV network into a HetNet with $N = 10$ cells, where there are 7 T1 cells and 3 T2 cells with $\eta = 0.085$. Algorithms for calculating MCST average cell availability, ST system availability are depicted in Alg. 7 and Alg. 8 respectively.

Fig. 3.13 illustrates how the cell unavailability and system unavailability vary for a HetNet considering a MCST scenario. Illustrated by the green (dashed) curve is the individual cell unavailability, in blue (solid with triangle marks) curve is the average cell unavailability and the system unavailability shown in red (solid with plus marks) lines as the BS coverage increases, for the HetNet scenario.

**Algorithm 7: Algorithm to estimate the cell availability for MCST in HetNets.**

**Input:** $x_B, y_B$ : Cartesian coordinates of the BS
**Input:** $N$ : Number of cells in the topology
**Input:** $\eta$ : Cell area threshold
**Input:** $R_1$ : Radius of the coverage of a T1 cell
**Input:** $R_2$ : Radius of the coverage of a T2 cell
**Output:** $A_s^c(:, j)$ : The average cell availability of any cell in the topology $j$

[1] Generate the Voronoi diagram using $(x_B, y_B)$ pairs
[2] Find the vertices of the cell, $(x_l, y_l)$ from the Voronoi diagram
[3] Input $(x_l, y_l)$ pairs to calculate the cell area $S(i, j)$ using Eq. (3.24)
[4] **if** $(S(i, j)) \leq \eta$ **then**
[5] $\quad C(i, j) = \pi(R_1)^2$;
[6] $\quad$ **if** $(C(i, j)) \leq S(i, j)$ **then**
[7] $\quad\quad A_s^c(i, j) = \frac{C(i,j)}{S(i,j)}$;
[8] $\quad$ **else**
[9] $\quad\quad A_s^c(i, j) = 1$
[10] $\quad$ **end**
[11] **else**
[12] $\quad C(i, j) = \pi(R_2)^2$;
[13] $\quad$ **if** $(C(i, j)) \leq S(i, j)$ **then**
[14] $\quad\quad A_s^c(i, j) = \frac{C(i,j)}{S(i,j)}$;
[15] $\quad$ **else**
[16] $\quad\quad A_s^c(i, j) = 1$
[17] $\quad$ **end**
[18] **end**
[19] Calculate $A_s^c(:, j) = \frac{1}{N} \sum_{i=1}^{N} A_s^c(i, j)$

**Algorithm 8: Algorithm to estimate the system availability for ST in HetNets.**

**Input:** $xB, yB$ : x, y coordinates of the BS
**Input:** $N$ : Number of cells in the topology
**Input:** $\eta$ : Cell area threshold
**Input:** $R_1$ : Radius of the coverage of a T1 cell
**Input:** $R_2$ : Radius of the coverage of a T2 cell
**Output:** $A_s^s(j)$ : System availability of topology $j$

[1] Generate the Voronoi diagram using $(x_B, y_B)$ pairs
[2] Find the vertices of the cell, $x_l, y_l$ of the Voronoi diagram
[3] Input $(x_l, y_l)$ pairs to calculate the cell area $S(i, j)$ using Eq. (3.24)
[4] **if** $(S(i, j)) \leq \eta$ **then**
[5] $\quad C(i, j) = \pi(R_1)^2$
[6] **else**
[7] $\quad C(i, j) = \pi(R_2)^2$
[8] **end**
[9] Calculate the total BS coverage outside the unit square region $C_{exurban}(j)$
[10] Calculate the total overlaps between BS coverages $C_{overlap}(j)$
[11] Calculate $C_{tot}(j) = \sum_{i=1}^{N} C(i, j) - C_{exurban}(j) - C_{overlap}(j)$
[12] **if** $C_{tot}(j) \leq \sum_{i=1}^{N} S(i, j)$ **then**
[13] $\quad A_s^s(j) = \frac{C_{tot}(j)}{\sum_{i=1}^{N} S(i,j)}$
[14] **else**
[15] $\quad A_s^s(j) = 1$
[16] **end**

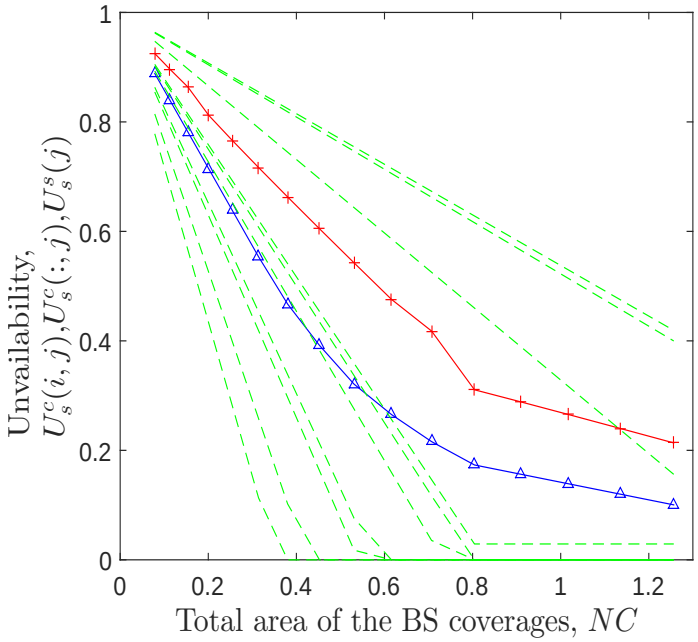


Figure 3.13: SCST, MCST cell and ST system unavailability in a HetNet with 3(7) T2(T1) cells for topology $j = 1$ .

### 3.6.5 Availability and transmission power tradeoff

Fig. 3.14 brings out a comparison of average cell unavailability (blue plots) and system unavailability (red plots) of HomNet and HetNet. Blue (solid with circle marks) curve and blue (solid with plus marks) curve illustrate the average cell unavailability of topology 1 for HomNet and HetNet respectively. Red (solid with circle marks) curve and red (solid with plus marks) curve illustrate the system unavailability of topology 1 for HomNet and HetNet respectively.

When compared with the average unavailability of HomNet (in which all cells have the same radius as $R_2$) with HetNet, we observe that unavailability of the HetNet is higher for the coverage area defined for the T2 cells. This is because the coverage of those T1 cells is lower than that of the T2 cells. This is reasonable since received power is inversely proportional to the distance between the transmitter and the receiver, according to the radio propagation model in the free space. Although this is not favorable from the mobile user's perspective, service provider can compensate the tradeoff via the reduced transmission power levels obtained after the introduction of micro cells (T1 cells).

To study the tradeoff between system availability and transmission power, we calculate and compare the total BS transmission power in the HomNet versus in the HetNet. For illustration simplicity, the free space propagation model is adopted in our calculation, i.e.,

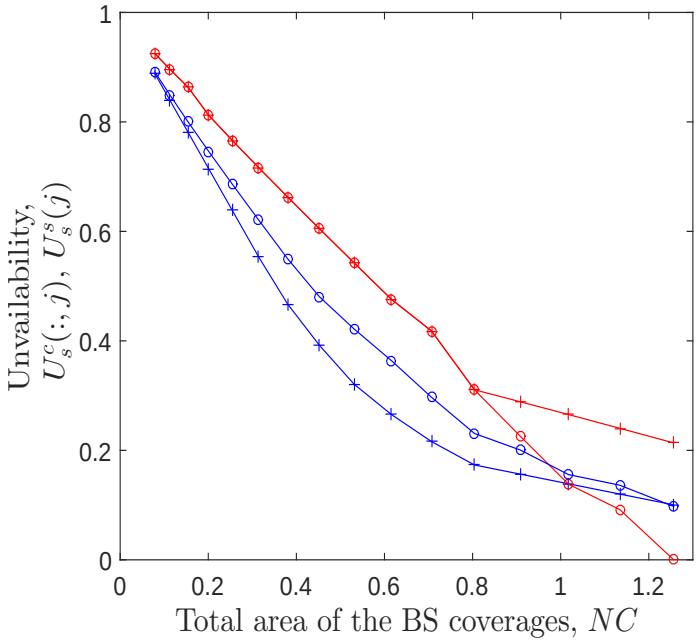


Figure 3.14: Comparison of MCST cell/ST system unavailability in a HomNet with $N = 10$ cells and HetNet with 3(7) T2(T1) cells for topology $j = 1$ .

$$P_R(d) = \frac{P_T G_T G_R \lambda^2}{(4\pi)^2 d^\alpha L} \tag{3.25}$$

where, $P_R(d)$ is the reception power at the UE which is $d$ distance away from the BS, $P_T$ is the transmission power, $G_T$ and $G_R$ are the antenna gains of the transmitter and the receiver respectively, $\lambda$ is the wavelength in meters, $\alpha$ is the path loss coefficient, and $L$ is the system loss factor. Assume that $G_t = G_r = 1$, $\alpha = 2.5$, $L = 1$, and $\lambda = 15$ cm. Configure $P_R(R) = 0.1$ $\mu$W as the required $P_R$ for a UE which is located at the boundary of the BS coverage, with radius $R$. Consider the $N = 10$ cell network shown in Fig. 3.1.

Tab. 3.4 illustrates the numerical results on the obtained system availability and the total (i.e., for 10 cells together) required transmission power for both HomNet and HetNet. Keep the same threshold as $\eta = 0.085$ km$^2$. There are respectively 7 T1 cells (with coverage radius $R_1$) and 3 T2 cells (with coverage radius $R_2$) in the HetNet case. In the HomNet case, all 10 cells are homogeneous with coverage radius $R_2$.

With four different combinations of cell coverage for T1 (with radius $R_1$) and T2 (with radius $R_2$) cells, we illustrate the tradeoff between system availability and total transmission power. For instance, the last row tells us that to increase the system availability from $A_s^s(1) = 63.48\%$ (obtained by the HetNet) to $A_s^s(1) = 100\%$ (obtained by the HomNet) which indicates that URC is supported, a 70% higher power level is required.

Table 3.4: The tradeoff between availability and transmission power

| $R_1$ (km) | $R_2$ (km) | HetNet | | HomNet | |
|---|---|---|---|---|---|
| | | $A_s^s(1)$ | Total $P_T$ (W) | $A_s^s(1)$ | Total $P_T$ (W) |
| 0.11 | 0.17 | 0.4395 | 1416.85 | 0.7739 | 2644.60 |
| 0.11 | 0.20 | 0.5030 | 1814.53 | 1.0000 | 3970.20 |
| 0.14 | 0.17 | 0.5736 | 1932.72 | 0.7739 | 2644.60 |
| 0.14 | 0.20 | 0.6348 | 2330.40 | 1.0000 | 3970.20 |

It can be seen that the required transmission power is much lower in a HetNet compared to a HomNet although the availability is higher. This is an advantage in the service provider's eye, eventhough the mobile user might suffer from lack of connectivity in certain occasions.

### 3.6.6 Guaranteed cell availability

The algorithm which has been followed to analyze the guaranteed cell availability is given below by Alg. 9.

**Algorithm 9: Algorithm to estimate the guaranteed cell availability.**

**Input:** $x_B, y_B$ : x, y coordinates of the BS
**Input:** $N$ : Number of cells in the topology
**Input:** $\beta$ : Required availability level
**Input:** $R$ : Radius of the BS coverage
**Output:** $P\left(A_s^c \geq \beta\right)$ : The guaranteed cell availability corresponding to the BS at $(x_B, y_B)$

**[1]** Generate the Voronoi diagram using $(x_B, y_B)$ pairs
**[2]** Find the vertices of the cell, $x_l, y_l$ of the Voronoi diagram
**[3]** Input $(x_l, y_l)$ pairs to calculate the cell area $S(i,j)$ using Eq. (3.24)
**[4]** Calculate $\bar{S} = \frac{\sum_{i=1}^{N} S(i,j)}{N}$
**[5]** Calculate $C = \pi(R)^2$
**[6]** Calculate $y = \frac{C}{\beta \bar{S}}$
**[7]** Calculate $P\left(A_s^c \geq \beta\right) = \int_0^y f_{2D}\left(y\right) dy$

Fig. 3.15 illustrates this probability for 2 cell radius values of a HomNet where the mean cell coverage is calculated as $MCA = \pi R^2$. To obtain the definite integral in Eq. (3.21), the CDF of the normalized cell areas derived in [68] is adopted. Evidently, the higher the required availability level, the lower the probability to achieve it. Meanwhile, a larger cell coverage would increase the probability for providing a guaranteed availability level for a particular cell which may in turn provide URC.

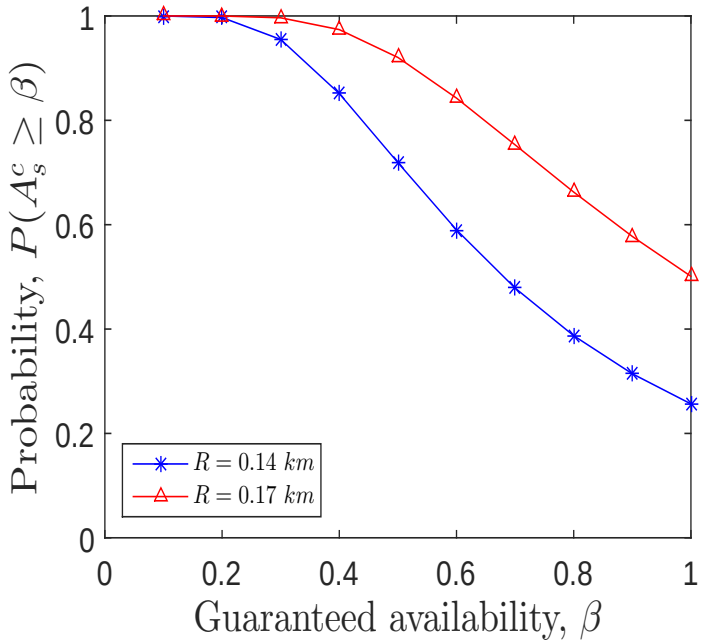


Figure 3.15: The probability for providing a guaranteed cell availability level.

## 3.7 Chapter Summary

This chapter discloses the study we carried out to obtain connectivity-based availability definitions assuming circular BS coverages. Firstly, the developed system model was introduced along with the different scenarios and assumptions considered. Then the cell availability definitions were explained for SCST, MCST, SCMT and MCMT cases and for HomNet and HetNet cell deployments. Similarly, system availability definitions were described for ST and MT for HomNets and ST HetNets. Followed by the cell and system availability, we also present a definition for guaranteed cell availability using a stochastic approach. Algorithms for all the scenarios are enclosed as well. A comparison was carried out in between HomNets and HetNets to evaluate the availability and transmission power tradeoff.

# Chapter 4

# SINR-based URC Concepts and Analysis

*In Chap. 3, we proposed a cellular system which is modeled using SG tools with an assumption on circular-shaped BS coverage for each cell. However, one may argue that this assumption might not be valid to characterize the real life cellular networks. Thus, in Chap. 4 we derive expressions for cell availability and system availability assuming that the BS coverage is affected by SINR, hence not certainly circular-shaped coverages.*

## 4.1 System Model

In this chapter we continue studying the previously introduced system model in Sec. 3.1 of Chap. 3, which is modeled as a PV network with $N$ cells. In contrast to the previous system model, our underlying assumptions are differed as follows.

- All BSs are formed based on homogeneous PPP of intensity $\lambda_B$ in the Euclidean plane.
- In each cell, one BS is deployed and one omni-directional antenna is mounted on each of them. However, SINR deterioration over distance has a significant impact on the coverage of each BS.
- Frequency re-use factor of the system is one. Therefore, the whole band of frequency used in a particular cell is reused in each of the adjacent cells.
- Same channel type and propagation conditions are considered.

## 4.2 SINR and Coverage

From rewriting the Eq. (2.13) after expanding the denominator and nominator we get,

$$SINR^{0,j} = \frac{P_T^{i,j} L_p^i u_g^i u_l^i G_R^i}{kT_{sys}\Delta f + \sum_{i=1}^{M} P_T^{i,j} L_p^i u_g^i u_l^i G_R^i}. \tag{4.1}$$

Followed by the assumption that the interference term $I^{0,j}$ in the denominator may be much higher than the noise term $N$, (especially since the frequency reuse factor of system is tight), we could assume that $N \approx 0$ and ignore the noise term in Eq. (2.13) for the ease of our analysis. This is sometimes also called as signal to interference ratio (SIR). Having the knowledge of SINR, we now advance to investigate the relationship between the SINR and the coverage of a cell or the whole system. Thereby, we can relate the spatial characteristics of a cellular network to SINR and derive expressions for availability.

We begin with the assumption, that $P_T^{i,j}, u_g^i, u_l^i, G_R^i$ are same for all the cells in the system. Therefore, we can rewrite Eq. (4.1) as follows.

$$SINR^{0,j} = \frac{L_p^i}{\sum_{i=1}^{M} L_p^i}. \tag{4.2}$$

Also, $L_p^i$ which is the propagation loss between the transmitter and the receiver for user, is given by,

$$L_p^i = \frac{\lambda^2}{(4\pi)^2 (d^i)^\alpha} \tag{4.3}$$

where, $d$ is the distance between the mobile user and the BS, $\lambda$ is the wavelength in meters and $\alpha$ is the path loss coefficient as introduced in Eq. (3.25). Substituting from Eq. (4.3) and using the assumption of unity frequency reuse factor, we get the mathematical expression which relates SINR and distance as in Eq. (4.4).

$$SINR^{0,j} = \frac{(d^i)^{-\alpha}}{\sum_{i=1}^{M} (d^i)^{-\alpha}}. \tag{4.4}$$

For the further clarification of the work documented in the rest of the chapter, we define the terminology of SINR threshold as below.

**SINR threshold:** is the minimum SINR that a UE should achieve in order to get a sufficient level of service from the BS.

By setting an appropriate SINR threshold, we can find the maximum allowable distance from the BS that a mobile user should fall within a cell. If a user fall inside the maximum allowable distance, we assume that a successful demodulation can be attained at the UE. This distance defines the maximum coverage area offered by a BS to meet a given required level of SINR.

## 4.3 SINR-based Cell Availability

Bringing forward the concept of the availability definition from the space domain as proposed in Eq. (3.2), we define the SINR-based cell availability as the area covered by the minimum SINR or the SINR threshold contour over the area of the cell of interest. Thus, we can express the SINR-based cell availability in the space domain, $A_s^c(i,j)$ as,

$$A_s^c(i,j) = \begin{cases} \frac{C_{SINR}(i,j)}{S(i,j)}, & \text{if } C_{SINR}(i,j) < S(i,j); \\ 1, & \text{otherwise.} \end{cases} \tag{4.5}$$

where, $C_{SINR}(i,j)$ and $S(i,j)$ denote area covered by the SINR threshold and area (or size) of the PV cell respectively for a randomly selected cell $i$ of topology $j$.

To provide coherent definitions as proposed in Sec. 3.3, we can further develop cell availability definitions for SCMT, MCST and MCMT scenarios.

## 4.4 SINR-based System Availability

System availability is the availability defined for the whole system considering the total area covered by the SINR threshold of each cell and the total area of the region considered which contains all the cells. Accordingly, we express the SINR-based system availability considering a particular topology $j$, $A_s^s(j)$ as,

$$A_s^s(j) = \begin{cases} \frac{\sum_{i=1}^{N} C_{SINR}(i,j) - \Delta}{\sum_{i=1}^{N} S(i,j)}, & \text{if } \sum_{i=1}^{N} C_{SINR}(i,j) - \Delta < \sum_{i=1}^{N} S(i,j); \\ 1, & \text{otherwise} \end{cases} \tag{4.6}$$

where, $\Delta$ represents the overlap between the contours defined by the SINR threshold among neighboring BSs and the area which belongs to an outer-tier cell but falls outside the region of interest. Furthermore, we can also define the SINR-based system availability by considering the MT scenario separately as in Sec. 3.4.

## 4.5 SINR Threshold Contours

According to the definitions proposed above, in order to analyze the SINR-based cell or system availability in the space domain, we have to estimate the coverage area of the SINR threshold contour. Alg. 10 shows the algorithm which is employed to create the SINR threshold contour in the MATLAB simulations. Unless otherwise stated, parameters are configured as $\alpha = 2.5, Th = 0.4 : 0.05 : 0.6, N = 10, M = 5$.

Fig. 4.1 and Fig. 4.2 illustrate how the contour for a comparably low and high SINR

**Algorithm 10: Algorithm to estimate the SINR threshold contour.**

**Input:** $x_B, y_B$ : Cartesian coordinates of the BS of the RC
**Input:** $N$ : Number of cells in the topology
**Input:** $Th$ : SINR threshold
**Input:** $\alpha$ : Path loss coefficient
**Output:** $x_p, y_p$ : Cartesian coordinates along the SINR threshold contour

```
[1]  for z = π/180 : π/180 : 2π do
[2]      d = 0.001      : d is the initial distance from the BS of the RC to any user
[3]      x_p(z) = x_B + d cos(z)
[4]      y_p(z) = y_B + d sin(z)
[5]      I(z) = 0      : I(z) is the interference at the point (x_p(z), y_p(z))
[6]      for i = 1 : N do
[7]          dist(z,i) = sqrt((x_p(z) − x_B(i))^2 + (y_p(z) − y_B(i))^2)      : dist(z,i) is the distance to the point
               (x_p(z), y_p(z)) from the i^th BS
[8]          I(z) = I(z) + dist(z,i)^−α
[9]      end
[10]     SINR(z) = d^−α / (I(z) − d^−α)
[11]     while SINR(z) ≥ Th do
[12]         d = d + 0.001;
[13]         x_p(z) = x_B + d cos(z)
[14]         y_p(z) = y_B + d sin(z)
[15]         for i = 1 : N do
[16]             dist(z,i) = sqrt((x_p(z) − x_B(i))^2 + (y_p(z) − y_B(i))^2)
[17]             I(z) = I(z) + dist(z,i)^−α
[18]         end
[19]         SINR(z) = d^−α / (I(z) − d^−α)
[20]     end
[21] end
```

thresholds are distributed spatially within the RC respectively. Fig. 4.1(a) (or Fig. 4.2(a)) presents the RC and its SINR threshold contour within the system of interest and Fig. 4.1(b) (or Fig. 4.2(b)) illustrates the zoomed-in view of the SINR threshold contour of the RC. As it is evident from Fig. 4.1 and Fig. 4.2, now the coverage of the BS can not be considered as circular, as we assumed in Chap. 3 even though omni-directional antennas are mounted on the BS.

When comparing Fig. 4.1 with Fig. 4.2 we observe that contour drawn for high SINR threshold is a smoother contour with less bounces along it. In contrast, the contour corresponding to the low SINR threshold is not smooth and takes a random shape. This can be explained, by focusing on the nominator and the denominator of the SINR expression given in Eq. (4.4).

A lower SINR threshold indicates that the UE can receive a lesser power from the BS thus, can locate remotely to the tagged BS. Meanwhile moving away from the tagged BS within the cell means the received power from the neighboring BSs or the interference becomes substantial with comparison to the received power from the tagged BS. By thorough examination of Fig. 4.1(a), we can identify that the contour is biased towards the tagged cell,

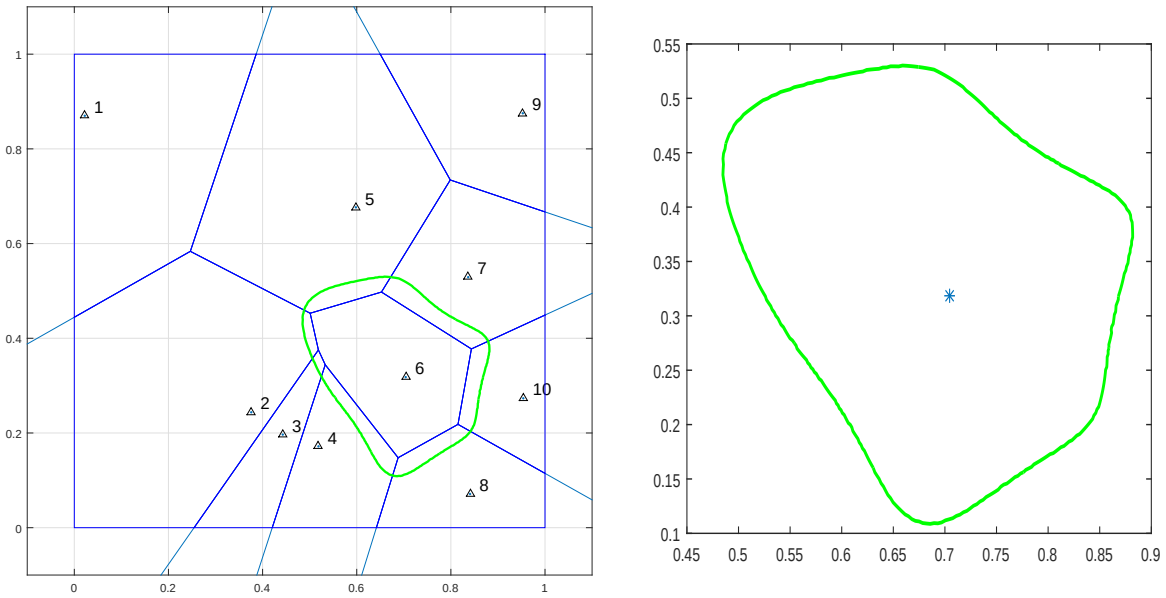


(a) The whole system (b) The RC alone

Figure 4.1: The coverage contour for a low SINR threshold.

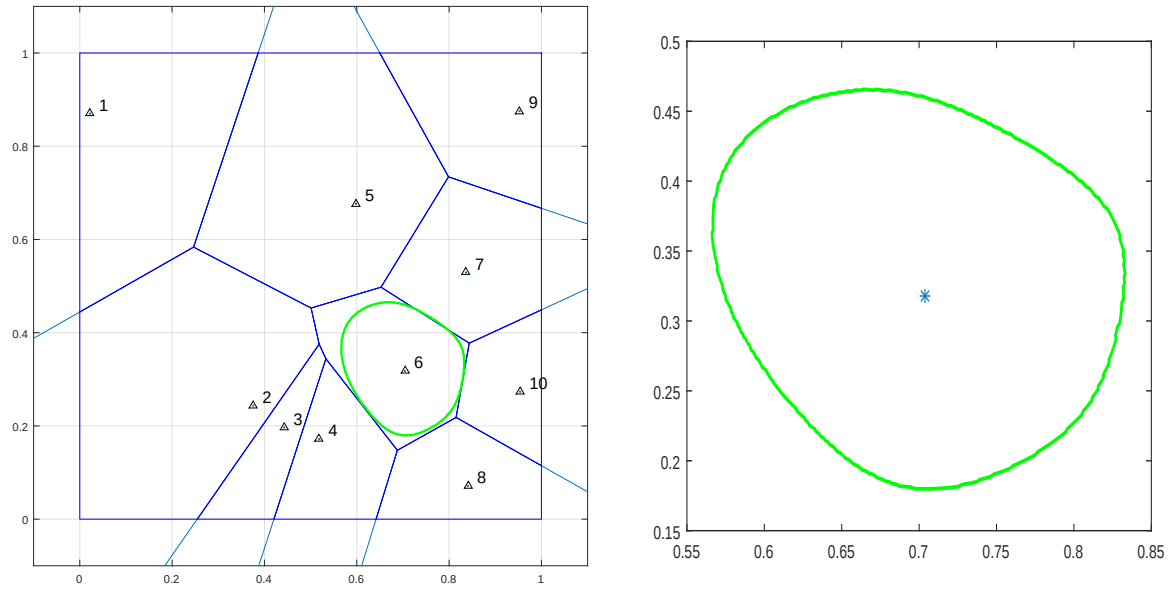


(a) The whole system (b) The RC alone

Figure 4.2: The coverage contour for a high SINR threshold.

i.e., cell number 6 in the where in the proximity of neighbor BSs and contour fold outwards where neighbor BSs are located much farther.

When a higher SINR threshold is set for the cell, UE should locate within the range where received power from the tagged BS is dominant over the interference from other BSs in the system. Since the effect from neighbor BSs are low in this case, the contour becomes much smoother and approximately recreates a circular coverage area as shown from Fig. 4.2(a).

## 4.6 SINR-based Cell Availability of a PV Network

The SINR-based cell availability for SCST scenario was simulated using the Alg. 11 as shown below. Simulations were carried out for cell number 6 in Fig. 3.7 which is considered as the RC in this study. The set of the Cartesian coordinates $(x_p, y_p)$ along the SINR threshold contour which is obtained from Alg. 10 is denoted as $S'$ when explaining the algorithms from here onwards.

**Algorithm 11: Algorithm to estimate the SCST cell availability for a given SINR threshold.**

**Input:** $x_B, y_B$ : Cartesian coordinates of the BS of the RC
**Input:** $N$ : Number of cells in the topology
**Input:** $Th$ : SINR threshold
**Input:** $\alpha$ : Path loss coefficient
**Output:** $A_s^c(i,j)$ : SINR-based cell availability of the corresponding BS $i$ of the topology $j$
**[1]** Run Alg. 10 and obtain the set of Cartesian coordinates along the SINR threshold contour $S'(i,j)$
**[2]** Input $S'(i,j)$ to calculate the coverage area defined by SINR threshold $C_{SINR}(i,j)$ using Eq. (3.24)
**[3]** Find the vertices of the cell, $(x_l, y_l)$ of the Voronoi diagram
**[4]** Input $(x_l, y_l)$ pairs to calculate the cell area $S(i,j)$ using Eq. (3.24)
**[5]** **if** $C_{SINR}(i,j) \leq S(i,j)$ **then**
**[6]** $\quad A_s^c(i,j) = \frac{C_{SINR}(i,j)}{S(i,j)}$
**[7]** **else**
**[8]** $\quad A_s^c(i,j) = 1$
**[9]** **end**

Fig. 4.3 illustrates the obtained $U_s^c(i,j)$ variation for RC as the estimated SINR threshold increases. It can be observed that unavailability increases with the increment of the SINR threshold. According to Eq. (4.4) when the SINR is high, the boundary or the contour is tight because the distance between the BS and a UE cannot be too large. Therefore, the area covered by the contour becomes comparably small which consequently make the unavailability high. Correspondingly, unavailability reaches zero for a sufficiently low SINR threshold. URC can be achieved in the space domain, when a user can access the services provided by BS with a lower SINR threshold. Then the BS can assure availability within the cell almost anywhere. With a higher SINR threshold, URC can be achieved if the BS has a higher transmission power and the neighboring BSs are located distantly to the UE's location.

For in depth analysis of cell unavailability, we consider $M = 5$ different cell deployments for the same PV network with $N = 10$ cells but still select the cell number 6 as the RC as shown in Fig. 3.7. The algorithm presented in Alg. 12 is used to run the simulations for SCMT scenario.

Fig. 4.4 illustrates the SCST cell unavailability behavior for the RC under each topology in dashed plots and SCMT cell unavailability over 5 topologies in blue (solid with triangle

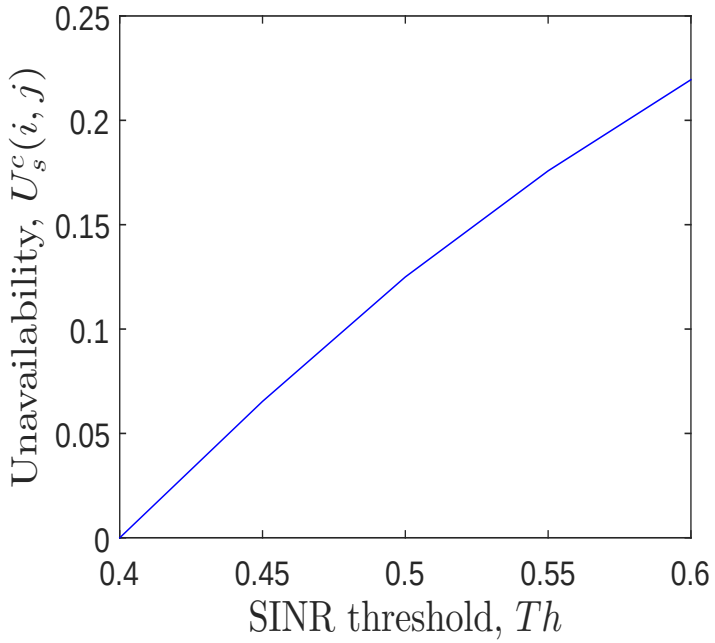


Figure 4.3: SCST cell unavailability of the RC ($i = 6$) for topology $j = 6$ as SINR threshold increases.

**Algorithm 12: Algorithm to estimate the SCMT cell availability for a given SINR threshold.**

**Input:** $x_B, y_B$ : Cartesian coordinates of the corresponding BS
**Input:** $N$ : Number of cells in the topology
**Input:** $M$ : Number of topologies
**Input:** $Th$ : SINR threshold
**Input:** $\alpha$ : Path loss coefficient
**Output:** $A_s^c(i,:)$ : SINR-based cell availability of the corresponding BS $i$ considering $M$ topologies

[1] **for** $j = 1 : M$ **do**
[2] | Run Alg. 11 to obtain $A_s^c(i,j)$
[3] **end**
[4] $A_s^c(i,:) = \sum_{j=1}^{M} A_s^c(i,j)$

marks) line. As depicted from Fig. 4.4, SCST cell unavailability $U_s^c(6,2)$ and $U_s^c(6,3)$ remains at zero, where $U_s^c(6,1)$, $U_s^c(6,4)$, $U_s^c(6,5)$ show non-zero values. Further, it can be observed that $U_s^c(6,5) < U_s^c(6,1) < U_s^c(6,4)$. This can be explained by carefully examining Fig. 3.3 and Fig. 3.4.

For a proper explanation concerning SINR we have to assess the positioning of the RC with respect to neighboring cells that produce interference. Among the 5 topologies, RC, i.e., the cell number 6 is placed in the middle only in topology 1. In all other 4 topologies, RC is placed in an edge of the unit square, but in different cell sizes and with different distances to the closest neighbor BSs. For instance, in topology 2 the RC has only one neighbor in a reasonable distance which can immensely affect the SINR. Contrary to that deployment, in topology 4, the neighboring BSs are placed in the vicinity to RC thus, the interference is very

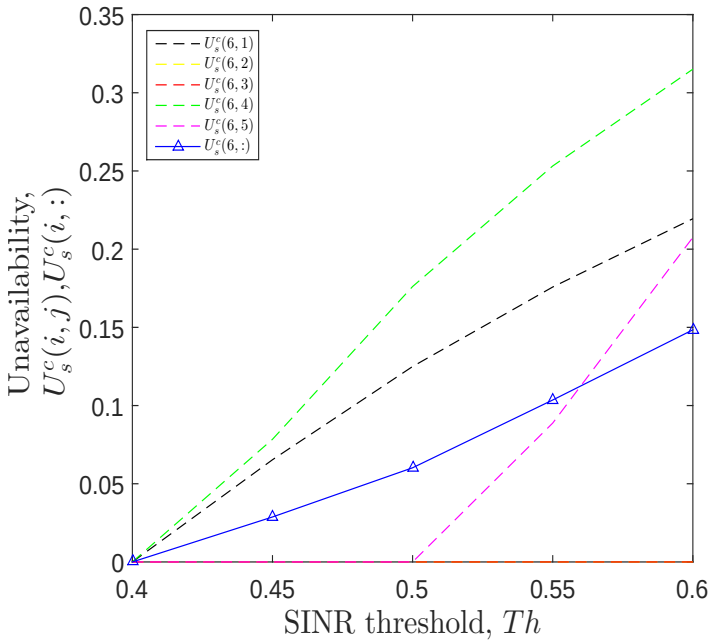


Figure 4.4: SCST and SCMT cell unavailability for $i = 6$ and $M = 5$ topologies as SINR threshold increases.

Table 4.1: Comparison of SCST and SCMT SINR-based cell availability

| SINR Threshold | 0.4 | 0.45 | 0.5 | 0.55 | 0.6 |
|---|---|---|---|---|---|
| $A_s^c(6,1)$ | 1.0000 | 0.9346 | 0.8750 | 0.8242 | 0.7805 |
| $A_s^c(6,2)$ | 1.0000 | 1.0000 | 1.0000 | 1.0000 | 1.0000 |
| $A_s^c(6,3)$ | 1.0000 | 1.0000 | 1.0000 | 1.0000 | 1.0000 |
| $A_s^c(6,4)$ | 1.0000 | 0.9216 | 0.8239 | 0.7468 | 0.6849 |
| $A_s^c(6,5)$ | 1.0000 | 1.0000 | 1.0000 | 0.9112 | 0.7925 |
| $A_s^c(6,:)$ | 1.0000 | 0.9712 | 0.9398 | 0.8964 | 0.8516 |

high which in turn degrades the availability. However, at a glance it can be understood that the unavailability increases along with the SINR threshold. Through the SINR-based SCMT cell availability analysis, we understand that the URC can be achieved in the cell deployments where the neighboring BSs are positioned distantly to each other.

Tab. 4.1 shows the numerical results obtained for SINR-based cell availability definitions. Note that $A_s^c(6,j)$ and $A_s^c(6,:)$ are obtained for SINR-based cell availability with correspondence to Eq. (3.3) and Eq. (3.5) respectively where covered area $C(i,j)$ has to be replaced by $C_{SINR}(i,j)$. This is also clearly illustrated by Alg. 11 and Alg. 12 respectively. The RC is cell number $i = 6$ and there are $M = 5$ topologies, i.e., $j = 1,2,3,4,5$.

Now we consider all $N = 10$ cells in the system in general and simulate the results for MCST SINR-based cell availability. Alg. 13 proposes the algorithm which was used to carry out the simulations for MCST scenario.

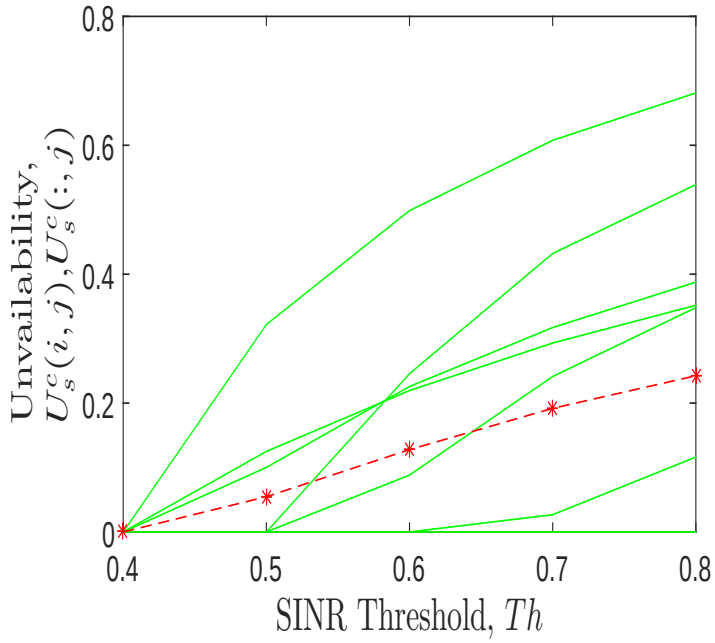


Figure 4.5: SCST and MCST cell unavailability for $N = 10$ cells of topology $j$ as SINR threshold increases.

**Algorithm 13: Algorithm to estimate the MCST cell availability for a given SINR threshold.**

**Input:** $x_B, y_B$ : Cartesian coordinates of the corresponding BS
**Input:** $N$ : Number of cells in the topology
**Input:** $Th$ : SINR threshold
**Input:** $\alpha$ : Path loss coefficient
**Output:** $A_s^c(:,j)$ : SINR-based cell availability of the $j^{th}$ topology
[1] **for** $i = 1 : N$ **do**
[2] | Run Alg. 11 and obtain $A_s^c(i,j)$
[3] **end**
[4] $A_s^c(:,j) = \sum_{i=1}^{N} A_s^c(i,j)$

Fig. 4.5 depicts the change of unavailability with the change of SINR threshold considering SCST and MCST scenarios. SCST cell unavailability are plotted in green solid curves and the average MCST cell unavailability is plotted in red (dashed-asterisks) curve. As illustrated from the results (refer to Tab. 4.2), we observe that many of the corner cells achieve zero unavailability for the considered SINR threshold range. However, we could say generally that MCST cell unavailability shows an increase when the SINR threshold increases.

Tab. 4.2 presents the values of MCST cell unavailability obtained with considered SINR threshold range for more clarity.

SINR-based cell availability was also evaluated for MCMT scenario. The algorithm used for this scenario is shown in Alg. 14 and the obtained results are shown in Fig. 4.6. The plots

Table 4.2: SINR-based SCST and MCST cell availability for $N = 10$ cells in topology 1

| SINR Threshold | 0.4 | 0.45 | 0.5 | 0.55 | 0.6 |
|---|---|---|---|---|---|
| $A_s^c(1,1)$ | 1.0000 | 1.0000 | 1.0000 | 1.0000 | 1.0000 |
| $A_s^c(2,1)$ | 1.0000 | 0.6781 | 0.5014 | 0.3923 | 0.3189 |
| $A_s^c(3,1)$ | 1.0000 | 1.0000 | 0.7544 | 0.5679 | 0.4610 |
| $A_s^c(4,1)$ | 1.0000 | 1.0000 | 0.9117 | 0.7587 | 0.6519 |
| $A_s^c(5,1)$ | 1.0000 | 0.8999 | 0.7743 | 0.6828 | 0.6124 |
| $A_s^c(6,1)$ | 1.0000 | 0.8750 | 0.7805 | 0.7068 | 0.6482 |
| $A_s^c(7,1)$ | 1.0000 | 1.0000 | 1.0000 | 0.9732 | 0.8838 |
| $A_s^c(8,1)$ | 1.0000 | 1.0000 | 1.0000 | 1.0000 | 1.0000 |
| $A_s^c(9,1)$ | 1.0000 | 1.0000 | 1.0000 | 1.0000 | 1.0000 |
| $A_s^c(10,1)$ | 1.0000 | 1.0000 | 1.0000 | 1.0000 | 1.0000 |
| $A_s^c(:,1)$ | 1.0000 | 0.9453 | 0.8722 | 0.8082 | 0.7576 |

shown in black (dashed) are the MCST cell unavailability of individual topologies and the average MCMT cell unavailability is shown in blue (solid with triangle marks) plot. It can be observed that, a similar trend is depicted which is increasing cell unavailability with increasing SINR threshold. For instance, topology 2 shows the lowest unavailability, with BSs placed comparably distant to each other causing low interference at each of the BSs and topology 4 has the highest unavailability, with BSs positioned closer to each other which created high interference at each.

**Algorithm 14: Algorithm to estimate the MCMT cell availability for a given SINR threshold.**

**Input:** $x_B, y_B$ : Cartesian coordinates of the corresponding BS
**Input:** $N$ : Number of cells in the topology
**Input:** $M$ : Number of topologies
**Input:** $Th$ : SINR threshold
**Input:** $\alpha$ : Path loss coefficient
**Output:** $\bar{A}_s^c$ : SINR-based average cell availability for any cell in any topology

```
[1] for j = 1 : M do
[2]     for i = 1 : N do
[3]         Run Alg. 11 and obtain A_s^c(i, j)
[4]     end
[5] end
```

[6] $\bar{A}_s^c = \frac{1}{M}\sum_{j=1}^{M}\left(\frac{1}{N}\sum_{i=1}^{N} A_s^c(i,j)\right)$

Tab. 4.3 presents the values of MCST and MCMT cell unavailability obtained with considered SINR threshold range. The given values are obtained from the simulations, which used Eq. (3.7) and Eq. (3.11) as the basis definitions.

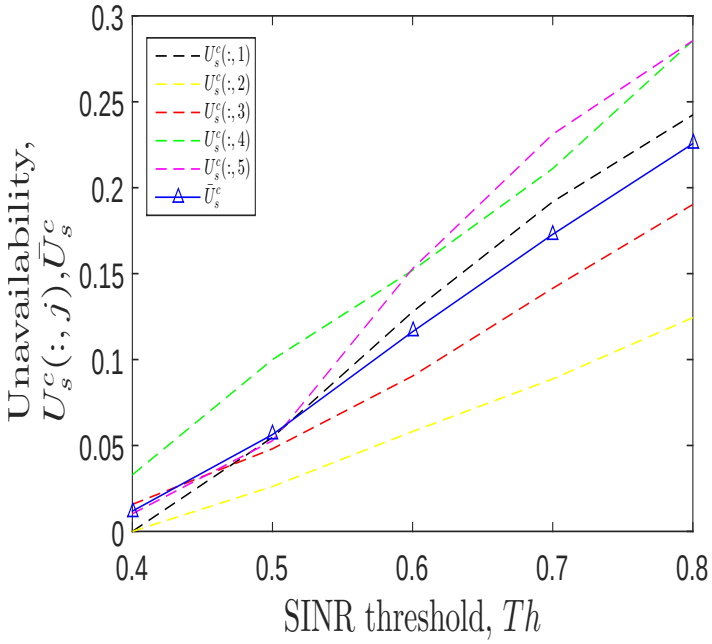


Figure 4.6: MCMT cell unavailability for $N = 10$ cells and $M = 5$ topologies as SINR threshold increases.

Table 4.3: Average SINR-based MCST and MCMT cell availability for $N = 10$ cells and $M = 5$ topologies

| SINR Threshold | 0.4 | 0.45 | 0.5 | 0.55 | 0.6 |
|---|---|---|---|---|---|
| $A_s^c(:,1)$ | 1.0000 | 0.9453 | 0.8722 | 0.8082 | 0.7576 |
| $A_s^c(:,2)$ | 1.0000 | 0.9739 | 0.9418 | 0.9113 | 0.8756 |
| $A_s^c(:,3)$ | 0.9843 | 0.9519 | 0.9096 | 0.8585 | 0.8098 |
| $A_s^c(:,4)$ | 0.9671 | 0.9000 | 0.8481 | 0.7888 | 0.7144 |
| $A_s^c(:,5)$ | 0.9897 | 0.9472 | 0.8471 | 0.7689 | 0.7144 |
| $\bar{A}_s^c$ | 0.9882 | 0.9437 | 0.8838 | 0.8271 | 0.7744 |

## 4.7 SINR-based System Availability of a PV Network

For a comprehensive analysis of SINR-based availability analysis, one must consider the variation of the system availability with SINR threshold as well. The algorithm which can be used to calculate SINR-based system availability for ST is given by Alg. 15.

However, due to the calculation complexity, estimating the overlaps between the adjacent SINR threshold contours accurately is complicated. Especially, for a low SINR threshold as the SINR threshold contour takes a irregular shape, finding the intersection and calculating the exact overlap are composite tasks. Even though for a higher SINR threshold, the contour may take a almost circular or elliptical shape, the calculation of overlaps is still complex. For a contour created for higher SINR threshold, one may estimate average radius of the each of the contours, however, calculating the overlaps between each other still becomes complicated. The overlap scenarios for a low threshold and high threshold are illustrated by Fig.4.7 to

**Algorithm 15: Algorithm to estimate the system availability for ST in HomNets.**

**Input:** $x_B, y_B$ : Cartesian coordinates of the corresponding BS
**Input:** $N$ : Number of cells in the topology
**Input:** $Th$ : SINR threshold
**Input:** $\alpha$ : Path loss coefficient
**Output:** $A_s^s(j)$ : SINR-based system availability of topology $j$

**for** $i = 1 : N$ **do**
  Find $S'(i) = (x_p(i), y_p(i))$ using Alg. 10
  **for** $z = 1 : length(x_p(i))$ **do**
    $d(i,z) = sqrt((x_B(i) - x_p(i,z))^2 + (y_B(i) - y_p(i,z))^2)$;
  **end**
  $dist(i) = mean(d(i,:))$ : $dist(i)$ is the average radius of the SINR threshold contour $(i)$
**end**
Input $S'(i)$ to calculate the coverage area defined by SINR threshold $C_{SINR}(i,j)$ using Eq. (3.24)
Find the vertices of the cell, $x_l, y_l$ of the Voronoi diagram
Input $(x_l, y_l)$ pairs to calculate the cell area $S(i,j)$ using Eq. (3.24)
Calculate the total BS coverage outside the unit square region $C_{exurban}(j)$
Calculate the total overlaps between BS coverages $C_{overlap}(j)$
Calculate $C_{tot}(j) = \sum_{i=1}^{N} C_{SINR}(i,j) - C_{exurban}(j) - C_{overlap}(j)$
**if** $C_{tot}(j) \leq \sum_{i=1}^{N} S(i,j)$ **then**
  $A_s^s(j) = \frac{C_{tot}(j)}{\sum_{i=1}^{N} S(i,j)}$
**else**
  $A_s^s(j) = 1$
**end**

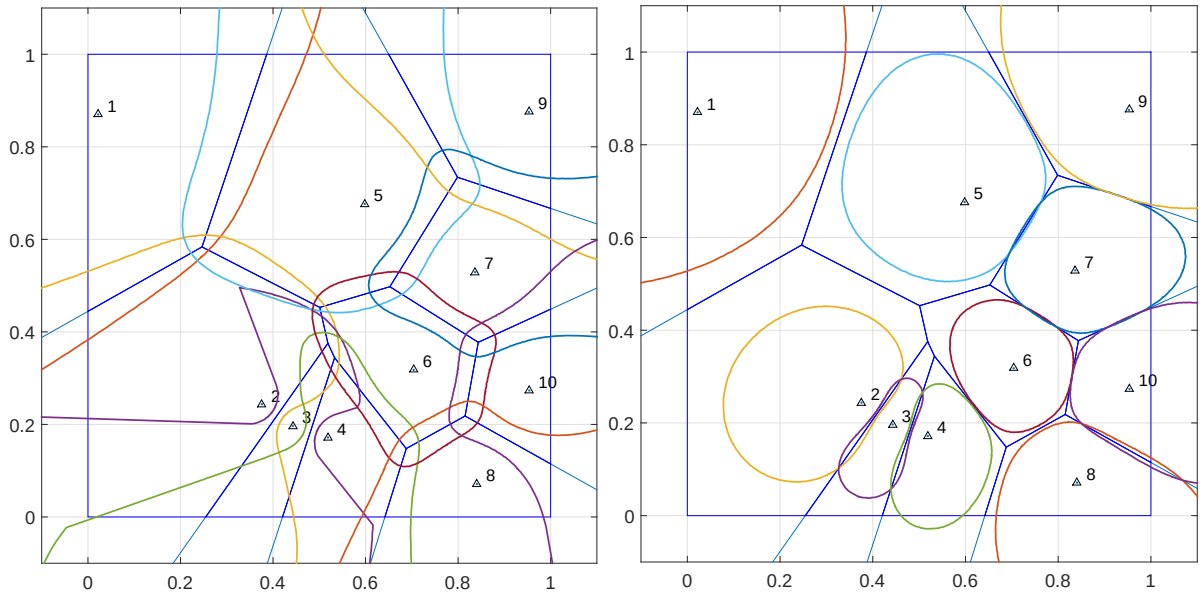


(a) Overlaps for low SINR threshold (b) Overlaps for high SINR threshold

Figure 4.7: Illustration of the overlaps between SINR threshold contours.

provide a clear idea. Therefore, evaluating SINR-based system availability using as given above simulations was not performed in this thesis.

An option is to set a sufficiently high SINR threshold which creates no overlaps in between the contours. Then we can assume that the overlap area becomes zero and deduct the calculate exurban area from the sum of the area of the SINR threshold contours which can be

divided my total area of the region to obtain the system availability. However, it should be noted from the above observations that the unavailability of the system may probably reach a higher value for unavailability which is not desirable.

In Chap. 6, we deploy PPP distributed users along with the PPP distributed BSs and find the user-oriented system availabilities considering SINR thresholds. Those results can be referred in order to get an overview of the SINR-based system availability.

## 4.8 Chapter Summary

This chapter was committed to conduct the availability analysis in the space domain with the focus to SINR perspective. Firstly, the relevant background for the rest of the chapter was laid by giving necessary theoretical explanation to show the relationship between the coverage and SINR. Then, the SINR-based availability definitions were proposed which can be adapted for cell-wise availability and system-wise availability with correspondence to the definitions of Chap. 2. Followed by the definitions, the estimations for SINR threshold contour was explained. Towards the end of the chapter, the respective algorithms followed and the figures and tables illustrating the obtained results are provided.

# Chapter 5

# Capacity-based URC Concepts and Analysis

*Now we have understood how the availability can be defined considering connectivity-based and SINR-based perspectives from Chap. 3 and Chap. 4 respectively. In Chap. 5, we will be focusing on the capacity variation along with the distance with respect to the placement of BSs. Therein, we attempt to define capacity-based cell availability and system availability definitions by the analysis conducted in this chapter.*

## 5.1 System Model

Analogous to Chap. 4, we continue with the same system model introduced in Chap. 3. The system consists of $N = 10$ PV cells within a unit region with one BS deployed in each of it. The underlying assumptions related to this chapter is as same as Chap. 4 which are listed in Sec. 4.1, except that the BS coverage is governed by the capacity threshold of the system.

## 5.2 Capacity and Coverage

We reviewed the expression for capacity in an OFDM system by Eq. (2.15). In this section, we are going to discover the relationship between the capacity and the distance. Since capacity is related with $SNR$ in a system, we start by looking at SNR in a different perspective. Eq. (5.1) indicates an expression which concerns SNR and the number of data symbols in the constellation $M_{mod}$ of the OFDM system.

$$SNR = \frac{E_b \ f_s \ log_2 M_{mod}}{N_0 \ W} \tag{5.1}$$

where $f_s$ is the baud rate and $E_b$ is the energy per bit. We can further simply the above expression and yield an expression for $log_2 M$ by substituting $N_0 = kT_{sys}\Delta f$ from Eq. (2.12) and $f_s = \frac{\Delta f}{1+G}$ as follows .

$$log_2 M_{mod} = \frac{(SNR)\ K\ T_{sys}\ (1+G)}{E_b}. \tag{5.2}$$

Besides, SNR achieved by user $(i)$ can be also expressed as,

$$SNR(i) = \frac{P_R(i)}{k_b T_{sys} \Delta f} \tag{5.3}$$

where $P_r(i)$ is given by $P_R(i) = \frac{P_T \lambda^2}{(4\pi)^2 d^\alpha}$. Now from the combinations of Eq. (2.15) and Eq. (5.1)-Eq. (5.3), it is evident that a system with higher capacity can provide services to users dispersed in a larger area than a system with a lower capacity. Also, the connected users would have to share the total capacity.

The capacity offered by a BS has to be decided upon how far the UE and how good the propagation environment is. Since we assume similar channel conditions and propagation conditions we can only focus on the distance between the BS and a particular UE. In general, the UEs would be geographically distributed closer to the BS or far from the BS. Thus, the actual bit rate that can be supplied by a BS will vary. If the UE is close enough to the BS to achieve a desired SNR in order to support a favorable modulation constellation, the user will achieve the required capacity to fulfill its high bandwidth requirements. Also, the UEs located too far from the BSs cannot achieve a sufficient capacity with a supportive modulation constellation.

Also, we can understand that smaller the cell, higher the capacity is because smaller the cell, the closer UEs are to the BS, and the more efficient the modulation can be supported. However,smaller the cells, more cells are needed to cover the considered region. Hence, there exists a tradeoff between the coverage of the system and the achieved capacity.

Before advancing to the rest of the chapter, we define the terminology, capacity threshold as follows.

**Capacity threshold:** is the maximum capacity that the system or the BS can offer to a certain area within its proximity in order to satisfy the capacity requirements of the users within it.

## 5.3 Capacity-based Cell Availability

Bringing forward the concept of the availability definition from the space domain as proposed in Eq. (3.2), we define the capacity-based cell availability as the area covered by the required capacity or the capacity threshold contour over the area of the cell of interest. Thus, we can express the capacity-based cell availability for cell $i$ under network topology $j$ in the space

domain, $A_s^c(i,j)$ as,

$$A_s^c(i,j) = \begin{cases} \frac{C_{cap}(i,j)}{S(i,j)}, & \text{if } C_{cap}(i,j) < S(i,j); \\ 1, & \text{otherwise.} \end{cases} \tag{5.4}$$

where, $C_{cap}(i,j)$ and $S(i,j)$ denote area covered by the capacity threshold and area of the PV cell respectively for a randomly selected cell $i$ of the $j^{th}$ topology.

To maintain the consistency, we could also propose definitions for cell availability for SCMT, MCST and MCMT scenarios as presented in Sec. 3.3.

## 5.4 Capacity-based System Availability

Capacity-based system availability is the availability defined for the whole system considering the total area covered by the capacity threshold of each cell and the total area of the region considered which contains all the cells. Accordingly, we express the capacity-based system availability for $j^{th}$ network topology, $A_s^s(j)$ as,

$$A_s^s(j) = \begin{cases} \frac{\sum_{i=1}^{N} C_{cap}(i,j) - \Delta}{\sum_{i=1}^{N} S(i,j)}, & \text{if } \sum_{i=1}^{N} C_{cap}(i,j) - \Delta < \sum_{i=1}^{N} S(i,j); \\ 1, & \text{otherwise} \end{cases} \tag{5.5}$$

where, $\Delta$ represents the overlap between the contours defined by the capacity threshold among neighboring BSs and the area which belongs to an outer-tier cell but falls outside the region of interest. Furthermore, we can also define the capacity-based system availability by considering MT scenario separately as in Sec. 3.4.

## 5.5 Capacity Threshold Contours

Given the required capacity or the capacity threshold of the system or a cell, one can calculate the distance (radius) within which that required capacity can be met. Thus, the coverage area bounded by the capacity threshold can be estimated. Alg. 16 shows the algorithm which has been employed in creating the capacity threshold contour in the simulations.

Unless otherwise stated, parameters are configured as, $N = 10$, $M = 5$, $rc = 6$, $Th = 1\ Gbps : 1\ Gbps : 10\ Gbps$, $\alpha = 2.5$, $\lambda = 3/20\ m$, $P_t = 1.5\ W$, $u_g = u_l = 1$, $T_{sys} = 290\ K$, $\Delta f = 10937.5\ Hz$, $N_{FFT} = 1024$, $N_{used} = 841$, $R_{err} = 3/4$, $p = 24/28$, $G = 1/8$, $n = 28/25$, $W = 10\ Mbps$, $E_b = 9.5 * 10^{-17}$ for the MATLAB simulations conducted in this chapter.

The set of the Cartesian coordinates $(x_p, y_p)$ along the capacity threshold contour which is obtained from Alg. 16 is denoted as $S''$ when explaining the algorithms from here onwards.

**Algorithm 16: Algorithm to estimate the capacity threshold contour.**

**Input:** $x_B, y_B$ : Cartesian coordinates of the BS of the RC
**Input:** $Th$ : Capacity threshold
**Input:** $\alpha$ : Path loss coefficient
**Input:** $P_T$ : Transmitted power from the BS
**Input:** $u_g, u_l$ : System gains
**Input:** $k_b$ : Boltzmanns constant
**Input:** $T_{sys}$ : Temperature of the system
**Input:** $\Delta f$ : Frequency spacing between subcarriers
**Input:** $N_{FFT}$ : Total number of subcarriers
**Input:** $N_{used}$ : Number of used subcarriers
**Input:** $\lambda$ : Wavelength of the signal
**Input:** $R_{err}$ : Error-correcting code rate
**Input:** $p$ : Ratio of the number of data subcarriers to the number of pilot subcarriers and data subcarriers
**Input:** $G$ : Ratio of guard time for an OFDM symbol to useful OFDM symbol time
**Input:** $n$ : Oversampling factor
**Input:** $W$ : Total bandwidth of the BSs
**Input:** $E_b$ : Energy per bit
**Output:** $x_p, y_p$ : Cartesian coordinates along the capacity threshold contour

[1] **for** $z = \frac{\pi}{180} : \frac{\pi}{180} : 2\pi$ **do**
[2] $d = 0.001$
[3] $x_p(z) = x_B + d\ cos(z)$
[4] $y_p(z) = y_B + d\ sin(z)$
[5] $dist(z) = \sqrt{(x_p((z) - x_B)^2 + (y_p(z) - y_B)^2}$ : $dist(z)$ : is the distance from $(x_p(z), y_p(z))$ to the BS which is apparently equal to $d$
[6] $P_R(z) = \frac{P_T \lambda^2}{(4\pi)^2 dist(z)^\alpha}$
[7] $SNR(z) = \frac{P_R(i)}{k_b T_{sys} \Delta f}$
[8] $log_2 M_{mod}(z) = \frac{SNR(z)\ k_b\ T_{sys}\ (1+G)}{E_b}$
[9] $R_b(z) = \frac{n\ W\ (N_{used}-1)\ log_2 M_{mod}(z)\ R_{err}\ p}{N_{FFT}\ (1+G)}$ : $R_b$ is the capacity of the cell
[10] **while** $R_b(z) \geq Th$ **do**
[11] $d = d + 0.001$
[12] $x_p(z) = x_B + d\ cos(z)$
[13] $y_p(z) = y_B + d\ sin(z)$
[14] $dist(z) = \sqrt{(x_p((z) - x_B)^2 + (y_p(z) - y_B)^2}$
[15] $P_R(z) = \frac{P_T \lambda^2}{(4\pi)^2 dist(z)^\alpha}$
[16] $SNR(z) = \frac{P_R(z)}{k_b T_{sys} \Delta f}$
[17] $log_2 M_{mod}(z) = \frac{SNR(z)\ k_b\ T_{sys}\ (1+G)}{E_b}$
[18] $R_b(z) = \frac{n\ W\ (N_{used}-1)\ log_2 M_{mod}(z)\ R_{err}\ p}{N_{FFT}\ (1+G)}$
[19] **end**
[20] **end**

Fig. 5.1 illustrates how the contours can vary with different capacity thresholds. As seen, the capacity threshold contours take a circular shape, since we have ignored the interference from the neighboring cells. For high capacity thresholds, the circular contour has a smaller radius compared to low capacity thresholds with larger radius of the contour. This is because, the SINR deteriorates over distance and this in turn results in a poor modulation constellation thus, reducing the area in which the allocated capacity threshold could serve.

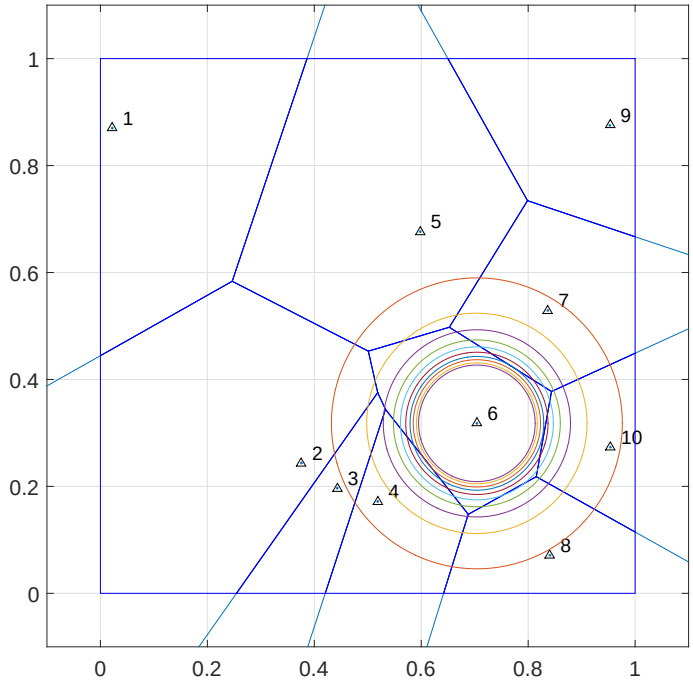


Figure 5.1: The coverage contours for various capacity thresholds.

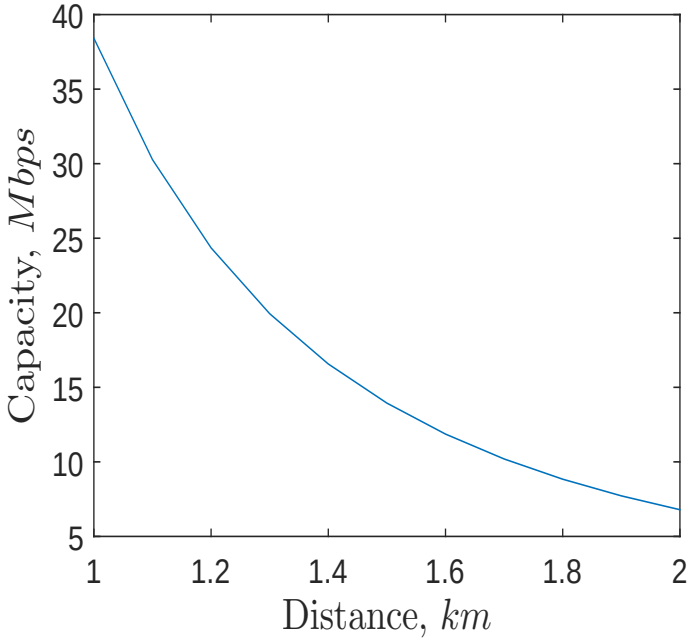


Figure 5.2: The achieved capacity variation over distance.

The above explanation can be also supported from the illustration in Fig. 5.2. The achieved capacity is plotted against the distance in between the BS and the reference point. It proves that the achieved capacity degrades when the distance increases.

## 5.6 Capacity-based Cell Availability of a PV Network

The cell availability for SCST scenario was simulated using the Alg. 17 as shown below. Simulations were carried out for the RC, which is the cell number 6, in Fig. 3.7.

**Algorithm 17: Algorithm to estimate the SCST cell availability for a given capacity threshold.**

**Input:** $x_B, y_B$ : Cartesian coordinates of the BS of the RC
**Input:** $Th$ : Capacity threshold
**Input:** $\alpha$ : Path loss coefficient
**Input:** $P_t$ : Transmitted power from the BS
**Input:** $u_g, u_l$ : System gains
**Input:** $k_b$ : Boltzmanns constant
**Input:** $T_{sys}$ : Temperature of the system
**Input:** $\Delta f$ : Frequency spacing between subcarriers
**Input:** $N_{FFT}$ : Total number of subcarriers
**Input:** $N_{used}$ : Number of used subcarriers
**Input:** $\lambda$ : Wavelength of the signal
**Input:** $R_{err}$ : Error-correcting code rate
**Input:** $p$ : Ratio of the number of data subcarriers to the number of pilot subcarriers and data subcarriers
**Input:** $G$ : Ratio of guard time for an OFDM symbol to useful OFDM symbol time
**Input:** $n$ : Oversampling factor
**Input:** $W$ : Total bandwidth of the BSs
**Input:** $E_b$ : Energy per bit
**Output:** $A_s^c(i,j)$ : Capacity-based cell availability of the corresponding BS $i$ of the topology $j$

[1] Run Alg. 16 and obtain the Cartesian coordinates along the capacity threshold contour $S''(i,j)$
[2] Input $S''(i,j)$ to calculate the coverage area defined by capacity threshold $C_{cap}(i,j)$ using Eq. (3.24)
[3] Find the vertices of the cell, $(x_l, y_l)$ of the Voronoi diagram
[4] Input $(x_l, y_l)$ pairs to calculate the cell area $S(i,j)$ using Eq. (3.24)
[5] Calculate the exurban coverage area $C_{out}(i,j)$
[6] **if** $(C_{cap}(i,j) - C_{out}(i,j)) \leq S$ **then**
[7] $\quad A_s^c(i,j) = \frac{C_{cap}(i,j) - C_{out}(i,j)}{S}(i,j)$
[8] **else**
[9] $\quad A_s^c(i,j) = 1$
[10] **end**

Fig. 5.3 illustrates the $U_s^c(i,j)$ variation for RC with the capacity thresholds. It is observed that lower the capacity threshold is, lower the unavailability turns and vice versa. Since the BS coverage rely on the capacity threshold, the BS coverage or the area which can be served by a particular capacity shrinks for a higher threshold. Therefore, the actual service area by the BS is smaller indicating a higher value for unavailability. Similarly, lower capacity threshold could expand the serviceable coverage area of a BS and reduce the unavailability. Therefore, achieving URC would require the cell to require a lower capacity level.

In the above analysis, as also depicted from Alg. 16, we have not considered any particular modulation scheme such as quadrature amplitude modulation (QAM) when calculating $log_2 M_{mod}$. Fig. 5.4 illustrates the behavior of SCST cell unavailability of the RC ($i = 6$) under topology $j = 6$ assuming QAM for the modulation constellation, as an example.

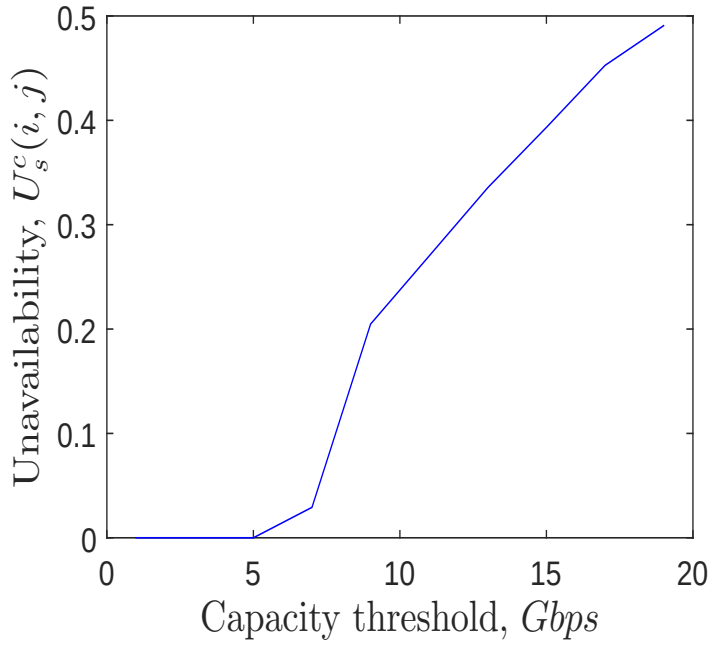


Figure 5.3: SCST cell unavailability of the RC ($i = 6$) for topology $j = 6$ as capacity threshold increases.

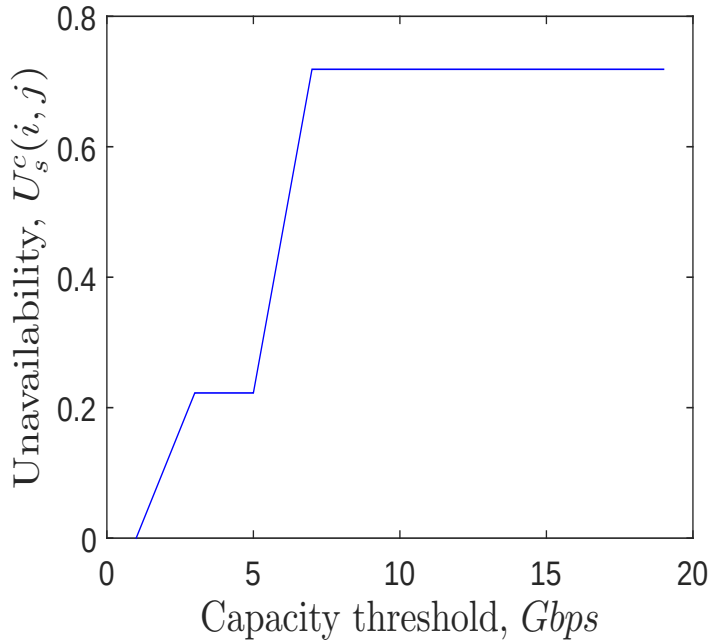


Figure 5.4: SCST cell unavailability of the RC ($i = 6$) for topology $j = 6$ as capacity threshold increases assuming QAM.

Now we consider the SCMT cell availability by taking the average of $M = 5$ topologies for RC. Presented by the Alg. 18 is the algorithm used for simulating the SCMT capacity-based cell availability.

**Algorithm 18: Algorithm to estimate the SCMT cell availability with given capacity threshold.**

**Input:** $x_B, y_B$ : Cartesian coordinates of the corresponding BS
**Input:** $Th$ : Capacity threshold
**Input:** $\alpha$ : Path loss coefficient
**Input:** $P_t$ : Transmitted power from the BS
**Input:** $u_g, u_l$ : System gains
**Input:** $k_b$ : Boltzmanns constant
**Input:** $T_{sys}$ : Temperature of the system
**Input:** $\Delta f$ : Frequency spacing between subcarriers
**Input:** $N_{FFT}$ : Total number of subcarriers
**Input:** $N_{used}$ : Number of used subcarriers
**Input:** $\lambda$ : Wavelength of the signal
**Input:** $R_{err}$ : Error-correcting code rate
**Input:** $p$ : Ratio of the number of data subcarriers to the number of pilot subcarriers and data subcarriers
**Input:** $G$ : Ratio of guard time for an OFDM symbol to useful OFDM symbol time
**Input:** $n$ : Oversampling factor
**Input:** $W$ : Total bandwidth of the BSs
**Input:** $E_b$ : Energy per bit
**Output:** $A_s^c(i,:)$ : Capacity-based cell availability of the corresponding BS $i$ considering $M$ topologies
[1] **for** $j = 1 : M$ **do**
[2] | Run Alg. 17 to obtain $A_s^c(i,j)$
[3] **end**
[4] $A_s^c(i,:) = \sum_{j=1}^{M} A_s^c(i,j)$

Fig. 5.5 demonstrates how the cell unavailability averaged over 5 topologies could differ with various capacity thresholds. As seen, for non-zero values of individual cell unavailability, highest values are indicated by topology 2 for a given capacity threshold and for topology 5, the cell unavailability remains at zero. Cell 6 contains a larger area in topology 2 and also the BS is placed with a biasing towards an edge. As a result, the BS coverage for a given capacity threshold cannot cover the total cell area. For instant, cell 6 in topology 5 inhere the smallest cell area among the 5 topologies, resulting in zero cell unavailability for the given range of capacity threshold. Average cell unavailability for the 5 topologies in blue (solid with triangle marks) curve indicates that $A_s^c(i,:)$ decreases when the capacity offered by the BS becomes larger. This analysis show that a smaller cell would have a better chance of obtaining URC, compared to a larger cell, provided with a lower capacity threshold.

Tab. 4.3 shows the numerical results obtained for above presented capacity-based cell availability definitions. Note that $A_s^c(6,j)$ and $A_s^c(6,:)$ are obtained for capacity-based cell availability with correspondence to Eq. (3.3) and Eq. (3.5) respectively by replacing covered area $C(i,j)$ by $C_{cap}(i,j)$. The cell of interest is cell number $i = 6$ and there are $M = 5$ topologies.

Cohering into a single topology we can define MCST capacity-based cell availability considering $N = 10$ cells in topology 1, corresponding to Eq. (3.7). Alg. 19 proposes the algorithm which was used to carry out the simulations for MCST scenario.

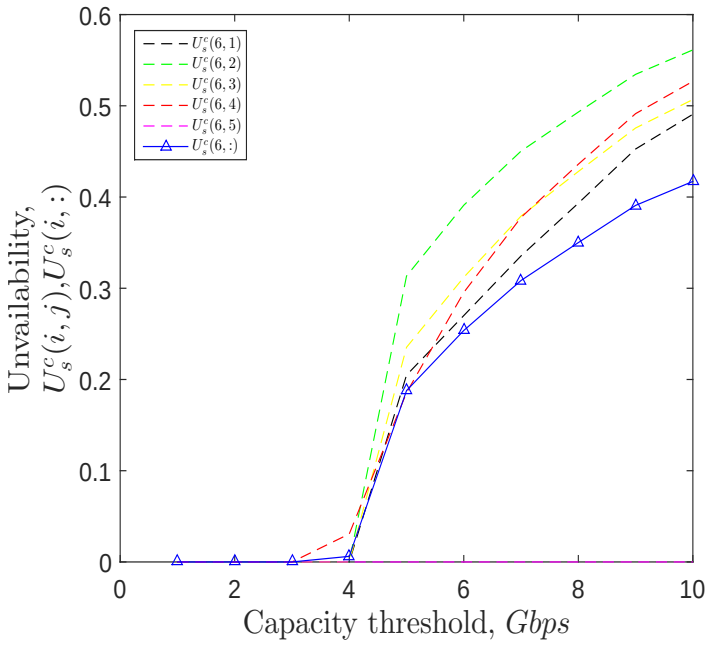


Figure 5.5: SCST and SCMT cell unavailability for $i = 6$ and $M = 5$ topologies as capacity threshold increases.

Table 5.1: Comparison of SCST and SCMT capacity-based cell availability

| Capacity Threshold (*Gbps*) | 1 | 2 | 3 | 4 ‘ | 5 | 6 | 7 | 8 | 9 | 10 |
|---|---|---|---|---|---|---|---|---|---|---|
| $A_s^c(6,1)$ | 1.0000 | 1.0000 | 1.0000 | 1.0000 | 0.7952 | 0.7299 | 0.6645 | 0.6068 | 0.5474 | 0.5093 |
| $A_s^c(6,2)$ | 1.0000 | 1.0000 | 1.0000 | 1.0000 | 0.6866 | 0.6090 | 0.5497 | 0.5069 | 0.4655 | 0.4388 |
| $A_s^c(6,3)$ | 1.0000 | 1.0000 | 1.0000 | 1.0000 | 0.7647 | 0.6880 | 0.6209 | 0.5720 | 0.5244 | 0.4932 |
| $A_s^c(6,4)$ | 1.0000 | 1.0000 | 1.0000 | 0.9693 | 0.8145 | 0.7046 | 0.6223 | 0.5640 | 0.5086 | 0.4732 |
| $A_s^c(6,5)$ | 1.0000 | 1.0000 | 1.0000 | 1.0000 | 1.0000 | 1.0000 | 1.0000 | 1.0000 | 1.0000 | 1.0000 |
| $A_s^c(6,:)$ | 1.0000 | 1.0000 | 1.0000 | 0.9939 | 0.8122 | 0.7463 | 0.6915 | 0.6499 | 0.6092 | 0.5829 |

Fig. 5.6 illustrates the change of unavailability with the change of capacity threshold considering MCST scenario. Average MCST cell unavailability is plotted in purple (dashed-asterisks) curve whereas the individual SCST cell unavailability are plotted in colored solid curves. It is observed from Fig. 5.6, that individual cell unavailability of cell 2 is the highest, more specifically the individual cell unavailability vary as $U_s^c(2,1) > U_s^c(5,1) > U_s^c(1,1) > U_s^c(7,1) > U_s^c(9,1) > U_s^c(3,1) > U_s^c(4,1) > U_s^c(6,1) > U_s^c(8,1) > U_s^c(10,1)$, i.e. individual cell unavailability of cell 10 being the lowest. By carefully examining topology 1 demonstrated in Fig. 3.3, we see that cells 2, 5, 1 have larger sizes compared to other cells and also BSs of cell 2 and 5 are placed closer to a cell edge. Hence, it is clear that $U_s^c(2,1) > U_s^c(5,1) > U_s^c(1,1) > .....$ Also cell 10 has the smallest size therefore it could achieve a higher availability for a given capacity threshold. Moreover, the MCST cell unavailability shows an increase when the capacity threshold increases.

**Algorithm 19: Algorithm to estimate the MCST cell availability for a given capacity threshold.**

**Input:** $x_B, y_B$ : Cartesian coordinates of the corresponding BS
**Input:** $Th$ : Capacity threshold
**Input:** $\alpha$ : Path loss coefficient
**Input:** $P_t$ : Transmitted power from the BS
**Input:** $u_g, u_l$ : System gains
**Input:** $k_b$ : Boltzmanns constant
**Input:** $T_{sys}$ : Temperature of the system
**Input:** $\Delta f$ : Frequency spacing between subcarriers
**Input:** $N_{FFT}$ : Total number of subcarriers
**Input:** $N_{used}$ : Number of used subcarriers
**Input:** $\lambda$ : Wavelength of the signal
**Input:** $R_{err}$ : Error-correcting code rate
**Input:** $p$ : Ratio of the number of data subcarriers to the number of pilot subcarriers and data subcarriers
**Input:** $G$ : Ratio of guard time for an OFDM symbol to useful OFDM symbol time
**Input:** $n$ : Oversampling factor
**Input:** $W$ : Total bandwidth of the BSs
**Input:** $E_b$ : Energy per bit
**Output:** $A_s^c(:, j)$ : Capacity-based cell availability of the $j^{th}$ topology
[1] **for** $i = 1 : N$ **do**
[2] | Run Alg. 17 and obtain $A_s^c(i, j)$
[3] **end**
[4] $A_s^c(:, j) = \sum_{i=1}^{N} A_s^c(i, j)$

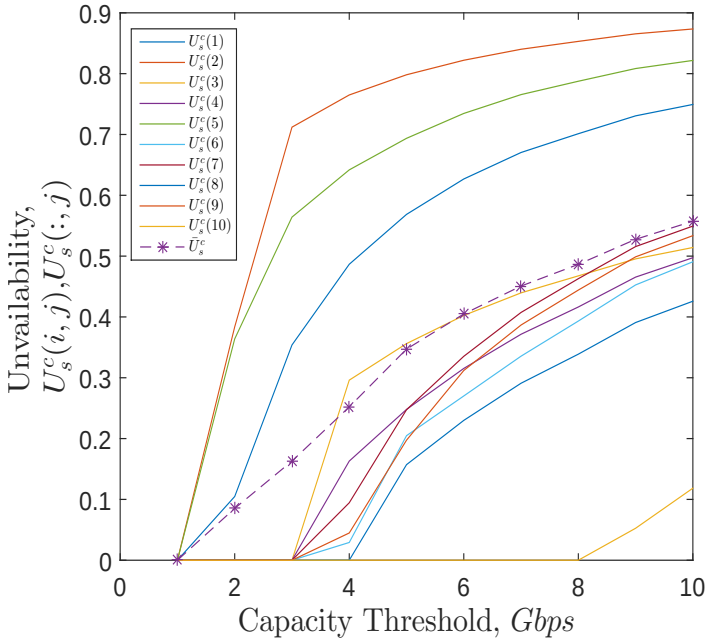


Figure 5.6: SCST and MCST cell unavailability for $N = 10$ cells of topology 1 as capacity threshold increases.

Tab. 5.2 presents the values of SCST and MCST capacity-based cell unavailability of topology 1 obtained with considered capacity threshold range to verify the above explanation.

The most general definition for average cell availability can be obtained through MCMT

Table 5.2: Capacity-based SCST and MCST cell availability of $N = 10$ cells in topology 1

| Capacity Threshold (*Gbps*) | 1 | 2 | 3 | 4 | 5 | 6 | 7 | 8 | 9 | 10 |
|---|---|---|---|---|---|---|---|---|---|---|
| $A_s^c(1,1)$ | 1.0000 | 0.8952 | 0.6461 | 0.5134 | 0.4314 | 0.3732 | 0.3296 | 0.2987 | 0.2694 | 0.2506 |
| $A_s^c(2,1)$ | 1.0000 | 0.6163 | 0.2880 | 0.2350 | 0.2018 | 0.1780 | 0.1599 | 0.1469 | 0.1345 | 0.1265 |
| $A_s^c(3,1)$ | 1.0000 | 1.0000 | 1.0000 | 0.7039 | 0.6439 | 0.5975 | 0.5604 | 0.5325 | 0.5045 | 0.4858 |
| $A_s^c(4,1)$ | 1.0000 | 1.0000 | 1.0000 | 0.8370 | 0.7521 | 0.6847 | 0.6285 | 0.5836 | 0.5345 | 0.5027 |
| $A_s^c(5,1)$ | 1.0000 | 0.6361 | 0.4358 | 0.3582 | 0.3063 | 0.2654 | 0.2344 | 0.2125 | 0.1916 | 0.1783 |
| $A_s^c(6,1)$ | 1.0000 | 1.0000 | 1.0000 | 0.9708 | 0.7952 | 0.7299 | 0.6645 | 0.6068 | 0.5474 | 0.5093 |
| $A_s^c(7,1)$ | 1.0000 | 1.0000 | 1.0000 | 0.9055 | 0.7525 | 0.6647 | 0.5926 | 0.5371 | 0.4843 | 0.4506 |
| $A_s^c(8,1)$ | 1.0000 | 1.0000 | 1.0000 | 1.0000 | 0.8429 | 0.7701 | 0.7090 | 0.6612 | 0.6092 | 0.5742 |
| $A_s^c(9,1,1)$ | 1.0000 | 1.0000 | 1.0000 | 0.9552 | 0.8026 | 0.6880 | 0.6133 | 0.5558 | 0.5012 | 0.4663 |
| $A_s^c(10,1)$ | 1.0000 | 1.0000 | 1.0000 | 1.0000 | 1.0000 | 1.0000 | 1.0000 | 1.0000 | 0.9475 | 0.8816 |
| $A_s^c(:,1)$ | 1.0000 | 0.9148 | 0.8370 | 0.7479 | 0.6529 | 0.5951 | 0.5492 | 0.5135 | 0.4724 | 0.4426 |

scenario. The algorithm which is employed to simulate MCST scenario is shown in Alg. 20. The variation of average cell availability with the capacity threshold can be observed via Fig. 5.7. It is evidenced that the MCMT cell availability curves for the 5 topologies fall very close to each other, implying a more realistic variation of the average MCMT cell availability in a capacity point of view. Tab. 5.3 presents the values of MCMT cell unavailability obtained with considered capacity threshold range.

**Algorithm 20: Algorithm to estimate the MCMT cell availability for a given capacity threshold.**

**Input:** $x_B, y_B$ : Cartesian coordinates of the corresponding BS
**Input:** $Th$ : Capacity threshold
**Input:** $\alpha$ : Path loss coefficient
**Input:** $P_t$ : Transmitted power from the BS
**Input:** $u_g, u_l$ : System gains
**Input:** $k_b$ : Boltzmanns constant
**Input:** $T_{sys}$ : Temperature of the system
**Input:** $\Delta f$ : Frequency spacing between subcarriers
**Input:** $N_{FFT}$ : Total number of subcarriers
**Input:** $N_{used}$ : Number of used subcarriers
**Input:** $\lambda$ : Wavelength of the signal
**Input:** $R_{err}$ : Error-correcting code rate
**Input:** $p$ : Ratio of the number of data subcarriers to the number of pilot subcarriers and data subcarriers
**Input:** $G$ : Ratio of guard time for an OFDM symbol to useful OFDM symbol time
**Input:** $n$ : Oversampling factor
**Input:** $W$ : Total bandwidth of the BSs
**Input:** $E_b$ : Energy per bit
**Output:** $\bar{A}_s^c$ : Capacity-based average cell availability for any cell in any topology

**[1]** **for** $j = 1 : M$ **do**
**[2]** | **for** $i = 1 : N$ **do**
**[3]** | | Run Alg. 17 and obtain $A_s^c(i,j)$
**[4]** | **end**
**[5]** **end**
**[6]** $\bar{A}_s^c = \frac{1}{M}\sum_{j=1}^{M}\left(\frac{1}{N}\sum_{i=1}^{N} A_s^c(i,j)\right)$

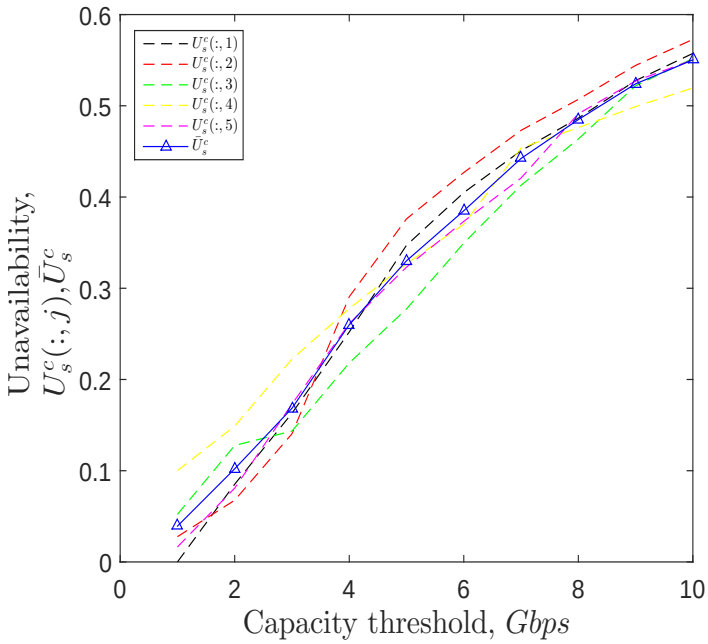


Figure 5.7: MCST and MCMT cell unavailability for $N = 10$ cells and $M = 5$ topologies as capacity threshold increases.

Table 5.3: Average capacity-based MCST and MCMT cell availability for $N = 10$ cells and $M = 5$ topologies

| Capacity Threshold (*Gbps*) | 1 | 2 | 3 | 4 | 5 | 6 | 7 | 8 | 9 | 10 |
|---|---|---|---|---|---|---|---|---|---|---|
| $A_s^c(:,1)$ | 1.0000 | 0.9148 | 0.8370 | 0.7479 | 0.6529 | 0.5951 | 0.5492 | 0.5135 | 0.4724 | 0.4426 |
| $A_s^c(:,2)$ | 0.9723 | 0.9323 | 0.8595 | 0.7093 | 0.6239 | 0.5731 | 0.5269 | 0.4930 | 0.4557 | 0.4272 |
| $A_s^c(:,3)$ | 0.9479 | 0.8723 | 0.8565 | 0.7819 | 0.7226 | 0.6505 | 0.5871 | 0.5365 | 0.4779 | 0.4482 |
| $A_s^c(:,4)$ | 0.8999 | 0.8510 | 0.7777 | 0.7222 | 0.6732 | 0.6298 | 0.5463 | 0.5239 | 0.5009 | 0.4805 |
| $A_s^c(:,5)$ | 0.9836 | 0.9191 | 0.8269 | 0.7388 | 0.6768 | 0.6267 | 0.5792 | 0.5087 | 0.4728 | 0.4497 |
| $\bar{A}_s^c$ | 0.9607 | 0.8979 | 0.8315 | 0.7400 | 0.6699 | 0.6151 | 0.5577 | 0.5151 | 0.4760 | 0.4497 |

## 5.7 Capacity-based System Availability of a PV Network

We also analyze the availability of the whole system consisting of $N = 10$ cells in a capacity perspective. The capacity-based system availability is evaluated for both ST and MT scenarios. The algorithms which can be used to calculate capacity-based system availability for ST and MT are given by Alg. 21 and Alg. 22 respectively. Tab. 5.4 presents the numerical values obtained from performing the simulations for ST and MT scenarios of capacity-based system availability.

Fig. 5.8 depicts the capacity-based system unavailability considering both ST and MT scenarios for $M = 5$ topologies, each consisting of $N = 10$ cells. It can be seen that for the 5 topologies the system unavailability increases when the capacity threshold increases which is understandable from above explanations. Also the curves lie much closer to each other so

Table 5.4: Comparison of ST and MT system availability

| Capacity Threshold ($Gbps$) | 3 | 4 | 5 | 6 | 7 | 8 | 9 | 10 |
|---|---|---|---|---|---|---|---|---|
| $A_s^s(1)$ | 0.8175 | 0.6398 | 0.5659 | 0.4770 | 0.4257 | 0.3891 | 0.3540 | 0.3315 |
| $A_s^s(2)$ | 0.7675 | 0.6194 | 0.5245 | 0.4903 | 0.4384 | 0.4015 | 0.3663 | 0.3439 |
| $A_s^s(3)$ | 0.7954 | 0.6466 | 0.5521 | 0.5148 | 0.4565 | 0.4146 | 0.3555 | 0.3328 |
| $A_s^s(4)$ | 0.8232 | 0.6628 | 0.5677 | 0.4836 | 0.4319 | 0.3886 | 0.3520 | 0.3287 |
| $A_s^s(5)$ | 0.7660 | 0.6263 | 0.5315 | 0.4639 | 0.4104 | 0.3393 | 0.3098 | 0.2912 |
| $\bar{A}_s^s$ | 0.7939 | 0.6390 | 0.5484 | 0.4859 | 0.4326 | 0.3866 | 0.3475 | 0.3256 |

**Algorithm 21: Algorithm to estimate the ST system availability for a given capacity threshold.**

**Input:** $x_B, y_B$ : Cartesian coordinates of the corresponding BS
**Input:** $Th$ : Capacity threshold
**Input:** $\alpha$ : Path loss coefficient
**Input:** $P_t$ : Transmitted power from the BS
**Input:** $u_g, u_l$ : System gains
**Input:** $k_b$ : Boltzmanns constant
**Input:** $T_{sys}$ : Temperature of the system
**Input:** $\Delta f$ : Frequency spacing between subcarriers
**Input:** $N_{FFT}$ : Total number of subcarriers
**Input:** $N_{used}$ : Number of used subcarriers
**Input:** $\lambda$ : Wavelength of the signal
**Input:** $R_{err}$ : Error-correcting code rate
**Input:** $p$ : Ratio of the number of data subcarriers to the number of pilot subcarriers and data subcarriers
**Input:** $G$ : Ratio of guard time for an OFDM symbol to useful OFDM symbol time
**Input:** $n$ : Oversampling factor
**Input:** $W$ : Total bandwidth of the BSs
**Input:** $E_b$ : Energy per bit
**Output:** $A_s^s(j)$ : Capacity-based system availability of topology $j$

**[1]** **for** $i = 1 : N$ **do**
**[2]** | Find $S''$ using Alg. 16
**[3]** **end**
**[4]** Input $S''(i,j)$ to calculate the coverage area defined by capacity threshold $C_{cap}(i,j)$ for each topology using Eq. (3.24)
**[5]** Find the vertices of the cell, $x_l, y_l$ of the Voronoi diagram
**[6]** Input $(x_l, y_l)$ pairs to calculate the cell area $S(i,j)$ using Eq. (3.24) for each topology
**[7]** Calculate the total coverage outside the unit square region $C_{exurban}(j)$
**[8]** Calculate the total overlaps between coverages $C_{overlap}(j)$
**[9]** Calculate $C_{tot}(j) = \sum_{i=1}^{N} C_{cap}(i,j) - C_{exurban}(j) - C_{overlap}(j)$
**[10]** **if** $C_{tot}(j) \leq \sum_{i=1}^{N} S(i,j)$ **then**
**[11]** | $A_s^s(j) = \frac{C_{tot}(j)}{\sum_{i=1}^{N} S(i,j)}$
**[12]** **else**
**[13]** | $A_s^s(j) = 1$
**[14]** **end**

that the average system unavailability which is shown in blue (solid with triangle marks) plot also provide a slight variation with each ST system unavailability.

**Algorithm 22: Algorithm to estimate the MT system availability for a given capacity threshold.**

**Input:** $x_B, y_B$ : Cartesian coordinates of the corresponding BS
**Input:** $Th$ : Capacity threshold
**Input:** $\alpha$ : Path loss coefficient
**Input:** $P_t$ : Transmitted power from the BS
**Input:** $u_g, u_l$ : System gains
**Input:** $k_b$ : Boltzmanns constant
**Input:** $T_{sys}$ : Temperature of the system
**Input:** $\Delta f$ : Frequency spacing between subcarriers
**Input:** $N_{FFT}$ : Total number of subcarriers
**Input:** $N_{used}$ : Number of used subcarriers
**Input:** $\lambda$ : Wavelength of the signal
**Input:** $R_{err}$ : Error-correcting code rate
**Input:** $p$ : Ratio of the number of data subcarriers to the number of pilot subcarriers and data subcarriers
**Input:** $G$ : Ratio of guard time for an OFDM symbol to useful OFDM symbol time
**Input:** $n$ : Oversampling factor
**Input:** $W$ : Total bandwidth of the BSs
**Input:** $E_b$ : Energy per bit
**Output:** $\bar{A}_s^s$ : Capacity-based average system availability
**[1]** For $j = 1 : M$ Calculate $A_s^s(j)$ from Alg. 21
**[2]** Calculate $\bar{A}_s^s = \frac{1}{M} \sum_{j=1}^{M} A_s^c(j)$

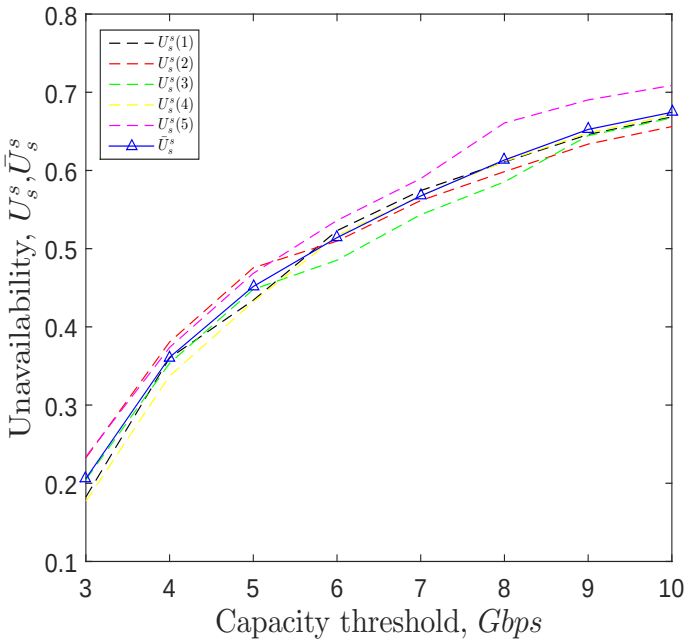


Figure 5.8: ST and MT system unavailability as capacity threshold increases.

## 5.8 Chapter Summary

This chapter is dedicated for the analysis of capacity-based availability both cell-wise and system-wise. In the first part of the chapter we explained how the capacity of BSs could affect the BS coverage which in turn impacts the availability. Then we developed an algorithm in order to obtain the coordinates along the contour beyond in which the capacity threshold

cannot be achieved. This algorithm is then used for the simulations done for capacity-based cell availability and system availability, followed by the availability definitions.

# Chapter 6

# User-oriented URC Concepts and Analysis

*In the previous chapters, i.e., Chaps. 3, 4, 5, we analyzed the space domain availability based on connectivity, SINR and capacity respectively. In Chap. 6 we conduct the analysis with a user-oriented approach. The UE locations are assumed to form a realization of a homogeneous two-dimensional spatial PPP. We introduce the concepts of individual user availability and user-oriented system availability in the space domain.*

## 6.1 System Model

We consider a cellular network which consists of $N$ randomly deployed BSs in a Euclidean plane according to some homogeneous PPP as shown in Fig. 2.4. We also consider multiple UEs distributed randomly in the same network according to another independent homogeneous PPP. Illustrated by Fig. 6.1 is the system model to which we refer in Chap. 6. In what follows, the underlying assumptions taken for this system model can be found.

- All BSs and UEs are formed based on two independent homogeneous PPPs of intensity $\lambda_B$ and intensity $\lambda_U$ in the Euclidean plane respectively.
- Each UE is associated with a serving BS which may or may not be the nearest one. For instance, if the association scheme is to pair the UE with the BS with the given SINR threshold, then the serving BS may or may not be the closest one because of propagation losses.
- In each cell, one BS is deployed, and one omni-directional antenna is mounted on each of them. However, SINR deterioration over distance has a significant impact on the coverage of each BS.
- Frequency re-use factor of the system is one.
- Same channel type and propagation conditions are considered.

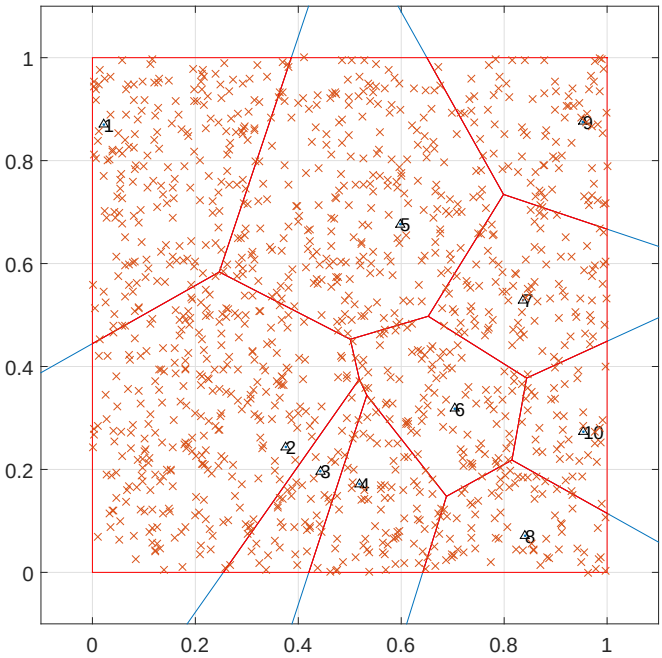


Figure 6.1: A cellular network of N = 10 BSs modeled with a homogeneous PPP of intensity $\lambda_B = 10$ and a collection of UEs following an independent homogeneous PPP of intensity $\lambda_U = 1500$ in the Euclidean plane.

Followed by the foundation laid in Sec. 3.2, we continue to extend the concept in the space domain availability in users' perspective. In this chapter, $MCA$ in Eq. (3.2), will be reflected by the number of users within the covered area $UE_{covered}$. Note that, this covered area can be defined by either of the perspectives analyzed in the previous chapters, i.e. connectivity-based, SINR-based or capacity-based.

## 6.2 Individual User Availability

In this section, we propose the space domain user availability for a randomly selected UE. If the randomly chosen user $m$ falls within the covered area, the space domain user availability, which is denoted by $A_s^u(m)$ becomes 1. Otherwise, $A_s^u(m)$ becomes 0, since the user is not served by any BS. Thus, in this criteria, $A_s^u(m)$ can be either 1 or 0.

$$A_s^u(m) = \begin{cases} 1, & \text{if } user\ m\ is\ covered; \\ 0, & \text{otherwise.} \end{cases} \tag{6.1}$$

Also the individual user unavailability for user $m$ in the space domain, denoted as $U_s^u(m)$ is given by,

$$U_s^u(m) = 1 - A_s^c(m). \tag{6.2}$$

## 6.3 User-oriented System Availability

Now we consider the whole cluster of UEs and propose the space domain user availability considering all the users as a system. User-oriented system availability determines the availability of the BSs' service to a collection of UEs dispersed within a unit area despite of the distribution which characterizes it. We define the user-oriented system availability $A_s^u$ as,

$$A_s^u = \begin{cases} \frac{no.\ of\ users\ covered}{total\ no.\ of\ users} = \frac{UE_{covered}}{N_{UE}}, & \text{if } UE_{covered} < N_{UE}; \\ 1, & \text{otherwise.} \end{cases} \tag{6.3}$$

The user-oriented system unavailability $U_s^u$ is expressed as,

$$U_s^u = 1 - A_s^c. \tag{6.4}$$

## 6.4 Individual User Availability of a PV Network with PPP Distributed Users

Now we evaluate the individual user availability of the system which is introduced in Fig. 6.1 using MATLAB simulations. Following algorithm given by Alg. 23 has been employed for individual user scenario.

**Algorithm 23: Algorithm to estimate the individual user availability of a PV network with PPP distributed users considering SINR-based coverages.**

**Input:** $x_B, y_B$ : Cartesian coordinates of the BS
**Input:** $N$ : Number of cells in the topology
**Input:** $Th$ : SINR threshold
**Input:** $\lambda_U$ : Intensity of the user PPP
**Input:** $\alpha$ : Path loss coefficient
**Output:** $A_s^u(m)$ : Individual user availability of user $m$
[1] Generate the Voronoi diagram using $(x_B, y_B)$ pairs
[2] Generate the user distribution of $\lambda_U$ intensity
[3] Create SINR threshold contours using Alg. 10 and obtain its coordinates $S'$
[4] Select a random user $m$ and obtain the coordinates $(x_U(m), y_U(m))$
[5] **if** $(x_U(m), y_U(m))$ *lies within* $(x_p, y_p)$ **then**
[6] | $A_s^u(m) = 1$
[7] **else**
[8] | $A_s^u(m) = 0$
[9] **end**

From the simulations done for the individual user availability for a randomly selected user, 2 possible scenarios can be observed. A UE can either lie closer to the BS, within the territory of the covered area or either lie closer to an edge of the cell, completely outside the coverage of the BS of the cell to which it belongs. These 2 scenarios can be recognized clearly from Figs. 6.2 and 6.3. The illustrated SINR threshold contours correspond to the SINR threshold range given by $Th = 0.5 : 0.05 : 0.7$ and the random UE is picked up from a homogeneous

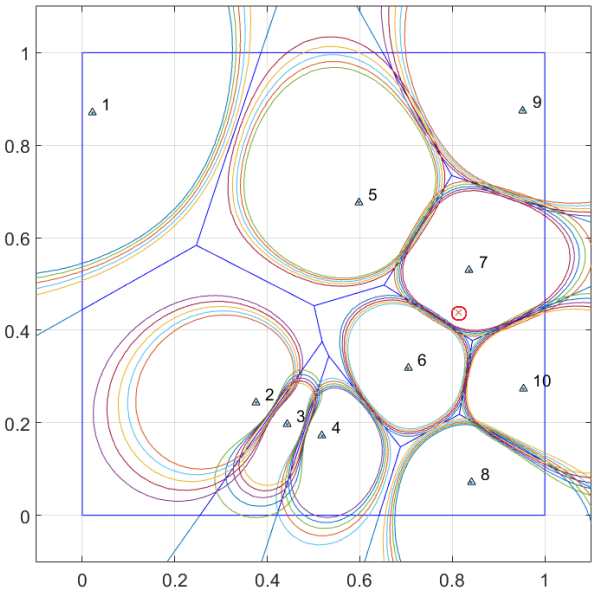


(a) The randomly chosen UE lies in the middle of a cell.

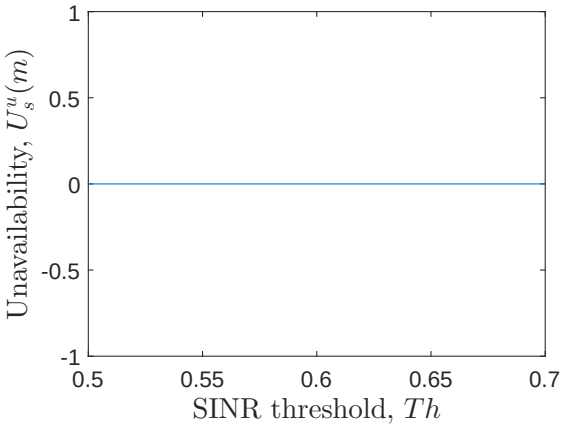


(b) The variation of individual user unavailability.

Figure 6.2: The individual user unavailability for a randomly chosen UE which lies in the middle of a cell.

PPP of intensity $\lambda_U = 1500$.

When a UE is placed closer to a BS, its user availability is obvious to become 1, unless a very tight SINR threshold is set to the BS. However, when a UE falls far away to the BS of the cell in which it belongs to, or rather lies near to an edge of the cell, the probability of the user availability becoming 0 is very high. But, there's a slight possibility that the user availability could become still 1. This could happen with the following scenarios.

- When a tight SINR threshold is given to all the BSs, and the BS is placed biased towards the edge to which the user is placed closely.
- When a relaxed SINR threshold is given to all the BSs, and the BSs is situated at the middle of the cell or closer to the edge in interest.
- When a relaxed SINR threshold is given to all the BSs, and the BS is situated away from the edge in interest but a neighboring BS is placed bias to the edge in interest. This assumes that no association policy is given such that a UE has to be paired with the closest BS.

Fig. 6.2(b) and Fig. 6.3(b) show the variation of the individual user unavailability with the increment of SINR threshold which determines the coverage area of a BS when the random UE is located as in Fig. 6.2(a) and Fig. 6.3(a) respectively. Fig. 6.4 shows the the variation of the individual user unavailability accordingly when the random UE falls in between the coverages corresponding to considered SINR threshold range.

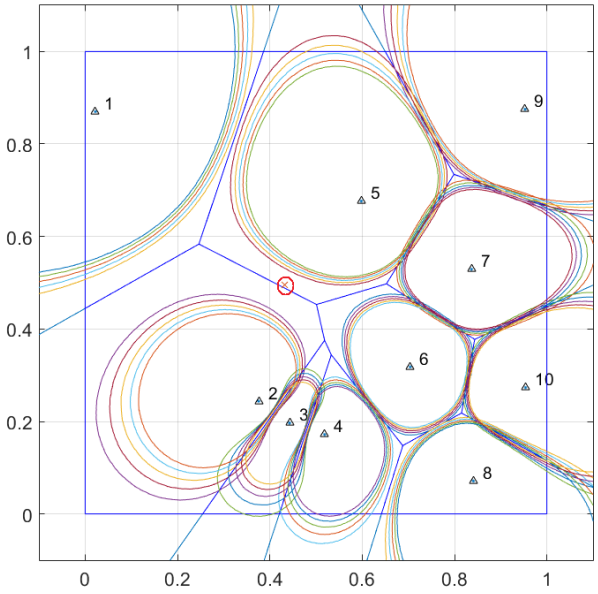


(a) The randomly chosen UE lies closer to an edge of a cell.

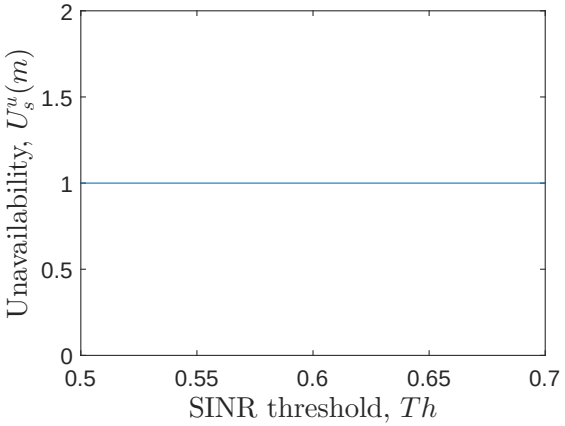


(b) The variation of individual user unavailability.

Figure 6.3: The individual user unavailability for a randomly chosen UE which lies closer to an edge of a cell.

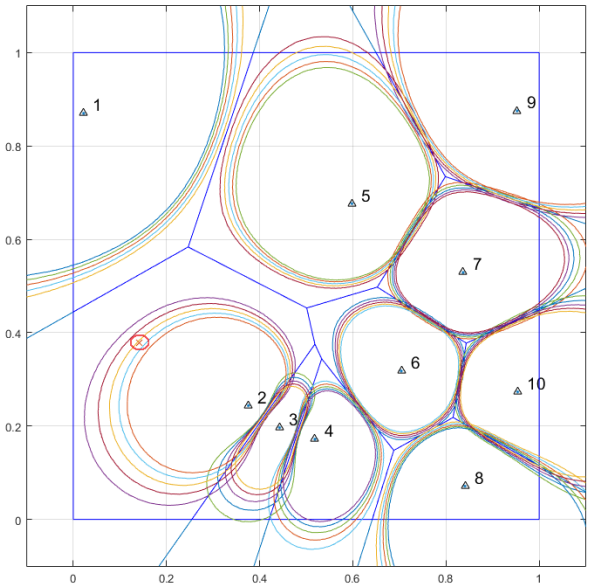


(a) The randomly chosen UE lies in between the SINR threshold contours.

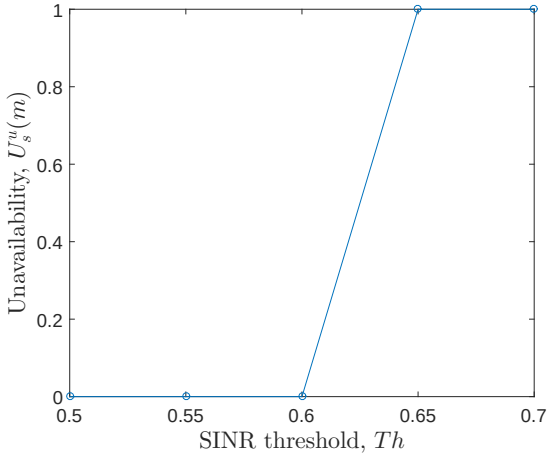


(b) The variation of individual user unavailability.

Figure 6.4: The individual user unavailability for a randomly chosen UE which lies in between the SINR threshold contours.

## 6.5 User-oriented System Availability of a PV Network with PPP Distributed Users

From the service provider's point of view, it is worth to know the indicated availability for the users within the system as a measure to evaluate the offered service. Therefore, we simulated

the user-oriented system availability, which apparently is the ratio between the number of users falling within the coverage $UE_{covered}$ and total number of users $N_{UE}$ within the system. Alg. 24 presents the algorithm which was used to simulate the user-oriented system availability considering that the coverage is defined by a given SINR threshold.

**Algorithm 24: Algorithm to estimate the user-oriented system availability of a PV network with PPP distributed users considering SINR-based coverage.**

**Input:** $x_B, y_B$ : Cartesian coordinates of the corresponding BS
**Input:** $N$ : Number of cells in the topology
**Input:** $Th$ : SINR threshold
**Input:** $\lambda_U$ : Intensity of the user PPP
**Input:** $\alpha$ : Path loss coefficient
**Output:** $A_s^u$ : User-oriented system availability
**[1]** Generate the Voronoi diagram using $(x_B, y_B)$ pairs
**[2]** Generate the user distribution of $\lambda_U$ intensity and obtain the Cartesian coordinates of UEs $(x_U, y_U)$
**[3]** Create SINR threshold contours using Alg. 10 and obtain its coordinates $S'$
**[4]** Count no. of UEs covered by the BSs $UE_{covered}$
**[5]** **if** $UE_{covered} \leq N_{UE}$ **then**
**[6]** $\quad A_s^u = \frac{UE_{covered}}{N_{UE}}$
**[7]** **else**
**[8]** $\quad A_s^u = 1$
**[9]** **end**

Fig. 6.5(a) illustrates the PV network in our interest consisting of PPP distributed users of intensity $\lambda_U = 1500$ along with the contours drawn for each SINR threshold. Fig. 6.5(b) depicts the variation of user-oriented system unavailability with each given SINR threshold. User-oriented system unavailability shows an increment when the SINR threshold increases. When the SINR threshold is higher, the coverage area of the BS shrinks such that lesser number of users fall within it and vice versa.

The simulations were also carried out considering different distributions to model the UEs within the PV network. We considered 2 distributions namely the PPP and uniform distribution, with 2 intensities of each. The simulations are carried out for $\lambda_U = 750$ and 1000 for PPP distribution and $N_{UE} = 750$ and 1000 for the uniform distribution. Also, it should be noted that, for a homogeneous PPP of intensity $\lambda_U = \rho$, number of UEs also can be approximated to $\rho$, i.e., $N_{UE} \approx \rho$.The results are shown in Fig. 6.6 and Tab. 6.1. It is observed that for the same intensity, PPP distribution indicates a higher system user unavailability compared to that of the uniform distribution. And for the same distribution unavailability decreases when the intensity increases.

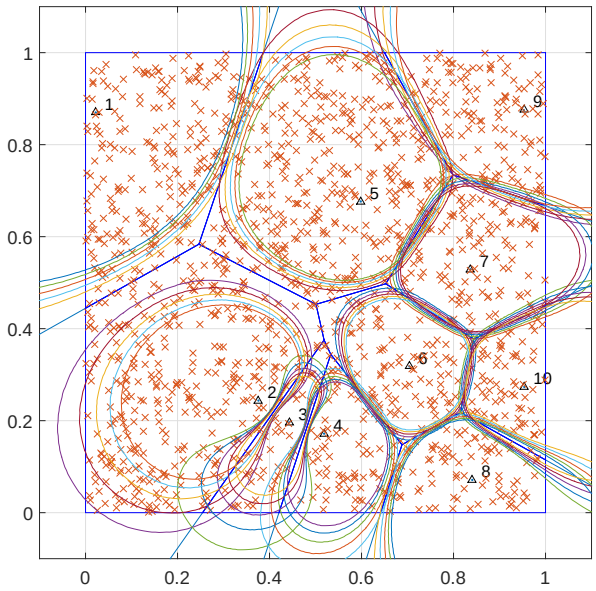


(a) The PV network with PPP distributed users and SINR threshold contours.

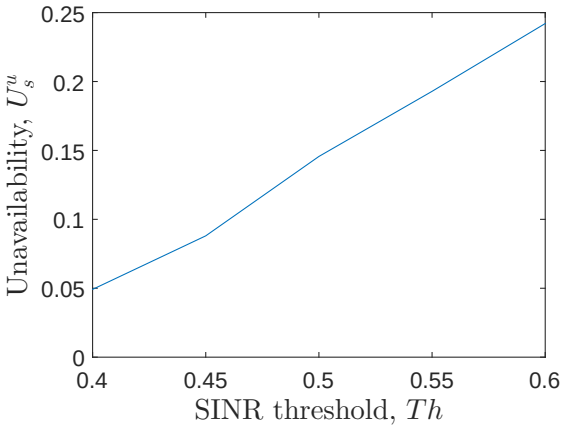


(b) The variation of system user unavailability with the SINR threshold variation.

Figure 6.5: The variation of user-oriented system unavailability as the SINR threshold increases.

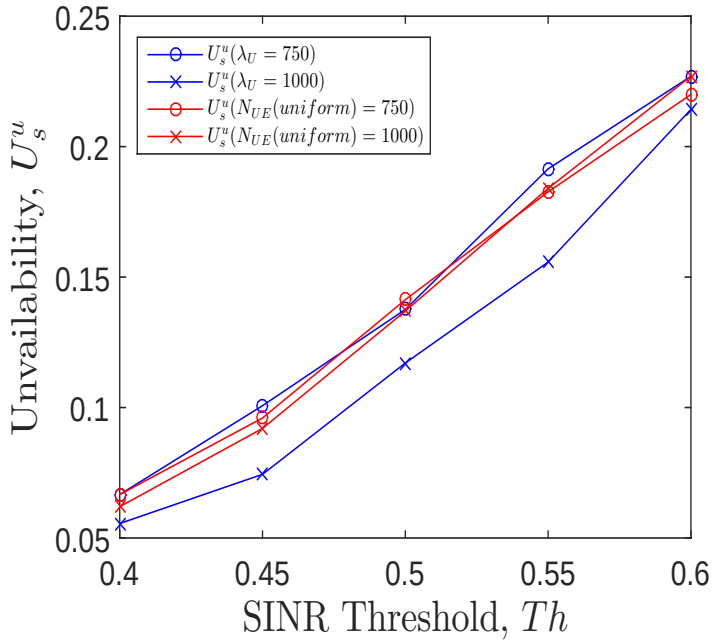


Figure 6.6: The variation of user-oriented system unavailability with the SINR threshold variation for different user distributions.

For a uniform distribution, the probability that there are $K$ out of $N$ nodes are distributed within a certain region of $A_0$, given the total system area as $A$ is given by Eq. (6.5), where, $p = \frac{A_0}{A}$.

$$P(N = K) = \binom{N}{K}(p)^K(1-p)^{N-K}. \tag{6.5}$$

Table 6.1: Numerical results of user-oriented system availability for PPP and uniform distributions

| SINR Threshold | 0.4 | 0.45 | 0.5 | 0.55 | 0.6 |
|---|---|---|---|---|---|
| $A_s^u(\lambda_U = 750)$ | 0.9333 | 0.8993 | 0.8624 | 0.8085 | 0.7730 |
| $A_s^u(\lambda_U = 1000)$ | 0.9444 | 0.9256 | 0.8829 | 0.8442 | 0.7857 |
| $A_s^u(N_{UE}(uniform) = 750)$ | 0.9333 | 0.9040 | 0.8587 | 0.8173 | 0.7800 |
| $A_s^u(N_{UE}(uniform) = 1000)$ | 0.9380 | 0.9080 | 0.8630 | 0.8160 | 0.7730 |

The probability that there are $K$ out of $N$ nodes within an area of $A_0$ for a PPP distribution of intensity of $\lambda_U$ is given by,

$$P(N = K) = \frac{(\lambda A_0)^K \ e^{-\lambda A_0}}{K!}. \tag{6.6}$$

For a given intensity of $\lambda_U$, $K, N$, $A_0$ and $A$, we find that the uniform distribution has a higher probability of having $K$ out of $N$ nodes compared to the PPP distribution containing the same number of nodes using Eq. (6.5) and Eq. (6.6). From a different perspective, we can also explain the behavior of user-oriented system availability illustrated in Fig. 6.6. When the number of nodes in a uniform distribution increases, the number of users covered by the BSs also increases since the users are distributed in a uniform manner. Yet, for a PPP distribution, since the distances between the neighboring nodes follow an exponential distribution, nodes (or the UEs) lie closer as the intensity increases. Therefore for a higher intensity $\lambda_U$, number of covered users increase significantly. However, there should exist a tradeoff between the intensity of the user distribution or the total number of users within the system, with the capacity offered from the system to achieve URC in the space domain.

## 6.6 PPP Distributed Users with Specific Resource Requirements

With the growing usage of sophisticated applications in the wireless communication, users tend to expect different resource requirements from the BSs in terms of capacity. Therefore, in this section we examine the effect on the user-oriented system unavailability with different resource requirements of the users.

### 6.6.1 Homogeneous resource requirements

When the resource requirements are homogeneous, every user in the system demands the same capacity to satisfy their demands. The algorithm used to simulate the user-oriented system availability for homogenous resource requirement scenario in a PV network is presented in Alg. 25. Fig. 6.7(a) illustrates the various capacity threshold boundaries along with

the PPP distributed users, having homogeneous resource requirements, dispersed within a PV network. Fig. 6.7(b) shows the user-oriented system unavailability for users having homogeneous resource requirements, in a system with capacity-based BS coverages.

**Algorithm 25: Algorithm to estimate the user-oriented system availability of a PV network with PPP distributed users considering homogeneous resource requirements.**

**Input:** $x_B, y_B$ : x, y coordinates of the BSs
**Input:** $\lambda_U$ : Intensity of the user PPP
**Input:** $Th$ : Capacity threshold
**Input:** $\alpha$ : Path loss coefficient
**Input:** $P_t$ : Transmitted power from the BS
**Input:** $u_g, u_l$ : System gains
**Input:** $k_b$ : Boltzmanns constant
**Input:** $T$ : Temperature of the system
**Input:** $\Delta f$ : Frequency spacing between subcarriers
**Input:** $N_{FFT}$ : Total number of subcarriers
**Input:** $N_{used}$ : Number of used subcarriers
**Input:** $\lambda$ : Wavelength of the signal
**Input:** $R$ : Error-correcting code rate
**Input:** $p$ : Ratio of the number of data subcarriers to the number of pilot subcarriers and data subcarriers
**Input:** $G$ : Ratio of guard time for an OFDM symbol to useful OFDM symbol time
**Input:** $n$ : Oversampling factor
**Input:** $W$ : Total bandwidth of the BSs
**Input:** $E_b$ : Energy per bit
**Output:** $A_s^u$ : user-oriented system availability

[1] Generate the Voronoi diagram using $(x_B, y_B)$ pairs
[2] Generate the user distribution of $\lambda_U$ intensity and obtain the Cartesian coordinates of UEs $(x_U, y_U)$
[3] Create capacity threshold contours using Alg. 16 and obtain its coordinates $S''$
[4] Count no. of UEs covered by the BSs $UE_{covered}$
[5] **if** $UE_{covered} \leq N_{UE}$ **then**
[6] $\quad A_s^u = \frac{UE_{covered}}{N_{UE}}$
[7] **else**
[8] $\quad A_s^u = 1$
[9] **end**

As observed from Fig. 6.7, when the capacity threshold increases, user-oriented system unavailability also increases accordingly. More specifically, user-oriented system unavailability shows an intense variation for low capacity thresholds but slowly increases for high capacity thresholds. When the capacity threshold is high, the BS can only serve for a limited area in which the number of users are limited.

### 6.6.2 Heterogeneous resource requirements

In the real life scenarios, users have heterogeneous resource requirements which means that users may demand different the bandwidths or capacity for the different applications they use. For the simulations performed in this section we consider two types of users namely, low resource requiring (LRR) users and high resource requiring (HRR) users using a OFDM system with $N_{FFT}$ subcarriers. HRR users demand for more subcarriers from the system to

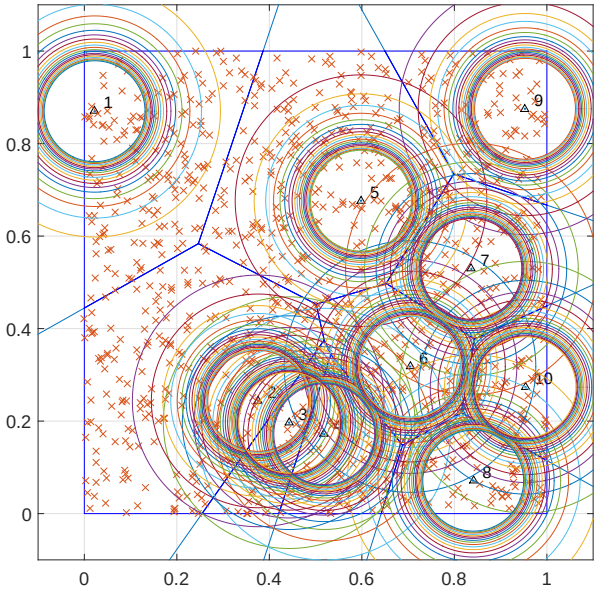


(a) The PV network with PPP distributed users and capacity threshold contours.

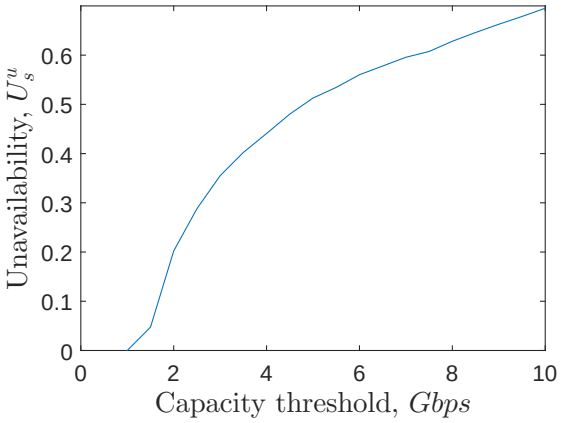


(b) The variation of user-oriented system unavailability with the capacity threshold variation.

Figure 6.7: User-oriented system unavailability for users with homogeneous user requirements.

fulfill their capacity requirements compared to LRR users. In Fig. 6.8 indicated by the crosses are the LRR users and indicated by the circles are the HRR users.

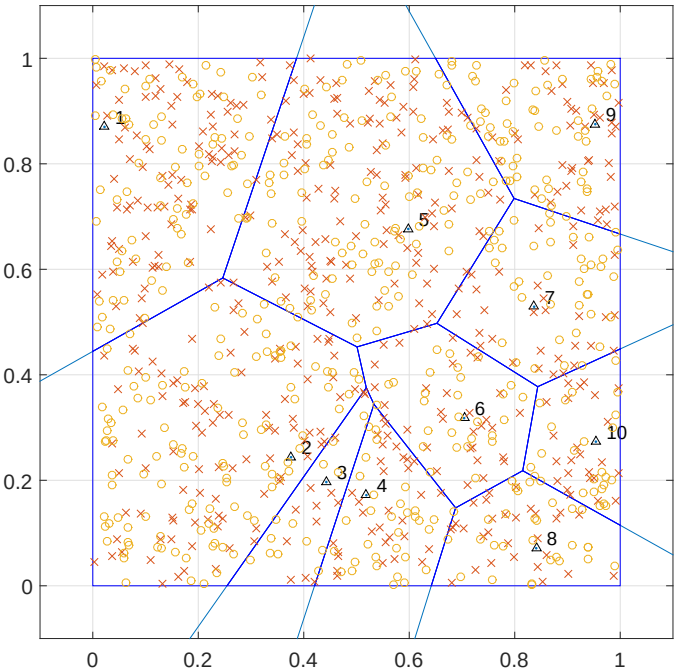


Figure 6.8: A PV network consisting of 10 BSs and LRR (illustrated by empty circles) and HRR (illustrated by cross symbols) users which follow 2 independent homogeneous PPP distributions of both having intensity of $\lambda_U = 500$.

Alg. 26 shows the algorithm used for performing the simulations for user-oriented system unavailability of a PV network with PPP distributed users considering low resource require-

ments. The same algorithm was modified for simulating system user availability of HRR users.

Fig. 6.9 illustrates the system user variation for heterogeneous scenario obtained for LRR and HRR users. It is evident that for both LRR and HRR users, the system user unavailability decreases when the capacity threshold increases. Further, it is observed that the unavailability of the HRR user system is higher than that of the LRR user system. It should be noted that the illustrated capacity threshold in Fig. 6.9 is the sum of the capacity offered for both LRR and HRR users by the system.

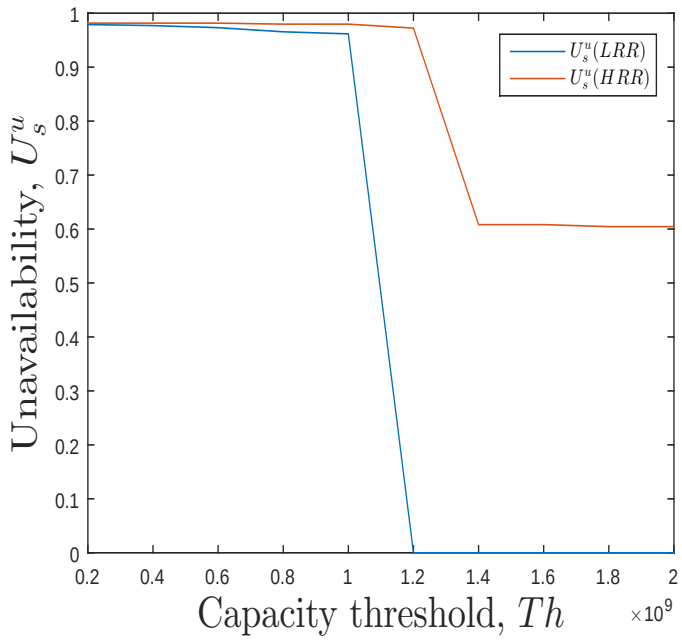


Figure 6.9: user-oriented system unavailability variation for LRR and HRR users when the capacity threshold increases.

The above behavior can be explained as follows. When the offered capacity by the system is low, system can only serve lesser number of users by satisfying their demands. Therefore the system user unavailability becomes substantial. Likewise, when the capacity offered by the system is high which is defined by means of the capacity threshold, system can serve more users resulting in lower system user unavailability. Also since a HRR user requires more capacity than a LRR user, for a given system capacity lesser number of HRR users can be satisfied, thus the unavailability of the HRR user system is higher than that of the LRR user system.

**Algorithm 26: Algorithm to estimate the user-oriented system availability of a PV network with PPP distributed users considering low resource requirements.**

**Input:** $x_B, y_B$ : x, y coordinates of the BSs
**Input:** $\lambda_U$ : Intensity of the user PPP
**Input:** $Th$ : Capacity threshold
**Input:** $\alpha$ : Path loss coefficient
**Input:** $P_t$ : Transmitted power from the BS
**Input:** $u_g, u_l$ : System gains
**Input:** $k_b$ : Boltzmanns constant
**Input:** $T$ : Temperature of the system
**Input:** $\Delta f$ : Frequency spacing between sub carriers
**Input:** $N_{L,FFT}$ : Total number of sub carriers for LRR users
**Input:** $N_1$ : Number of sub carriers required by LRR users
**Input:** $\lambda$ : Wavelength of the signal
**Input:** $R$ : Error-correcting code rate
**Input:** $p$ : Ratio of the number of data sub carriers to the number of pilot sub carriers and data sub carriers
**Input:** $G$ : Ratio of guard time for an OFDM symbol to useful OFDM symbol time
**Input:** $n$ : Oversampling factor
**Input:** $W$ : Total bandwidth of the BSs
**Input:** $E_b$ : Energy per bit
**Output:** $A_s^u$ : user-oriented system availability

[1] Generate the Voronoi diagram using $(x_B, y_B)$ pairs
[2] Generate the LRR user distribution of $\lambda_U$ intensity and obtain the Cartesian coordinates of UEs $(x_{U,L}, y_{U,L})$
[3] **for** $z = \frac{\pi}{180} : \frac{\pi}{180} : 2\pi$ **do**
[4] $d = 0.001 : d$ is the initial distance from the BS of the RC to any user
[5] $x_p(z) = x_B + d\ cos(z)$
[6] $y_p(z) = y_B + d\ sin(z)$
[7] $dist(z) = \sqrt{(x_p((z) - x_B)^2 + (y_p(z) - y_B)^2}$
[8] count $N_{L,covered}$ inside the circle defined by $d$ radius and $(x_B, y_B)$
[9] $N_{L,used} = N_{L,covered} \times N_1$
[10] $P_r(z) = \frac{P_t \lambda^2}{(4\pi)^2 dist(z)^\alpha}\ SNR(z) = \frac{P_r(z)}{k_b T \Delta f}$
[11] $log_2 M_{mod}(z) = \frac{SNR(z)\ k_b\ T\ (1+G)}{E_b}$
[12] $R_{b,L}(z) = \frac{n\ W\ (N_{L,used}-1)\ log_2 M_{mod}(z)\ R\ p}{N_{FFT}\ (1+G)}$
[13] **while** $R_{b,L}(z) \geq Th\ \&\ N_{L,used} \geq N_{L,FFT}$ **do**
[14] $d = d + 0.001$
[15] ; $x_p(z) = x_B + d\ cos(z)$
[16] $y_p(z) = y_B + d\ sin(z)$
[17] $dist(z) = \sqrt{(x_p((z) - x_B)^2 + (y_p(z) - y_B)^2}$
[18] count $N_{L,covered}$ inside the circle defined by $d$ radius and $xB, yB$
[19] $N_{L,used} = N_{L,covered} \times N_1$
[20] $P_r(z) = \frac{P_t \lambda^2}{(4\pi)^2 dist(z)^\alpha}\ SIR(z) = \frac{P_r(z)}{k_b T \Delta f}$
[21] $log_2 M_{mod}(z) = \frac{SNR(z)\ k_b\ T\ (1+G)}{E_b}$
[22] $R_{b,L}(z) = \frac{n\ W\ (N_{L,used}-1)\ log_2 M_{mod}(z)\ R\ p}{N_{FFT}\ (1+G)}$
[23] **end**
[24] **end**
[25] Count no. of LRR UEs covered by the BSs coverage $UE_{L,covered}$ : BS coverage is defined by the contour made of $(x_p, y_p)$ Cartesian coordinates
[26] **if** $UE_{L,covered} \leq N_{UE}$ **then**
[27] $A_s^u = \frac{UE_{L,covered}}{N_{UE}}$
[28] **else**
[29] $A_s^u = 1$
[30] **end**

## 6.7 Chapter Summary

In this chapter we analyzed the space domain availability in a novel approach considering the UEs of a cellular network. UEs are modeled as an independent homogeneous PPP and their spatial characteristics are used to obtain the definitions and the analysis of individual user availability ans system user availability. Furthermore, system user availability is more extensively analyzed considering both homogenous and heterogeneous resource requirements of users.

# Chapter 7

# Conclusions

*In this chapter, we conclude the thesis by providing a brief description of the progress made towards achieving the main objective of the thesis, a summary of the main conclusions and our contributions. We also suggest new research directions that have invoked as a result of our study.*

## 7.1 Conclusions

We presented the main objective of the research work done in this thesis as to advocate dependability-based availability definitions in the space domain in order to contribute the research work done in the context of URC. For achieving this goal, initially the existing work and the related concepts regarding the dependability analysis and URC are studied in detail. Thereafter, certain loopholes of the previous work done over dependability analysis and possible approaches to achieve URC are identified. Thus, the definitions for the availability in the space domain with a dependability perspective are derived using connectivity-based, SINR-based, capacity-based and user-oriented approaches.

To avoid certain limitations of previous models of cellular networks, SG is adapted to reflect more realistic spatial characteristics. The definitions for cell and system availability for connectivity-based, SINR-based, capacity-based perspectives are advocated and analyzed seperately. The probability of providing a guaranteed availability level is also deduced for the connectivity-based approach. Assuming UEs' distribution to be an independent PPP, the analysis is also extended to propose definitions for availability definitions in users' perspective. The proposed schemes are implemented in MATLAB in order to facilitate the evaluation of availability for the developed system models in each of the scenarios.

Therefore, it can be concluded that the main objectives of the thesis (as mentioned in Sec. 1.3) are achieved from the SG-based modelling, extensive simulations and analysis performed in Chaps. 3- 6. The findings of this thesis are expected to contribute towards the

progress of achieving URC in 5G networks.

## 7.2 Major Contributions

In the following, we highlight the main contributions that we have made through this thesis work.

- The concepts of cell availability and system availability in the space domain are solicited following a dependability perspective. According to the best of our knowledge, until now no such definitions exist in the literature. The definitions advocated based on the analysis presented in Chap. 3 have been disseminated as a journal paper in the IEEE Communication Letters.
- Connectivity-based cell availability and system availability considering both homogeneous and heterogeneous cellular networks have been analyzed. Also a comparison of the transmission power tradeoff between homogeneous and heterogeneous cellular networks has been presented.
- Guaranteed cell availability has been analyzed considering a PV network which employs SG characteristics. This is an important measure since many users are interested in the ability of the network to provide a certain level of availability. It is also worth to investigate the guaranteed cell availability of offering almost 100% availability, particularly for achieving URC.
- The threshold contours which define the boundary of exceeding the minimum achieved SINR and capacity are investigated. It is noteworthy identifying these boundaries that prescribe the borderlines in the space beyond which the BS cannot offer its service, i.e., network is unavailable in that particular space.
- Availability definitions in the space domain have been advocated in SINR and capacity driven deployments to provide a more extensive analysis of dependability in the space domain.
- User-oriented availability definitions have been also investigated by taking in to account the distribution of realistic user dispersions in cellular networks. Moreover, user requirements are identified as either homogeneous or heterogeneous and therein the respective user-oriented system availability is analyzed.

## 7.3 Future Work

During the work of this thesis, several interesting research areas have been emerged. Some of them are listed below.

- For this thesis work, proposed definitions were evaluated using MATLAB based simulations. More studies based on simulations can be performed via network simulators such as NS3 to perform extensive analysis. Also real-life test beds can be implemented to obtain more general results.

- The space domain availability analysis can be extended to obtain definitions for outage probability and area spectral efficiency (ASE). Outage probability can be defined as the probability that a UE can fall in to a region where a predetermined SINR or capacity threshold is not achieved. ASE can be defined as the maximum data rate per unit bandwidth per unit area achieved at a random UE location.

- Path availability, which can be defined as the availability that a UE attains by choosing a particular path within the network can also be analyzed. This path could be any random path a moving UE can follow. Within the selected path, an UE can pass path lengths where it is covered by a BS coverage, where it is not covered by any of the BS coverages or places where handovers can occur due to poor availability and overlapping of BS coverages are appeared. Considering UE's mobility patterns (for example random way point mobility), expressions can be formulated to evaluate the availability of a moving user in the space domain.

- Employing device-to-device (D2D) communication and relay assisted techniques to enhance the connectivity-based cell availability and thereby improving the system availability in the space domain.

# Bibliography

[1] J. Andrews, S. Buzzi, W. Choi, S. V. Hanly, A. Lozano, A. C. K. Soong, and J. C. Zhang, "What will 5G be?" *IEEE Journal on selected areas in communications*, vol. 32, no. 6, pp. 1065–1082, Nov. 2014.

[2] P. Popovski, "Ultra-reliable communication in 5G wireless systems," in *Proc. IEEE International Conference on 5G for Ubiquitous Connectivity (5GU)*, Nov. 2014, pp. 146–151.

[3] H. Shariatmadari, Z. Li, M. A. Uusitalo, S. Iraji, and R. Jäntti, "Link adaptation design for ultra-reliable communications," in *Proc. IEEE International Conference on Communications (ICC)*, Jul. 2016, pp. 1–5.

[4] E. Dahlman, G. Mildh, S. Parkvall, J. Peisa, J. Sachs, and Y. Selén, "5G radio access," *Ericsson review*, vol. 6, pp. 2–7, Jul. 2014.

[5] "IMT Vision - Framework and overall objectives of the future development of IMT for 2020 and beyond," ITU-R Recommendation M.2083, Tech. Rep., 2015, [Online] Available: https://www.itu.int/rec/R-REC-M.2083, Accessed on 20 May 2017.

[6] M. A. Marsan, L. Chiaraviglio, and D. Ciullo, "Optimal energy savings in cellular access networks," in *Proc. IEEE ICC*, Jun. 2009, pp. 1–5.

[7] G. Rubino and B. Sericola, *Markov chains and dependability theory*. Cambridge University Press, 2014, ISBN:978-1-107- 00757-4.

[8] E. Dubrova, *Fundamentals of dependability*. New York: Springer, 2013, pp. 5–20, [Online] Available: http://dx.doi.org/10.1007/978-1-4614-2113-92, Accessed on 20 May 2017.

[9] A. Snow, U. Varshney, and A. Malloy, "Reliability and survivability of wireless and mobile networks," *Computer*, vol. 33, no. 7, pp. 49–55, Jul. 2000.

[10] H. Pham, *System Software Reliability*. London: Springer, 2007, ch. System Reliability Concepts, pp. 9–75, [Online] Available: https://link.springer.com/chapter/10.1007%2F1-84628-295-0_2, Accessed on 20 May 2017.

[11] T. ITU, "Terms and definitions related to quality of service and network performance including dependability," *Recommendation E*, vol. 800, 1994.

[12] 3GPP-TR38.801, "Study on new radio access technology: Radio access architecture and interfaces," r14, v0.4.0 and v1.0.0, Aug. 2016 and Dec. 2016.

[13] S. M. Azimi, O. Simeone, O. Sahin, and P. Popovski, "Ultra-reliable cloud mobile computing with service composition and superposition coding," in *Proc. IEEE Annual Conference on Information Science and Systems (CISS)*, Mar. 2016, pp. 442–447.

[14] G. Durisi, T. Koch, and P. Popovski, "Toward massive, ultrareliable, and low-latency wireless communication with short packets," *Proceedings of the IEEE*, vol. 104, no. 9, pp. 1711–1726, Sep. 2016.

[15] J. J. Nielsen and P. Popovski, "Latency analysis of systems with multiple interfaces for ultra-reliable M2M communication," in *Proc. IEEE International Workshop on Signal Processing Advances in Wireless Communications (SPAWC)*, Jul. 2016, pp. 1–6.

[16] O. N. Yilmaz, K. V. Z. Li, M. Uusitalo, M. Moisio, P. Lundén, and C. Wijting, "Smart mobility management for D2D communications in 5G networks," in *Proc. IEEE Wireless Communications and Networking Conference Workshops (WCNCW)*, Apr. 2014, pp. 219–223.

[17] N. A. Johansson, Y.-P. E. Wang, E. Eriksson, and H. Martin, "Radio access for ultra-reliable and low-latency 5G communications," in *Proc. IEEE International Conference on Communication Workshop (ICCW)*, Jun. 2015, pp. 1184–1189.

[18] G. Pocovi, M. Lauridsen, B. Soret, K. I. Pedersen, and P. Mogensen, "Ultra-reliable communications in failure-prone realistic networks," in *Proc. International Symposium on Wireless Communication Systems (ISWCS)*, Sep. 2016, pp. 414–418.

[19] Z. Tao, P. V. Orlik, Z. Sahinoglu, A. F. Molisch, and J. Zhang, "Cooperative ultra-reliable wireless communications," Jul. 2012, US Patent 8218523 B2.

[20] M. J. Moisio, M. A. Uusitalo, O. Yilmaz, and Z. Li, "Ultra-reliable communication reliability and detection in mobile networks," Mar. 2014, US Patent 20160374136 A1.

[21] H. D. Schotten, R. Sattiraju, D. G. Serrano, Z. Ren, and P. Fertl, "Availability indication as key enabler for ultra-reliable communication in 5G," in *Proc. IEEE European Conference on Networks and Communications (EuCNC)*, Jun. 2014, pp. 1–5.

[22] U. Varshney and A. Malloy, "Improving the dependability of wireless networks using design techniques," in *Proc. IEEE Annual Conference on Local Computer Networks (LCN)*, Nov. 2001, pp. 122–131.

[23] D. Chen, C. Kintala, S. Garg, and K. S. Trivedi, "Dependability enhancement for IEEE 802.11 wireless LAN with redundancy techniques," in *Proc. International Conference on Dependable Systems and Networks*, Jun. 2003, pp. 521–528.

[24] I. A. M. Balapuwaduge, F. Y. Li, and V. Pla, "System times and channel availability for secondary transmissions in CRNs: A dependability-theory-based analysis," *IEEE Transactions on Vehicular Technology*, vol. 66, no. 3, pp. 2771–2788, Mar. 2017.

[25] Z. Jing and N. Zhisheng, "A reliable TCP-aware link layer retransmission for wireless networks," in *Proc. IEEE International Conference on Communication Technology (ICCT) Proceedings*, Aug. 2000, pp. 900–905.

[26] H. Balakrishnan, V. Padmanabhan, S. Seshan, and R. Katz, "Improving reliable transport and handoff performance in cellular wireless networks," *Wireless Networks*, vol. 1, no. 4, pp. 469–481, Dec. 1995.

[27] R. Vaze, "Throughput-delay-reliability tradeoff with ARQ in wireless ad hoc networks," *IEEE Transactions on Wireless Communications*, vol. 10, no. 7, pp. 2142–2149, Jul. 2011.

[28] Q. Chen and M. C. Gursoy, "Energy-efficient modulation design for reliable communication in wireless networks," in *Proc. IEEE Annual Conference on Information Sciences and Systems (CISS)*, Mar. 2009, pp. 811–816.

[29] M. Ghaderi, D. Towsley, and J. Kurose, "Network coding performance for reliable multicast," in *Proc. IEEE Military Communications Conference (MILCOM)*, Oct. 2007, pp. 1–7.

[30] D. Nguyen, T. Tran, T. Nguyen, and B. Bose, "Wireless broadcasting using network coding," *IEEE Transactions on Vehicular Technology*, vol. 58, no. 2, pp. 914–925, Feb. 2009.

[31] D. S. Lun, M. Médard, R. Koetter, and M. Effros, "On coding for reliable communication over packet networks," *Physical Communication*, vol. 1, no. 1, pp. 3–20, Mar. 2008.

[32] M. Ghaderi, D. Towsley, and J. Kurose, "Reliability benefit of network coding," *Department of Computer Science, University of Massachusetts Amherst, Tech. Rep. TR-07-08*, 2007, [Online] Available: https://link.springer.com/chapter/10.1007%2F1-84628-295-0_2, Accessed on 20 May 2017.

[33] M. Goyal, S. Prakash, W. Xie, Y. Bashir, H. Hosseini, and A. Durresi, "Evaluating the impact of signal to noise ratio on IEEE 802.15.4 PHY-level packet loss rate," in *Proc. IEEE International Conference on Network-Based Information Systems (NBiS)*, Sep. 2010, pp. 279–284.

[34] P. Fan and K. B. Letaief, "On MIMO transmission over fading channels: Reliable throughput vs. outage probability," in *Proc. IEEE Global Telecommunications Conference (GLOBECOM)*, Dec. 2011, pp. 1–5.

[35] R. Sattiraju and H. D. Schotten, "Reliability modeling, analysis and prediction of wireless mobile communications," in *Proc. IEEE Vehicular Technology Conference (VTC Spring)*, May. 2014, pp. 1–6.

[36] A. Birolini, *Reliability Engineering: Theory and Practice*. Springer, 2014.

[37] R. Sattiraju, P. Chakraborty, and H. D. Schotten, "Reliability analysis of a wireless transmission as a repairable system," in *Proc. IEEE Globecom Workshops (GC Wkshps)*, Dec. 2014, pp. 1397–1401.

[38] J. Sauv and F. S. Coelho, "Availability considerations in network design," in *Proc. IEEE Pacific Rim International Symposium on Dependable Computing*, Dec. 2001, pp. 119–126.

[39] G. Egeland and P. E. Engelstad, "The availability and reliability of wireless multi-hop networks with stochastic link failures," *IEEE Journal on Selected Areas in Communications*, vol. 27, no. 7, pp. 1132–1146, Sep. 2009.

[40] A. McDonald and T. Znati, "A path availability model for wireless ad hoc networks," in *Proc. IEEE Wireless Communications and Networking Conference (WCNC)*, Sep. 1999, pp. 35–40.

[41] F. Muhammad, Z. Abbas, and F. Y. Li, "Cell association with load balancing in non-uniform heterogeneous cellular networks: Coverage probability and rate analysis," *IEEE Transactions on Vehicular Technology*, Sep. 2016, early access available in IEEE Xplore, May 2017. DOI: 10.1109/TVT.2016.2614696.

[42] F. Baccelli, M. Klein, M. Lebourges, and S. Zuyev, "Stochastic geometry and architecture of communication networks," *Telecommunication Systems*, vol. 7, no. 1, pp. 209–227, Jun. 1997.

[43] F. Baccelli and S. Zuyev, "Stochastic geometry models of mobile communication networks," in *Frontiers in queueing: models and applications in science and engineering*, 1996, pp. 227–243.

[44] T. X. Brown, "Cellular performance bounds via shotgun cellular systems," *IEEE Journal on Selected Areas in Communications*, vol. 18, no. 11, pp. 2443–2455, Nov. 2000.

[45] S. Lee and K. Huang, "Coverage and economy of cellular networks with many base stations," *IEEE Communications Letters*, vol. 16, no. 7, pp. 1038–1040, 2012.

[46] J. G. Andrews, F. Baccelli, and R. K. Ganti, "A tractable approach to coverage and rate in cellular networks," *IEEE Transactions on Communications*, vol. 59, no. 11, pp. 3122–3134, Nov. 2011.

[47] T. Bai and R. W. Heath, "Location-specific coverage in heterogeneous networks," *IEEE Signal Processing Letters*, vol. 20, no. 9, pp. 873–876, Sep. 2013.

[48] S. Mukherjee, "Distribution of downlink SINR in heterogeneous cellular networks," *IEEE Journal on Selected Areas in Communications*, vol. 30, no. 3, pp. 575–585, Apr. 2012.

[49] P. Madhusudhanan, J. G. Restrepo, Y. Liu, T. X. Brown, and K. R. Baker, "Downlink performance analysis for a generalized shotgun cellular system," *IEEE Transactions on Wireless Communications*, vol. 13, no. 12, pp. 6684–6696, Dec. 2014.

[50] Y. J. Chun, M. O. Hasna, and A. Ghrayeb, "Modeling heterogeneous cellular networks interference using poisson cluster processes," *IEEE Journal on Selected Areas in Communications*, vol. 33, no. 10, pp. 2182–2195, Oct. 2015.

[51] H.-S. Jo, Y. J. Sang, P. Xia, and J. G. Andrews, "Heterogeneous cellular networks with flexible cell association: A comprehensive downlink SINR analysis," *IEEE Transactions on Wireless Communications*, vol. 11, no. 10, pp. 3484–3495, 2012.

[52] I. A. M. Balapuwaduge, "Channel access and reliability performance in cognitive radio networks: Modeling and performance analysis," Ph.D. dissertation, University of Agder - Norway, Jun. 2016, [Online] Available: https://brage.bibsys.no/xmlui/handle/11250/2413948, Accessed on 20 May 2017.

[53] V. K. Katukoori, "Standardizing availability definition," *University of New Orleans, New orleans, LA., USA*, 1995.

[54] V. H. Mac Donald, "Advanced mobile phone service: The cellular concept," *Bell System Technical Journal*, vol. 58, no. 1, pp. 15–41, Jan. 1979.

[55] A. Goldsmith, *Wireless Communications*. Cambridge University Press, 2005.

[56] T. S. Rappaport, *Wireless communications: principles and practice*. Prentice Hall PTR New Jersey, 1996, vol. 2.

[57] H. ElSawy, A. Sultan-Salem, M.-S. Alouini, and M. Z. Win, "Modeling and analysis of cellular networks using stochastic geometry: A tutorial," *IEEE Communications Surveys & Tutorials*, 2016.

[58] D. J. Daley and D. Vere-Jones, *An introduction to the theory of point processes*. Springer, 1988.

[59] M. Haenggi, J. G. Andrews, F. Baccelli, O. Dousse, and M. Franceschetti, "Stochastic geometry and random graphs for the analysis and design of wireless networks," *IEEE Journal on Selected Areas in Communications*, vol. 27, no. 7, pp. 1029–1046, May 2009.

[60] B. François and B. Bartłomiej, "Stochastic geometry and wireless networks. volume I. theory," 2009.

[61] S. N. Chiu, D. Stoyan, W. S. Kendall, and J. Mecke, *Stochastic geometry and its applications*. John Wiley & Sons, 2013.

[62] M. Quine and D. Watson, "Radial generation of n-dimensional Poisson processes," *Journal of Applied Probability*, vol. 21, no. 03, pp. 548–557, 1984.

[63] M. Tanemura, "Statistical distributions of Poisson Voronoi cells in two and three dimensions," *FORMA-TOKYO-*, vol. 18, no. 4, pp. 221–247, 2003.

[64] M. Tanemura, in Proceedings of Intersections of Art and Science, July 8-14, 2001, Sydney eds. G. Lugosi and D. Nagy.

[65] A. Hinde and R. Miles, "Monte carlo estimates of the distributions of the random polygons of the Voronoi tessellation with respect to a Poisson process," *Journal of Statistical Computation and Simulation*, vol. 10, no. 3-4, pp. 205–223, 1980.

[66] S. DiCenzo and G. Wertheim, "Monte carlo calculation of the size distribution of supported clusters," *Physical Review B*, vol. 39, no. 10, p. 6792, 1989.

[67] D. Weaire, J. Kermode, and J. Wejchert, philas. Mag. B 53 (5) (1986) L101.

[68] J.-S. Ferenc and Z. Néda, "On the size distribution of Poisson Voronoi cells," *Physica A: Statistical Mechanics and its Applications*, vol. 385, no. 2, pp. 518–526, Nov. 2007.

[69] A. Ghosh, J. Zhang, J. G. Andrews, and R. Muhamed, *Fundamentals of LTE*. Pearson Education, 2010.

[70] S. C. Yang, *OFDMA system analysis and design*. Artech House, 2010.

[71] C. E. Shannon, "A mathematical theory of communication," *Bell Labs Technical Journal*, vol. 27, no. 3, pp. 379–423, Jul. 1948.

[72] A. Goyal and A. N. Tantawi, "A measure of guaranteed availability and its numerical evaluation," *IEEE Transactions on Computers*, vol. 37, no. 1, pp. 25–32, Jan. 1988.

[73] A. Okabe, B. Boots, K. Sugihara, and S. Chiu, "Spatial tessellations: concepts and applications of voronoi diagrams. 1992," *Chichester, UK*, 1992.

[74] M. De Berg, M. Van Kreveld, M. Overmars, and O. C. Schwarzkopf, "Computational geometry," in *Computational geometry*. Springer, 2000, pp. 1–17.

[75] R. Pure and S. Durrani, "Computing exact closed-form distance distributions in arbitrarily-shaped polygons with arbitrary reference point," *The Mathematica Journal*, vol. 17, pp. 1–27, Jun. 2015.

# Appendix A

# A Published Paper based on Chap. 3

---

| | |
|---|---|
| **Title:** | Achieving Ultra Reliable Communication in 5G Networks:<br>A Dependability Perspective Availability Analysis in the Space Domain |
| **Authors:** | H. V. Kalpanie Mendis and Frank Y. Li |
| **Affiliation:** | Dept. of Information and Communication Technology, University of Agder (UiA),<br>N-4898 Grimstad, Norway |
| **Journal:** | *IEEE Communications Letters,* Early access available in IEEE Xplore,<br>April 2017, DOI: 10.1109/LCOMM.2017.2696958 |
| **Copyright ©:** | IEEE |

---

# Achieving Ultra Reliable Communication in 5G Networks: A Dependability Perspective Availability Analysis in the Space Domain

H. V. Kalpanie Mendis and Frank Y. Li

***Abstract* — As part of the 5G communication paradigm, ultra reliable communication (URC) is envisaged as an important technology pillar for providing anywhere and anytime services to end users. While most existing studies on reliable communication do not investigate this problem from a dependability theory perspective, those dependability based studies tend to define reliability merely in the time domain. In this letter, we advocate extending the concept of URC from the dependability perspective also *in the space domain*. We initiate definitions on cell availability and system availability. Correspondingly, the availability as well as the probability of providing a guaranteed level of availability in a network are analyzed both/either cell-wise and/or system-wise. Poisson point process (PPP) and Voronoi tessellation are adopted to model the spatial characteristics of cell deployment in both homogeneous and heterogeneous networks.**

*Keywords*—URC, dependability and availability, space domain analysis, Poisson point process, Voronoi tessellation.

## I. Introduction

Ultra reliable communication (URC) is foreseen as one of the essential service requirements for 5G mobile and wireless networks. It aims at achieving almost 100% reliability at a certain (satisfactory) level of services [1]. The terminology of URC is introduced by the METIS project which had the objective of laying the foundation for 5G technologies. A 3GPP technical report [2] also included the concept of URC.

Reliable communication for an end-user in its simplest term can be defined as having connectivity to the network at anywhere and anytime. However, most studies on reliability have solely focused on the anytime connectivity or the time domain analysis. Little work has been done regarding the anywhere aspect of reliable communication or the space domain analysis.

Manuscript received March 24, 2017; accepted April 13, 2017. The associate editor coordinating the review of this paper and approving it for publication was L. Wang. (Corresponding author: Frank Y. Li.)

The authors are with the Department of Information and Communication Technology, University of Agder, N-4898 Grimstad, Norway (email: hvmend15@uia.no; frank.li@uia.no).

Digital Object Identifier 10.1109/LCOMM.2017.2696958

With respect to the metrics used to characterize reliable communication, parameters such as packet delivery ratio, outage probability, signal to interference and noise ratio (SINR), bit error rate (BER) are popular ones. These metrics represent the conventional understanding of reliable communication, but they do not address the reliability issue from a dependability theory point of view. In the context of the dependability theory, metrics such as mean time to failure (MTTF), mean time between failures (MTBF), and mean time to repair (MTTR) have been defined to investigate reliability. These dependability terminologies are however applicable to the time domain, not the space domain.

Considering applying URC in the time domain, [3] investigated the tradeoff between mobile energy and latency for mobile cloud computing applications. Furthermore, [4] provided a review of recent advances for short packet communications through three examples in order to achieve massive, ultra reliable and low latency wireless communications.

For space domain analysis, one may apply a Poisson point process (PPP) to capture the randomness of cell deployments and user equipment (UE) distribution in today's cellular networks. For instance, [5] employed the PPP to model one-tier networks and obtained a tractable result for coverage probability and average data rate of UEs. A model to analyze the coverage probability for PPP-based heterogeneous networks (HetNets) was presented in [6]. The probability that a user is connected to a macro-cell or open access femto-cell was computed in [7] by using a realistic stochastic geometry (SG) model. [8] derived expressions for UE coverage probability in HetNets considering random fading with arbitrary distributions and non-homogeneous PPP base station (BS) distributions.

Although many existing studies have investigated BS or/and UE distributions and obtained coverage probability, SINR profile or outage probability, a proper definition of reliability and availability *in the space domain* is lacking from the dependability theory's perspective. To the best of our knowledge, so far no definition exists on the availability of UEs in the space domain dedicated to URC. In this letter, we introduce the concept of cell availability and system availability in the space domain and derive their expressions in both homogenous networks (HomNets) and HetNets.

## II. Network Scenario and Assumptions

To perform space domain analysis, the physical deployment of BS locations and UE distributions need to be considered. Traditionally, a cellular network is often assumed to be deployed on a hexagonal grid (for coverage calculation convenience). To model the spatial randomness of modern cellular networks consisting of typically heterogeneous cells with various sizes, SG is a powerful tool. When applying SG into wireless networks, PPP and Voronoi diagrams are popular mathematical models in order to retain tractability of BSs or/and UEs and to study cell tessellations.

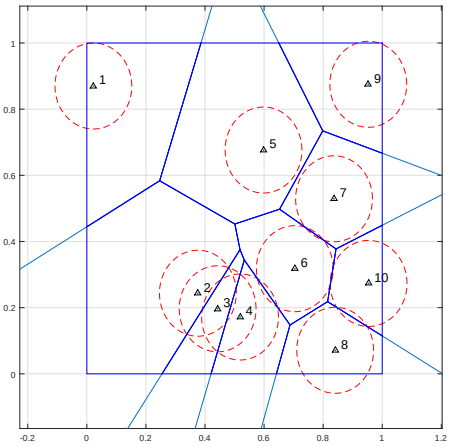


Figure A.1: A PV distributed cellular network with $N = 10$ cells/BSs. The cell boundaries are shown and the cells together form a Voronoi tessellation. The Voronoi cell boundaries which create the actual geographical area of each cell are indicated in blue (solid) lines. The BS coverage which the BS can communicate with the UEs within each cell is indicated in red (dashed) lines.

Consider a Poisson Voronoi (PV) distributed cellular network consisting of $N$ number of cells. In each cell there is a BS and the whole network is covered by a Voronoi tessellation with $N$ cells, as shown in Fig. 1. It is worth highlighting that each Voronoi cell might contain different cell size since the Voronoi cell boundaries are defined by lines bisecting the distances between each two neighboring BSs. For the ease of analysis, we focus on a $1 \times 1$ unit region of a cellular network.

Two cellular network deployment scenarios are considered in our study, i.e., HomNets and HetNets, as presented below. In both cases, the BS antenna is assumed to be omni-directional for all cells. Two types of cells, i.e., type 1 (T1) cells and type 2 (T2) cells, are considered with the same channel type and propagation condition but with different transmission ranges.

- HomNet: All BSs transmit with an identical transmission power level and have the same coverage radius, $R_2$. That is, there exists only one type of cells, T2.
- HetNet: It consists of both T1 and T2 cells. A T2 cell is deployed when its Voronoi cell size is greater than a predefined threshold value, $\eta$. Otherwise a T1 cell with radius $R_1$, where $R_1 < R_2$, is deployed.

Note that the Voronoi cell size is independent of the transmission power of its associated BS. Another underlying assumption of the above scenarios is that all BSs are distributed based on a homogeneous PPP with a constant intensity level in the Euclidean plane [5].

## III. Availability Definition

In this section, we firstly revisit the time domain definition of availability and then develop our concept which defines network availability in the space domain. The space domain network availability deals with the *anywhere* aspect of URC.

### *A. Availability Definition from the Time Domain*

For a repairable system, the available time or the uptime is the time duration during which the system is operational. Similarly, the unavailable time or the downtime for a repairable system is the time duration during which the system is not operational. Let MUT and MDT denote mean uptime and mean downtime respectively. The steady state availability in the time domain, $A_t$, can be expressed as,

$$A_t = \frac{MUT}{MUT + MDT}. \tag{A.1}$$

### *B. Availability Definition from the Space Domain*

Analogous to the time domain, we adopt a similar ratio to define space domain availability. Conceptually, the network availability in the space domain is defined as the ratio between the covered area by the BS(s) and the total area of a cell or network of interest. Consider the randomness of cell sizes in SG cellular networks and denote the mean covered area and the mean uncovered area as MCA and MUA respectively. We can express the availability in the space domain, $A_s$, as,

$$A_s = \frac{MCA}{MCA + MUA}. \tag{A.2}$$

Bringing forward the above concept, we further define two availability terminologies as follows.

- **Cell availability** $A_s^c$: defined as the covered area by the BS of an individual cell of interest divided by the area (or size) of the cell. Denote these two areas by $C(i)$ and $S(i)$ respectively for a randomly selected cell, $i$, *in a given network topology*. We have,

$$A_s^c(i) = \begin{cases} \frac{C(i)}{S(i)}, & \text{if } C(i) < S(i); \\ 1, & \text{otherwise.} \end{cases} \tag{A.3}$$

  Furthermore, the average cell availability $\bar{A}_s^c$ for *a given network topology* consisting of $N$ cells is expressed as,

$$\bar{A}_s^c = \frac{1}{N} \sum_{i=1}^{N} A_s^c(i). \tag{A.4}$$

- **System availability** $A_s^s$: For a specific network topology, $A_s^s$ is defined as the ratio

between the sum of the total covered area of all individual cells and the total area of the network including all $N$ cells. That is,

$$A_s^s = \begin{cases} \frac{\sum_{i=1}^{N} C(i) - \Delta}{\sum_{i=1}^{N} S(i)}, & \text{if } \sum_{i=1}^{N} C(i) - \Delta < \sum_{i=1}^{N} S(i); \\ 1, & \text{otherwise} \end{cases} \tag{A.5}$$

where $\Delta$ represents those overlapped coverage areas among neighboring BSs and the 'exurban' areas of outer-tier cells. While an overlapping area is an area mutually covered by two or more neighboring BSs, an exurban area is the area which belongs to an outer-tier cell but falls outside the region of interest, i.e., beyond the $1 \times 1$ border in Fig. 1.

Furthermore, the cell unavailability of cell $i$ and the system unavailability, denoted by $U_s^c(i)$ and $U_s^s$ respectively, are defined as,

$$U_s^c(i) = 1 - A_s^c(i); \quad U_s^s = 1 - A_s^s. \tag{A.6}$$

Therefore, the goal of achieving URC in the space domain is to diminish system unavailability to a sufficiently low level.

## III. Space Domain Availability in a PV Network

To apply the defined space domain availability to cellular networks, we need to calculate both $MCA$ and mean cell area.

### *A. The Size of a Voronoi Polygon: A Deterministic Expression*

To compute the area of each Voronoi polygon, i.e., $S(i)$, the well-known shoelace formula has been adopted. It is a mathematical algorithm to calculate the area of a simple 2-dimensional polygon whose vertices are represented by ordered pairs in the plane. Let $(x_j, y_j)$ be the coordinates of vertex $j$, $l$ be the number of edges of the Voronoi polygon, and $S$ be the area of the polygon. Then the formula to calculate the area of the Voronoi polygon is expressed as,

$$S = \frac{1}{2} \left| \sum_{j=1}^{l-1} x_j y_{j+1} + x_l y_1 - \sum_{j=1}^{l-1} x_{j+1} y_j - x_1 y_l \right|. \tag{A.7}$$

The above calculated individual cell area will be used to compute the cell and system availability defined in Sec. III by replacing $S$ with $S(i)$ for cell $i$ under a given topology.

Consider now a PV network with $N = 10$ cells distributed in a $1 \times 1$ unit region. A snapshot of a such a cellular network is shown in Fig. 1. We perform MATLAB based simulations for our space domain availability evaluation. For the HetNet scenario, the threshold to distinguish

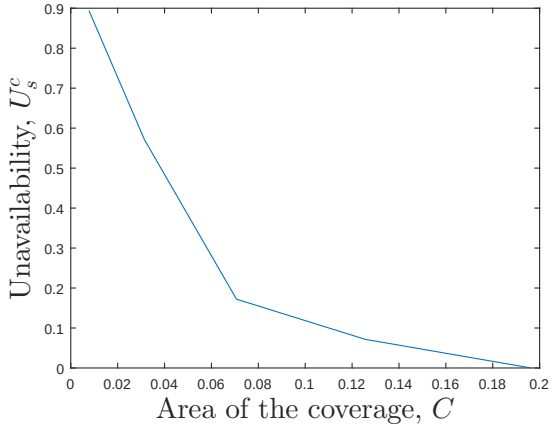


Figure A.2: Cell unavailability of the reference cell as BS coverage increases.

a cell as a T1 or T2 cell is configured as $\eta = 0.085$ unit$^2$. The radius of the BS coverage for a T1 or T2 cell varies as $R_1 = 0.1 \sim 0.16$ or $R_2 = 0.1 \sim 0.2$ unit respectively.

### *B. Cell Availability for HomNets*

Refer to cell number 6 in Fig. 1 as a reference cell (RC) in this study. Fig. 2 illustrates its obtained $U_s^c(i)$ variation as the BS coverage, i.e., $\pi R^2$, increases. With a very small BS coverage, i.e., at a very low transmission power level, the unavailability turns to be quite high. As the BS transmission power increases, the unavailability decreases monotonically to a substantially low level. The cell unavailability reaches zero when the BS coverage is sufficiently large, implying that all the users residing in the RC are connected to the network.

### *C. System Availability for HomNets and HetNets*

To obtain system availability, we need to include all cells in the studied network. To cover the whole network, we may deploy either the same type of cells (i.e., HomNets) or two types of cells (i.e., HetNets). Fig. 3 depicts the individual cell unavailability in green (dashed), average cell unavailability in blue (solid with triangle marks) and the system unavailability red (solid with plus marks) lines respectively as the BS coverage increases, for the HomNet scenario. When the BS coverage is low, the system unavailability is high since a user can very likely fall into an uncovered area. Increasing the BS coverage will obviously reduce the system unavailability for the whole network but it is not effective for lifting individual cell availability due to the diversity of cell sizes in a PV network. As shown from the plot, many cells reach zero unavailability much earlier than the system unavailability does. This result means that it is not smart to increase the BS transmission power for the whole network simultaneously. In other words, the deployment of a HetNet is appreciated.

Fig. 4 depicts how the cell unavailability and system unavailability vary for a HetNet. For the same PV network with $N = 10$ and $\eta = 0.085$, there are 7 T1 cells and 3 T2 cells. In addition to the individual cell unavailability, the blue (solid with triangle marks) curve

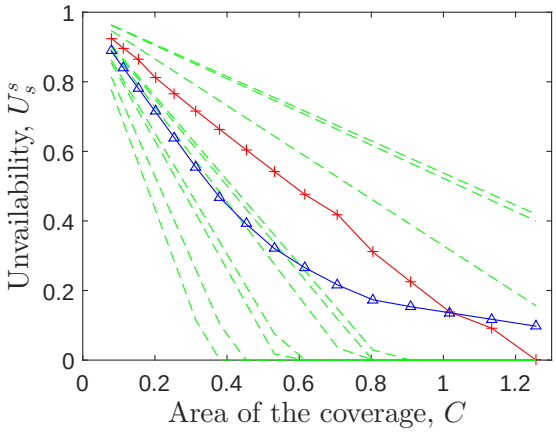


Figure A.3: Cell and system unavailability in a HomNet with $N = 10$ cells.

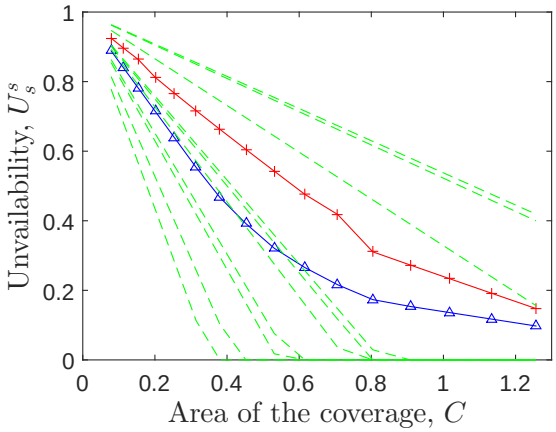


Figure A.4: Cell/system unavailability in a HetNet with 3(7) T2(T1) cells.

represents the average cell unavailability for T1 and T2 cells respectively. Another curve in red (solid with plus marks) illustrates the system unavailability for the whole HetNet.

When comparing the system unavailability of the HomNet (in which all cells have the same radius as $R_2$) with that of the HetNet, we observe that the unavailability of the HetNet is higher. This is because the coverage of those T1 cells is lower than that of the T2 cells. At the same time, the total transmission power of the whole network is reduced in a HetNet. Although providing lower availability to end-users may have negative effect on user satisfaction, a network service provider would be interested in identifying the tradeoff between BS transmission power levels and cell/system availability for its network deployment considering for instance a combination of macro- and small-cells.

### *D. System Availability for HomNets and HetNets*

To study the tradeoff between system availability and transmission power, we calculate and compare the total BS transmission power in the HomNet versus in the HetNet. For illustration simplicity, the free space propagation model is adopted in our calculation. That is, $P_r(d) = \frac{P_t G_t G_r \lambda}{(4\pi)^2 d^\alpha L}^2$ where $P_r(d)$ is the reception power at the UE which is $d$ distance away from the BS, $P_t$ is the transmission power, $G_t$ and $G_r$ are the antenna gains of the transmitter

Table A.1: The Tradeoff between Availability and Transmission Power

| $R_1$ (km) | $R_2$ (km) | HetNet | | HomNet | |
|---|---|---|---|---|---|
| | | $A_s^s$ | Total $P_t$ (W) | $A_s^s$ | Total $P_t$ (W) |
| 0.11 | 0.17 | 0.4395 | 1416.85 | 0.7739 | 2644.60 |
| 0.11 | 0.20 | 0.5030 | 1814.53 | 1.0000 | 3970.20 |
| 0.14 | 0.17 | 0.5736 | 1932.72 | 0.7739 | 2644.60 |
| 0.14 | 0.20 | 0.6348 | 2330.40 | 1.0000 | 3970.20 |

and the receiver respectively, $\lambda$ is the wavelength in meters, $\alpha$ is the path loss coefficient, and $L$ is the system loss factor.

Assume that $G_t = G_r = 1$, $\alpha = 2.5$, $L = 1$, and $\lambda = 15$ cm. Configure $P_r(R) = 0.1$ $\mu$W as the required $P_r$ for a UE which is located at the boundary of the BS coverage, with radius $R$. Consider the $N = 10$ cell network shown in Fig. 1. Table A.1 illustrates the numerical results on the obtained system availability and the total (i.e., for 10 cells together) required transmission power for both HomNet and HetNet. Keep the same threshold as $\eta = 0.085$ km$^2$. There are respectively 7 T1 cells (with coverage radius $R_1$) and 3 T2 cells (with coverage radius $R_2$) in the HetNet case. In the HomNet case, all 10 cells are homogeneous with coverage radius $R_2$.

With four different combinations of cell coverage for T1 and T2 cells, we illustrate the tradeoff between system availability and total transmission power. For instance, the last row tells us that to increase the system availability from $A_s^s = 63.48\%$ (obtained by the HetNet) to $A_s^s = 100\%$ (obtained by the HomNet), a 70% higher power level is required.

## V. Guaranteed Levels of Availability

Although a high level of availability is expected, there is no guarantee that it can be obtained in a network. The average availability itself does not provide a complete view regarding the obtained cell availability from the system's point of view. Network operators may additionally be interested in obtaining the probability of achieving a given level of availability. In this section, we introduce another dependability measure which expresses the probability of providing a predetermined or guaranteed level of availability [9].

### *A. The Normalized Size of a PV Polygon: A Stochastic View*

In the literature, there does no exist a standard closed-form expression to calculate the average area of a Voronoi cell. The size of a Voronoi cell, $g(S)$, is indeed one of the to-be-clarified aspects regarding PV diagrams. Instead of obtaining an explicit expression for $g(S)$, it is more convenient to use a general $f_{2D}(y)$ distribution function to express the normalized cell sizes $y = S/\bar{S}$, where $S$ is the area of Voronoi cell and $\bar{S} = \frac{1}{N}\sum_{i=1}^{N} S(i)$. Accordingly, it is shown that the probability density function (PDF) of a *normalized* PV cell area $y$ in a 2-dimensional space can be approximated as [10]

$$f_{2D}(y) = \frac{343}{15}\sqrt{\frac{7}{2\pi}}y^{2.5}exp\left(-3.5y\right). \tag{A.8}$$

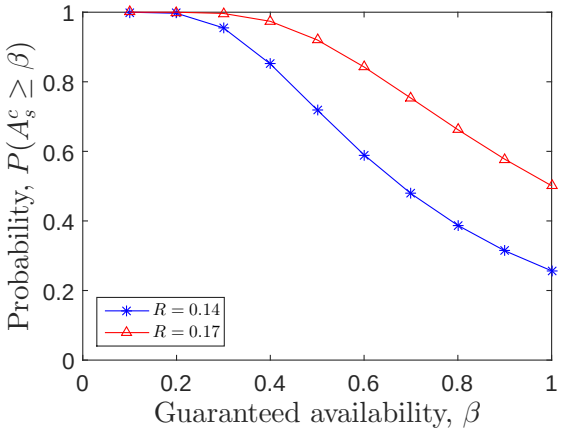


Figure A.5: The probability for providing a guaranteed cell availability level.

Moreover, from the cumulative distribution function (CDF) of (A.8) we obtain the probability that the normalized Voronoi cell area $y$ is smaller than or equal to a value $c$ and it is given by

$$P\left(y \leq c\right) = \int_0^c f_{2D}\left(y\right) dy. \tag{A.9}$$

### *B. Guaranteed Cell Availability*

As defined in (3), the cell availability equals to one when the cell size is smaller than or equal to the covered area of the BS. Accordingly, (A.9) is equivalent to the probability that $A_s^c = 1$ given that the value $c$, i.e., the upper limit of the integral, is equal to the normalized covered area of the BS covering that cell. Mathematically, it is expressed as

$$P\left(A_s^c = 1\right) \equiv P\left(c \geq y\right) = \int_0^c f_{2D}\left(y\right) dy. \tag{A.10}$$

Note that availability equals to one implies that full connectivity is obtained everywhere in the cell, indicating that URC can be achieved in this cell *in the space domain*.

Let us now target at a general guaranteed cell availability level of $\beta$ where $(0 < \beta < 1)$. Then the probability for providing a guaranteed availability level greater than or equal to $\beta$ by the cell is given by,

$$P\left(A_s^c \geq \beta\right) \equiv P(y \leq y_i) = \int_0^{y_i} f_{2D}\left(y\right) dy \tag{A.11}$$

where $y_i = MCA/(\bar{S}\beta)$ is the corresponding *normalized cell area*. Fig. 5 illustrates this probability by considering two cell radius values for a HomNet where the mean cell coverage is calculated as $MCA = \pi R^2$. To obtain the definite integral in (A.11), the CDF of the normalized cell areas derived in [10] is adopted. Evidently, the higher the required availability level, the lower the probability to achieve it. Meanwhile, a larger cell coverage would increase the probability for providing a guaranteed availability level.

### VI. Conclusions

This letter makes a contribution to the ongoing research work on URC by soliciting the concept of cell and system availability in the space domain from the perspective of dependability theory. Through PPP and Voronoi tessellation based analysis, we illustrate the relationship between BS coverage and cell/system availability for both homogenous and heterogeneous cellular networks. The probability of providing a guaranteed availability level is also deduced.

### Appendix A: References

[1] P. Popovski, "Ultra-reliable communication in 5G wireless systems," in *Proc. 1st Int. Conf. 5G for Ubiquitous Connectivity, 2014, pp. 1-6.*

[2] 3GPP TR38.801, "Study on New Radio Access Technology: Radio Access Architecture and Interfaces," *R14, v0.4.0*, Aug. 2016.

[3] S. M. Azimi, O. Simeone, O. Sahin, and P. Popovski, "Ultra-reliable cloud mobile computing with service composition and superposition coding," in *Proc. CISS, 2016, pp. 442-447.*

[4] G. Durisi, T. Koch, and P. Popovski, "Toward massive, ultra-reliable, and low-latency wireless communication with short packets," *Proc. IEEE*, vol. 104, no. 9, pp. 1711-1726, Sep. 2016.

[5] J. G. Andrews, F. Baccelli, and R. K. Ganti, "A tractable approach to coverage and rate in cellular networks," *IEEE Trans. Commun.*, vol. 59, no. 11, pp. 3122-3134, Nov. 2011.

[6] T. Bai and R. W. Heath, "Location-specific coverage in heterogeneous networks," *IEEE Signal Process. Lett.*, vol. 20, no. 9, pp. 873-876, Sep. 2013.

[7] S. Mukherjee, "Distribution of downlink SINR in heterogeneous cellular networks," *IEEE J. Sel. Areas Commun.*, vol. 30, no. 3, pp. 575-585, Apr. 2012.

[8] P. Madhusudhanan, J. G. Restrepo, Y. Liu, T. X. Brown, and K. R. Baker, "Downlink performance analysis for a generalized shotgun cellular system," *IEEE Trans. Commun.*, vol. 13, no. 12, pp. 6684-6696, Dec. 2014.

[9] A. Goyal and A. N. Tantawi, "A measure of guaranteed availability and its numerical evaluation," *IEEE Trans. Comput.*, vol. 37, no. 1, pp. 25-32, Jan. 1988.

[10] J.-S. Ferenc and Z. Néda, "On the size distribution of Poisson Voronoi cells," *Physica A: Statistical Mechanics and its Applications*, vol. 385, no. 2, pp. 518-526, Nov. 2007.

# Appendix B

# Example of MATLAB Codes

The outline of the MATLAB simulations used to obtain the results of this thesis is depicted by Tab. B.1. MATLAB programs were simulated in a computer with a RAM of 6 GB memory and Intel(R) Core(TM) i5-6200U processor with 2.4 GHz speed.

Table B.1: Summary of the MATLAB codes

| | |
|---|---|
| MATLAB version used | $R2015a$ |
| Number of MATLAB programs | 56 |
| Number of MATLAB functions | 18 |
| Maximum length of a MATLAB program/ function | 540 *lines* |
| Minimum length of a MATLAB program/ function | 26 *lines* |
| Maximum time to run a MATLAB program/ function | $\approx$ 10 *minutes* |
| Minimum time to run a MATLAB program/ function | $\approx$ 5 *seconds* |

## B.1 MATLAB Code for Connectivity-based System Availability of HetNet Scenario

```
File Name: Availability_HetNet

This program computes the MCST cell availability and the ST system availability
of the topology 1 which employs both T1 and T2 cells for a given radius
of the BS coverage.

xB = gallery('uniformdata',[1 10],1);
yB = gallery('uniformdata',[1 10],2);
S=SquareBV(xB,yB,0);  %Cell Area
Th=0.08;  %Threshold cell Area
```

```
index=find(S>Th);  %Index of T2 cells
jndex=find(S<Th);  %Index of T1 cells
R1=0.05:0.01:0.16; %radius of the BS coverage of T1 cells
R1(13:16)=0.16;
R2=0.05:0.01:0.2; %radius of the BS coverage of T2 cells

%--- ST system availability ---%
for z=1:length(R2)
%exurban area
OutofBoundArea(z)=boundaryOutAreaHet(x,y,S,Th,R2(z),R1(z));
%overlapping area
OverlappingArea(z)=AreaOverlapCirclesHet(x,y,S,Th,R2(z),R1(z));
%total BS coverage of the system
BSarea(z)=length(index)*pi*R2(z)^2+length(jndex)*pi*R1(z)^2;
%effective BS coverage of the system
CoveredArea(z)= BSarea(z)- OutofBoundArea(z)-OverlappingArea(z);
%ST system availability
STAvailability(z)=CoveredArea(z)/sum(S);
end

%--- MCST cell availability ---%
R=0.05:0.01:0.2;
IndAvailT2=zeros(length(xB),length(R));
IndAvailT1=zeros(length(xB),length(R));

for i=1:length(xB)
if S(i)>Th
R=0.05:0.01:0.2;
for z=1:length(R)
coverT2(z)=pi*R(z).^2;
if S(i)<coverT2(z)
IndAvailT2(i,z)=1;
else
IndAvailT2(i,z)= coverT2(z)/S(i);
end
end
else
R=0.05:0.01:0.16;
R(13:16)=0.16;
for z=1:length(R)
```

```
coverT1(z)=pi*R(z).^2;
if S(i)<coverT1(z)
IndAvailT1(i,z)=1;
else
IndAvailT1(i,z)= coverT1(z)/S(i);
end
end
end

 %eliminating nonzero elements
 [r_mac,c_mac]=find(IndAvailT2);
 IndAvailT2=IndAvailT2(unique(r_mac),:) ;
 [r_mic,c_mic]=find(IndAvailT1);
 IndAvailT1=IndAvailT1(unique(r_mic),:) ;

for k=1:length(R)
totAvailT1(k)=sum(IndAvailT1(:,k));
totAvailT2(k)=sum(IndAvailT2(:,k));
AvgAvail(k)=(totAvailT1(k)+totAvailT2(k))/length(xB);
end

%=========================================================================
Function Name: boundaryOutAreaHet

This function outputs the total exurban area produced by the BS coverages
outside the unit region.

Input: (x,y) coordintes of the BSs, CellArea, ThresholdArea,
Radius of T1 and T2  cells
Output: total exurban area


function OutOfBound=boundaryOutAreaHet(x,y,S,Th,R1,R2)

for i = 1 : length(x)
    if S(i)>Th
       R=R1;
       if x(i)<R
            h=R-x(i);
            OutboundArea(i)= R.^2.*acos(1-h/R)-(R-h).*sqrt(2*R.*h-h.^2);
```

```
       else if 1-x(i)<R
            h=R-1+x(i);
            OutboundArea(i)= R.^2.*acos(1-h/R)-(R-h).*sqrt(2*R.*h-h.^2);
        else if y(i)<R
            h=R-y(i);
            OutboundArea(i)= R.^2.*acos(1-h/R)-(R-h).*sqrt(2*R.*h-h.^2);
        else if 1-y(i)<R
            h=R-1+y(i);
            OutboundArea(i)= R.^2.*acos(1-h/R)-(R-h).*sqrt(2*R.*h-h.^2);
        %two boundary out area
        %x=0,y=0
        else if x(i)<R &  y(i)<R
            [Alpha_(i),Beta_(i)]=linecirc(infinity,0,x(i),y(i),R);
            if Beta_(i)> 0
                Alpha(i)=0;
                Beta(i)=Beta_(i);
            end
            [u_(i),v_(i)]=linecirc(0,0,x(i),y(i),R);
            if Beta_(i) > 0
                u(i)=u_(i);
                v(i)=0;
            end
            Triangle(i)=0.5*(abs(Alpha(i)*v(i)-u(i)*Beta(i)));
            Theta(i)=acos((2*R^2-(Alpha(i)-u(i))^2-(Beta(i)-v(i))^2)/2*R^2);
            Segment(i)=0.5*R^2*(2*Theta(i)-sin(2*Theta(i)));
            OutboundArea(i)=pi*R^2-(Triangle(i)+Segment(i));

%x=0,y=1
else if x(i)<R &  1-y(i)<R
[Alpha_,Beta_]=linecirc(infinity,0,x,y,R);
if Beta_ > 0
Alpha=0;
Beta=Beta_;
end

[u_,v_]=linecirc(0,1,x,y,R);
if Beta_ > 0
u=u_;
v=1;
end
```

```
Triangle(i)=0.5*(abs(Alpha(i)*v(i)+u(i)-Alpha(i)-u(i)*Beta(i)));
Theta(i)=acos((2*R^2-(Alpha(i)-u(i))^2-(Beta(i)-v(i))^2)/2*R^2);
Segment(i)=0.5*R^2*(2*Theta(i)-sin(2*Theta(i)));
OutboundArea(i)=pi*R^2-(Triangle(i)+Segment(i));

%x=1,y=0
else if 1-x(i)<R &  y(i)<R
[Alpha_,Beta_]=linecirc(infinity,-1,x,y,R);
if Beta_ > 0
Alpha=1;
Beta=Beta_;
end

[u_,v_]=linecirc(0,0,x,y,R);
if Beta_ > 0
u=u_;
v=0;
end
Triangle(i)=0.5*(abs(Alpha(i)*v(i)+Beta(i)-v(i))-u(i)*Beta(i));
Theta(i)=acos((2*R^2-(Alpha(i)-u(i))^2-(Beta(i)-v(i))^2)/2*R^2);
Segment(i)=0.5*R^2*(2*Theta(i)-sin(2*Theta(i)));
OutboundArea(i)=pi*R^2-(Triangle(i)+Segment(i));

%x=1,y=1
else if 1-x(i)<R &  1-y(i)<R
[Alpha_,Beta_]=linecirc(infinity,-1,x,y,R);
if Beta_ > 0
Alpha=1;
Beta=Beta_;
end

[u_,v_]=linecirc(0,1,x,y,R);
if Beta_ > 0
u=u_;
v=1;
end
Triangle=0.5*(abs(Alpha(i)*v(i)+u(i)+Beta(i)-Alpha(i)-v(i))-u(i)*Beta(i));
Theta(i)=acos((2*R^2-(Alpha(i)-u(i))^2-(Beta(i)-v(i))^2)/2*R^2);
Segment(i)=0.5*R^2*(2*Theta(i)-sin(2*Theta(i)));
OutboundArea(i)=pi*R^2-(Triangle(i)+Segment(i));
```

```
end
end
end
end
end
end
end
end
else
R=R2;
if x(i)<R
h=R-x(i);
OutboundArea(i)= R.^2.*acos(1-h/R)-(R-h).*sqrt(2*R.*h-h.^2);
else if 1-x(i)<R
h=R-1+x(i);
OutboundArea(i)= R.^2.*acos(1-h/R)-(R-h).*sqrt(2*R.*h-h.^2);
else if y(i)<R
h=R-y(i);
OutboundArea(i)= R.^2.*acos(1-h/R)-(R-h).*sqrt(2*R.*h-h.^2);
else if 1-y(i)<R
h=R-1+y(i);
OutboundArea(i)= R.^2.*acos(1-h/R)-(R-h).*sqrt(2*R.*h-h.^2);

%two boundary out area
%x=0,y=0
else if x(i)<R &  y(i)<R
[Alpha_(i),Beta_(i)]=linecirc(infinity,0,x(i),y(i),R);
if Beta_(i)> 0
Alpha(i)=0;
Beta(i)=Beta_(i);
end
[u_(i),v_(i)]=linecirc(0,0,x(i),y(i),R);
if Beta_(i) > 0
u(i)=u_(i);
v(i)=0;
end
Triangle(i)=0.5*(abs(Alpha(i)*v(i)-u(i)*Beta(i)));
Theta(i)=acos((2*R^2-(Alpha(i)-u(i))^2-(Beta(i)-v(i))^2)/2*R^2);
Segment(i)=0.5*R^2*(2*Theta(i)-sin(2*Theta(i)));
OutboundArea(i)=pi*R^2-(Triangle(i)+Segment(i));
```

```
%x=0,y=1
else if x(i)<R &  1-y(i)<R
[Alpha_,Beta_]=linecirc(infinity,0,x,y,R);
if Beta_ > 0
Alpha=0;
Beta=Beta_;
end

[u_,v_]=linecirc(0,1,x,y,R);
if Beta_ > 0
u=u_;
v=1;
end
Triangle(i)=0.5*(abs(Alpha(i)*v(i)+u(i)-Alpha(i)-u(i)*Beta(i)));
Theta(i)=acos((2*R^2-(Alpha(i)-u(i))^2-(Beta(i)-v(i))^2)/2*R^2);
Segment(i)=0.5*R^2*(2*Theta(i)-sin(2*Theta(i)));
OutboundArea(i)=pi*R^2-(Triangle(i)+Segment(i));

%x=1,y=0
else if 1-x(i)<R &  y(i)<R
[Alpha_,Beta_]=linecirc(infinity,-1,x,y,R);
if Beta_ > 0
Alpha=1;
Beta=Beta_;
end

[u_,v_]=linecirc(0,0,x,y,R);
if Beta_ > 0
u=u_;
v=0;
end
Triangle(i)=0.5*(abs(Alpha(i)*v(i)+Beta(i)-v(i))-u(i)*Beta(i));
Theta(i)=acos((2*R^2-(Alpha(i)-u(i))^2-(Beta(i)-v(i))^2)/2*R^2);
Segment(i)=0.5*R^2*(2*Theta(i)-sin(2*Theta(i)));
OutboundArea(i)=pi*R^2-(Triangle(i)+Segment(i));

%x=1,y=1
else if 1-x(i)<R &  1-y(i)<R
[Alpha_,Beta_]=linecirc(infinity,-1,x,y,R);
```

```
if Beta_ > 0
Alpha=1;
Beta=Beta_;
end

[u_,v_]=linecirc(0,1,x,y,R);
if Beta_ > 0
u=u_;
v=1;
end
Triangle=0.5*(abs(Alpha(i)*v(i)+u(i)+Beta(i)-Alpha(i)-v(i))-u(i)*Beta(i));
Theta(i)=acos((2*R^2-(Alpha(i)-u(i))^2-(Beta(i)-v(i))^2)/2*R^2);
Segment(i)=0.5*R^2*(2*Theta(i)-sin(2*Theta(i)));
OutboundArea(i)=pi*R^2-(Triangle(i)+Segment(i));
end
end
end
end
end
end
end
end
end
end
end
end

OutOfBound=sum(OutboundArea);


%=========================================================================
Function Name: AreaOverlapCirclesHet

This function calculates the overlapping area between 2 circles with
heterogeneous radius values.

Input: (x,y) coordintes of the BSs, CellArea, ThresholdArea,
Radius of T1 and T2  cells
Output: total overlapping area between all combinations of 2 cricles

function Overlap=AreaOverlapCirclesHet(x,y,S,Th,R1,R2)
```

```
Array_Overlap=zeros(length(x),length(x));

%computing overlap area between two circles
for i = 1 : length(x)
    for j = i : length(x)
    d(j)=sqrt((x(i)-x(j)).^2+(y(i)-y(j)).^2);
    if S(i)>Th && S(j)>Th
        R=R1;
        theta(j)=2.*acos(d(j)./(2*R));
        if d(j)>=2*R
            AreaOverlap(j)=0;
            else if i==j         %to avoid the circle compared with itself
                AreaOverlap(j)=0;
            else if d(j)==0        %to avoid the circle compared with itself
                AreaOverlap(j)=pi*R.^2;
                else
                AreaOverlap(j)=R.^2*(theta(j)-sin(theta(j)));
            end
            end
        end
        Array_Overlap(i,j)=AreaOverlap(j);

    else if S(i)<Th && S(j)<Th
            R=R2;
            theta(j)=2.*acos(d(j)./(2*R));
            if d(j)>=2*R
                AreaOverlap(j)=0;
                else if i==j         %to avoid the circle compared with itself
                    AreaOverlap(j)=0;
                else if d(j)==0        %to avoid the circle compared with itself
                    AreaOverlap(j)=pi*R.^2;
                else
                    AreaOverlap(j)=R.^2*(theta(j)-sin(theta(j)));
                end
                end
            end
            Array_Overlap(i,j)=AreaOverlap(j);

         else if S(i)>Th && S(j)<Th
            RR1=R1;
```

```
            RR2=R2;
            phi(j)=2.*acos((RR1.^2+d(j).^2-RR2.^2)./(2*RR1*d(j)));
            theta(j)=2.*acos((RR2.^2+d(j).^2-RR1.^2)./(2*RR2*d(j)));
            if d(j)>=(RR1+RR2)
                AreaOverlap(j)=0;
                else if i==j         %to avoid the circle compared with itself
                    AreaOverlap(j)=0;
                else if d(j)==0        %to avoid the circle compared with itself
                    AreaOverlap(j)=pi*RR2.^2;
                    else
                    area1(j)=0.5*phi(j)*RR1.^2 - 0.5*RR1.^2.*sin(phi(j));
                    area2(j)=0.5*theta(j)*RR2.^2 - 0.5*RR2.^2.*sin(theta(j));
                    AreaOverlap(j)=area1(j)+area2(j);
                end
                end
            end
            Array_Overlap(i,j)=AreaOverlap(j);

            else if S(i)<Th && S(j)>Th
            RR1=R2;
            RR2=R1;
            phi(j)=2.*acos((RR1.^2+d(j).^2-RR2.^2)./(2*RR1*d(j)));
            theta(j)=2.*acos((RR2.^2+d(j).^2-RR1.^2)./(2*RR2*d(j)));
            if d(j)>=(RR1+RR2)
                AreaOverlap(j)=0;
                else if i==j         %to avoid the circle compared with itself
                    AreaOverlap(j)=0;
                else if d(j)==0        %to avoid the circle compared with itself
                    AreaOverlap(j)=pi*RR2.^2;
                    else
                    area1(j)=0.5*phi(j)*RR1.^2 - 0.5*RR1.^2.*sin(phi(j));
                    area2(j)=0.5*theta(j)*RR2.^2 - 0.5*RR2.^2.*sin(theta(j));
                    AreaOverlap(j)=area1(j)+area2(j);
                end
                end
            end
            Array_Overlap(i,j)=AreaOverlap(j);
                end
     end
    end
```

```
    end
    end
end
% Array_Overlap
[row,col,val] =find(Array_Overlap);

if length(unique(row))< length(row)& length(unique(col))< length(col)
    %disp('there are more than two overlapping circles');
    Overlap=AreaOverlap3CirclesHet(x,y,S,Th,R1,R2,row,col,val);

else %calculating two circle overlap area
Overlap=sum(val);
end

%================================================================================

Function Name: AreaOverlap3CirclesHet

This function calculates the overlapping area between 3 circles with
heterogeneous radius values.

Input: (x,y) coordintes of the BSs, CellArea, ThresholdArea,
Radius of T1 and T2  cells
Output: total overlapping area between all combinations of 3 cricles

function Overlap=AreaOverlap3CirclesHet(x,y,S,Th,R1,R2,row,col,val)
R=R1;
%calculating the intersecting points of the overlapping circles
for k = 1 : length(row)
    i=row(k);
    j=col(k);
%     R(k)=0.1;
    [alpha,Beta]=circcirc(x(i),y(i),R,x(j),y(j),R);
    points(2*k-1,1)=alpha(1);
    points(2*k,1)=alpha(2);
    points(2*k-1,2)=Beta(1);
    points(2*k,2)=Beta(2);
end

%check if the three point lie incide the circles and sort out the common
```

```
%overlap area intersecting points

unique_r=unique(row);
unique_c=unique(col);



if length(unique_r)>length(unique_c)
    bb=setdiff(unique_c,unique_r);
    for v=1:length(bb)
        unique_r(length(unique(row))+v,1) = bb(v,1)
    end
    unique_array=unique_r;
else
    bb=setdiff(unique_r,unique_c);
    for v=1:length(bb)
        unique_c(length(unique(col))+v,1) = bb(v,1);
    end
    unique_array=unique_c;
end
% unique_array
% olap_circ=unique([unique_r,unique_c]);

if length(points)<length(unique_array)*2
 for m=1:length(unique_array)
   for n=1:(length(unique_array)*2)-2
in_dist(n,m)=sqrt((points(n,1)-x(unique_array(m))).^2+...
.........(points(n,2)-y(unique_array(m))).^2);
if in_dist(n,m)<R-0.0001
            trianglepoint(n,m)=in_dist(n,m);
        else
            trianglepoint(n,m)=0;
        end
end
end

else

for m=1:length(unique_array)
   for n=1:length(unique_array)*2
in_dist(n,m)=sqrt((points(n,1)-x(unique_array(m))).^2+...
```

```
.........(points(n,2)-y(unique_array(m))).^2);
if in_dist(n,m)<R-0.0001
            trianglepoint(n,m)=in_dist(n,m);
        else
            trianglepoint(n,m)=0;
        end
end
end
end

[r,c] =find(trianglepoint);
point_array=points(r,:);

if length(r)<3
chordlength=sqrt((point_array(1,1)-point_array(2,1))^2+...
.........(point_array(1,2)-point_array(2,2))^2);
angle=2*asin(chordlength/(2*R));
Overlap=R.^2*(angle-sin(angle));

else
%area of triangle formed by the intersecting points
triArea=polyarea(point_array(:,1),point_array(:,2));

%calculating the chord length
c1=sqrt((point_array(1,1)-point_array(2,1))^2+(point_array(1,2)-point_array(2,2))^2);
c2=sqrt((point_array(2,1)-point_array(3,1))^2+(point_array(2,2)-point_array(3,2))^2);
c3=sqrt((point_array(3,1)-point_array(1,1))^2+(point_array(3,2)-point_array(1,2))^2);


%assuming equal radius
Overlap=0.25*sqrt((c1+c2+c3)*(c2+c3-c1)*(c1+c3-c2)*(c1+c2-c3))+ ....
.....R^2*(asin(c1/(2*R))+asin(c2/(2*R))+asin(c3/(2*R))-(0.25*c1*sqrt(4*R^2-c1^2))-....
.....(0.25*c2*sqrt(4*R^2-c2^2))-(0.25*c3*sqrt(4*R^2-c3^2)));
end
```

## B.2 MATLAB Code for Creating SINR Threshold Contour and Finding The Cell Availability of The RC

```
File Name: SINR_Th_Contour

This program obtains the coordinates along the SINR threshold contour
and calculates the cell availability accordingly.

%x y coordinates of the 10 BSs
xB = gallery('uniformdata',[1 10],1);
yB = gallery('uniformdata',[1 10],2);

[XY,V,C]=Voronoi(xB,yB,'bs_ext',[0 0;0 1;1 1;1 0],'figure','on');
%The function Voronoi provides the Voronoi decomposition of a set of (x,y) data,
% but with all vertices limited to the unit square.
%V contains all vertices and C contains all vertices for each individual point.
%XY contains updated xy coordinates as limited by any input boundaries.
hold on

Th=0.6; %SINR threshold
alpha=2.5; %path loss coefficient

ref=6;  %index of the RC

xc=C(ref,1);
yc=C(ref,2);

xv=XY(V{ref},1);
yv=XY(V{ref},2);

Theta=0:1:360;

for j=1:length(Theta)
    d=0.001;  %calculating sinr at d=0.001
    xp(j)=xc+d*cosd(Theta(j));
    yp(j)=yc+d*sind(Theta(j));
```

```
Iloop(j)=0;
    for k=1:length(xB)
        dist(j,k) = sqrt((xp(j)-xB(k)).^2+(yp(j)-yB(k)).^2);
        Iloop(j)=Iloop(j)+ dist(j,k)^(-alpha);
    end
    I_r(j)=Iloop(j)-d.^(-alpha);

    sinr(j)= d.^(-alpha)/I_r(j);

 while sinr(j)>=Th
        d=d+0.001;
        xp(j)=xc+d*cosd(Theta(j));
        yp(j)=yc+d*sind(Theta(j));

        Iloop(j)=0;
        for k=1:length(xB)
            dist(j,k) = sqrt((xp(j)-xB(k)).^2+(yp(j)-yB(k)).^2);
            Iloop(j)=Iloop(j)+ dist(j,k)^(-alpha);
        end

        I_r(j)=Iloop(j)-d.^(-alpha);

        sinr(j)= d.^(-a)/I_r(j);
    end
end

% plotting the SINR threshold contour
plot(xp,yp,'b','LineWidth',2)
hold off

%Finding the cell availability
ThArea=polyarea(xp,yp);
CellArea=polyarea(xv,yv);

if CellArea<ThArea
    availability=1;
else
availability=ThArea/CellArea;
end
```